Biogeosciences Discuss., 11, 1187–1275, 2014
www.biogeosciences-discuss.net/11/1187/2014/
doi:10.5194/bgd-11-1187-2014

Biogeosciences Discussions
Open Access

Characterisation of NO production and consumption: new insights by an improved laboratory dynamic chamber technique

T. Behrendt[1], P. R. Veres[2], F. Ashuri[1], G. Song[1,3], M. Flanz[4], B. Mamtimin[1], M. Bruse[5], J. Williams[4], and F. X. Meixner[1]

[1]Biogeochemistry Department, Max Planck Institute for Chemistry, Mainz, Germany
[2]Cooperative Institute for Research in Environmental Sciences, Boulder, CO 80305, USA
[3]Institute of Applied Ecology, Chinese Academy of Sciences, Shenyang, China
[4]Atmospheric Chemistry Department, Max Planck Institute for Chemistry, Mainz, Germany
[5]Environmental Modelling Group (EMG), Johannes Gutenberg University Mainz, Mainz, Germany

Received: 1 January 2014 – Accepted: 2 January 2014 – Published: 17 January 2014

Correspondence to: T. Behrendt (thomas.behrendt@mpic.de)

Published by Copernicus Publications on behalf of the European Geosciences Union.

Abstract

Biogenic NO_x emissions from natural and anthropogenically influenced soils are currently estimated to amount to $9\,Tg\,a^{-1}$, hence a significant fraction of global NO_x emissions ($45\,Tg\,a^{-1}$). During the last three decades, a large number of field measurements have been performed to quantify biogenic NO emissions. To study biogenic NO emissions as a function of soil moisture, soil temperature, and soil nutrients, several laboratory approaches have been developed to estimate local/regional NO emissions by suitable up-scaling. This study presents an improved and automated laboratory dynamic chamber system (consisting of six individual soil chambers) for investigation and quantification of all quantities necessary to characterize biogenic NO release from soil (i.e., net NO release rate, NO production and consumption rate, and respective Q_{10} values). In contrast to former versions of the laboratory dynamic chamber system, the four experiments for complete characterization can now be performed on a single soil sample, whereas former studies had to be performed on four sub-samples. This study discovered that the sub-sample variability biased former measurements of net NO release rates tremendously. Furthermore, it was also shown that the previously reported variation of optimum soil moisture (i.e., where a maximum net NO release rate occurs) between individual sub-samples is most likely a methodical artefact of former versions of the laboratory dynamic chamber system.

A comprehensive and detailed methodical concept description of the improved laboratory dynamic chamber system is provided. Response of all quantities (necessary to characterize net NO release) to soil temperature and NO mixing ratio of the flushing air-stream are determined by automatic monitoring of these variables during one single drying-out experiment with one single soil sample only. The method requires precise measurements of NO mixing ratio at the inlet and outlet of each soil chamber; finally, four pairs of inlet/outlet NO mixing ratios are sufficient to derive all necessary quantities. Soil samples from drylands exhibit particularly low NO production, but even lower NO consumption rates. However, with the improved laboratory dynamic chamber

BGD
11, 1187–1275, 2014

system those low levels can be quantified, as well as corresponding NO compensation point mixing ratios and respective Q_{10} values. It could be shown, that the NO compensation point mixing ratio seems to be generally independent of gravimetric soil moisture content, but, particularly for dryland soils, strongly dependent on soil temperature.

New facilities have been included into the improved system (e.g. for investigation of net release rates of other trace gases, namely CO_2 and VOCs). First results are shown for net release rates of acetone (C_3H_6O), acetaldehyde (C_2H_4O) and CO_2. This new system is thus able to simultaneously investigate potential mechanistic links between NO, multitudinous VOC and CO_2.

1 Introduction

The turnover of nutrients in natural soils is predominantly driven by soil microbes and any control of production and consumption of trace gases in the soil is exerted on the level of microbes' metabolism. If production of the trace gas in the soil exceeds its consumption, the trace gas will be delivered to the atmosphere. In case of nitric oxide (NO), microbially produced NO is usually released from soils. Once in the atmosphere, it is immediately involved in important chemical reactions (Crutzen et al., 1999; Denman et al., 2007). It reacts with atmospheric oxidants (O_3, OH, NO_3·) and is converted first to nitrogen dioxide (NO_2), and finally to nitric acid (HNO_3, Williams et al., 1992). The concentration of both, NO_x (= NO + NO_2) and volatile organic compounds (VOCs), controls the production or destruction of tropospheric O_3 with a production threshold of approx. 30 ppt of NO (Sillman, 1999; Chameides et al., 1992). Particularly for understanding tropospheric chemistry of non-industrialized regions, it is important to know the strength of biogenic NO and VOCs emissions from natural sources. While there is rich literature with respect to soil biogenic NO emissions, relatively little is known about VOC emissions from and VOC deposition to soils.

The microbial release of NO from soils was first discovered by Galbally and Roy (1978). Underlying processes are nitrification and denitrification (Braker and Conrad,

BGD
11, 1187–1275, 2014

2011). It is well known that microbes can release VOCs but the mechanisms are still unknown (Insam and Seewald, 2010; Schulz and Dickschat, 2007). Historically, it has been assumed that the function of inter- and intraspecies communication as well as defence play an important role in VOC production (Schulz and Dickschat, 2007). Since (i) emissions of NO and VOCs from soils are highly variable in space and time, and (ii) corresponding field experiments are costly, laboratory incubation experiments are the ideal tool for studying mechanistic processes. Additionally, environmental conditions are usually highly variable in the field; consequently, identification and quantification of individual factors, which might influence soil biogenic NO and VOC (e.g., soil moisture, soil temperature; soil nutrients), is often impossible because of mutually masking effects.

Early pioneering studies of NO emission from soils found, that – within the top soil layer – NO is microbially produced and consumed as an intermediate within the process of nitrification and denitrification (Gödde and Conrad, 1999; Conrad, 1996; Schuster and Conrad, 1992). The major enzymatic pathways which generate NO are autotropic nitrification, heterotrophic nitrification and denitrification (Braker and Conrad, 2011). The enzymes involved differ in their half saturation constants, K_m, as well as in their maximum reaction rate, V_{max} (Koper et al., 2010, Betlach and Tiedje, 1981). In an earlier study (Kumon et al., 2002) co-denitrification of fungi, i.e. the formation of an N-product owing an oxidation number between the oxidation numbers of its educts, was found. It is still unclear how much this process contributes to the production and consumption of NO in soils. Within the process of dissimilatory nitrate reduction to ammonia (DNRA), N_2O can be produced (Rütting et al., 2011). Since DNRA is the reverse process of nitrification, where NO and N_2O can be produced, it might be possible that NO is formed, too. Besides the microbial production and consumption of NO, some abiotic processes are known that also result in the release of NO from soils (Van Cleemput and Samater, 1996). These processes are assumed to be of importance under acidic conditions, where microbial activity is limited. Since the kinetics of NO release follow a first order reaction, the net release of NO, which is usually measured in labora-

BGD
11, 1187–1275, 2014

tory incubation experiments, can be separated into production and consumption terms. However, it should be emphasized, that this concept has been shown to be valid only, if (i) production and consumption processes occur simultaneously, and (ii) are homogeneously distributed in the top soil layer (Rudolph et al., 1996, Rudolph and Conrad, 1996). Simultaneous occurrence of production and consumption processes imply the so-called compensation point; the mixing ratio, where production equals consumption and consequently the net NO release is zero is defined as the NO compensation point mixing ratio (Conrad, 1994).

The major environmental factors that control the release of NO from soil are (i) soil moisture, (ii) soil temperature, (iii) the atmospheric mixing ratio of NO, and (iv) nitrogen availability/fertilizer application (Ludwig et al., 2001). In addition to these factors, several other controlling factors have been recognized. Gödde and Conrad (2000) investigated net NO release rates for a series of different soils under constant soil moisture and soil temperature. They identified soil nitrate and nitrite (NO_3^-, NO_2^-), soil pH, soil texture, and soil nitrification rates as further influencing factors for NO production, while microbial respiration, soil texture and soil ammonium (NH_4^+) have affected the consumption of NO. Stark et al. (2002) found in an earlier study, that soils characterized by high organic carbon and C : N ratio showed lower biogenic NO emissions. This might be explained by the fact that high availability of C leads to a greater demand for N and thereby to an increase of consumption of NO. If this is the case, soil organic carbon and microbial respiration might be used to predict the consumption or even the release of NO (Ashuri, 2009; Dunfield and Knowles, 1998; Stark et al., 2002; Gödde and Conrad, 2000).

Steinkamp and Lawrence (2011; Supplement) provide a recent compilation of numerous (110 studies in the last 3 decades) field measurements of NO fluxes. However, the majority of the studies concentrated on fertilized agricultural soils, despite the fact that 47 % of the earth's surface is covered by drylands (UNEP, 1997) for which only a relatively small number of studies exists (Feig, 2009). Several field and laboratory methods have been established to study soil NO fluxes (in mass per area and time)

BGD
11, 1187–1275, 2014

as well as soil NO release rates (in mass per mass of dry soil and time) and their influencing factors, namely soil temperature, soil moisture, ambient NO mixing ratio, and more (Galbally and Johansson, 1989; Yang and Meixner, 1997; Pape et al., 2009; Gut et al., 1998; Wang et al., 2011; Gödde and Conrad, 1998). The most relevant parameter which has been determined either in field experiments (Slemr and Seiler, 1984) or during laboratory incubations is the NO compensation point mixing ratio, $m_{NO,comp}$ (Feig et al., 2008a, b; Bargsten et al., 2010; Remde et al., 1989). The NO production rate (P_{NO}), and the NO consumption rate coefficient (k_{NO}) need to be parameterized for the influencing factors separately, as they define $m_{NO,comp}$, which in turn is needed to calculate the so-called net potential NO flux using soil-diffusion algorithms described by Galbally and Johansson (1989) and Meixner and Yang (2006). Once, the net potential NO flux is parameterized for soil moisture and soil temperature, routine measured field data of soil temperature and soil moisture have been used to up-scale the laboratory derived net potential NO flux to different spatial (plot, ecosystem, region) and temporal scales. Up-scaled NO fluxes have been repeatedly shown to be in largely good agreement with those measured in the field (Mayer et al., 2011; Laville et al., 2009; van Dijk et al., 2002, Ludwig et al., 2001; Remde et al., 1993).

Laboratory incubation systems for the investigation of NO release from soil are usually dynamic chamber systems. Here, the net release rate of NO (J_{NO}) from an enclosed soil sample is determined from the NO concentration difference between incoming and outgoing air. All further quantities, which are necessary to characterize NO production and NO consumption (i.e., P_{NO}, k_{NO}, $m_{NO,comp}$, Q_{10} values J_{NO}) were usually derived from J_{NO} data, eventually obtained under different, mostly discrete soil temperature and soil moisture conditions. Particularly, the study of arid/hyper-arid as well as organic rich soils by laboratory dynamic chambers has manifested obvious and partly substantial difficulties for the determination of k_{NO}, $m_{NO,comp}$, or corresponding Q_{10} values (c.f., Feig, 2009; Gelfand et al., 2009; Yu et al., 2010, 2008; Bargsten et al., 2010; Laville et al., 2009). Since there was reasonable suspicion, that these difficulties are due to non-standardized pre-incubation protocols and sub-sample variability, it was

BGD
11, 1187–1275, 2014

decided to design an improved laboratory dynamic chamber system such, that these difficulties will be eliminated. In the next section, the methodical concept for the determination of J_{NO}, P_{NO}, k_{NO}, $m_{NO,comp}$, and corresponding Q_{10} values from only four pairs of NO mixing ratio is described in detail as well as the reasons to develop the improved laboratory dynamic chamber system. Furthermore, design of the improved system included the option to apply the system also for soil release studies of other trace gases. First attempts to determine (simultaneously with net NO release) the net release of CO_2, and two volatile organic compounds (VOCs), namely acetone (C_2H_4O) and acetaldehyde (C_3H_6O) are also reported.

2 The need for an improved laboratory dynamic chamber system: methodical concept vs. experimental reality

2.1 Methodical concept

The dynamic chamber technique is applied to determine the release of a trace gas from the enclosed soil sample. The mass balance of the dynamic chamber necessitates that all mass fluxes into and out of the chamber's volume sum up to zero (see Sect. S.1). The mass flux Φ_{in} entering the chamber (in mass per time; here: $ng\,s^{-1}$) is equal to $Q \cdot c_{in}$, where Q is the purging flow ($m^3\,s^{-1}$) and c_{in} is the trace gas' concentration at the chamber's inlet ($ng\,m^{-3}$). Given a well-mixed volume of the chamber, the concentration within the chamber (c_{cham}) is identical to that at its outlet; consequently, the mass flux Φ_{out} leaving the chamber is equal to $Q \cdot c_{cham}$. The mass flux of the trace gas out of (or into) the soil (Φ_{soil}) is usually related to the mass of the soil sample m_{soil} (kg) and is named the release rate J (in $ng\,kg^{-1}\,s^{-1}$). Conventionally, fluxes into the chamber's volume are counted positive, those out of it negative; therefore the chamber's mass

BGD
11, 1187–1275, 2014

balance equation delivers

$$J = \frac{\Phi_{soil}}{m_{soil}} = \frac{Q\,c_{cham} - Q\,c_{in}}{m_{soil}} = \frac{Q}{m_{soil}}(m_{cham} - m_{in})f_{C,NO} \quad (1)$$

where $f_{C,NO}$ is the factor to convert the incoming and chamber NO mixing ratios (m_{in} and m_{cham}, ppb) into corresponding NO concentrations ($f_{C,NO} = 572.5\,ng\,m^{-3}\,ppb^{-1}$, at 1013.25 hPa and $T = 25\,^{\circ}C$; see Sect. 3.4).

If the release of the trace gas is the result of microbial production and consumption processes in the soil sample, the release rate J is always a net release rate, which is defined by

$$J = P - U \quad (2)$$

where P and U ($ng\,kg^{-1}\,s^{-1}$) are the rates of trace gas production and consumption, respectively. If $P > U$, the net release rate J is positive, if $U > P$, then J becomes negative. According to Eq. (1) this is equivalent to $m_{cham} > m_{in}$ and $m_{cham} < m_{in}$, respectively. For $U = P$, J equals zero and the corresponding concentration in the chamber's headspace is called the compensation point mixing ratio $m_{NO,comp}$ (because here, the consumption of the trace gas in the soil sample compensates its production).

Since Remde et al. (1989), it has frequently been shown experimentally that there is a strong linear relationship between J_{NO} and the chamber's NO mixing ratio $m_{NO,cham}$:

$$J_{NO}\left(m_{NO,cham}\right) = P_{NO} + k_{NO}\,m_{NO,cham}\,f_{C,NO} \quad (3)$$

where k_{NO} is the so-called NO consumption rate coefficient (in $m^3\,kg^{-1}\,s^{-1}$, which is counted negative). This relation is linear for a wide range of $m_{NO,cham}$, and is schematically shown in Fig. 1. The relation implies, that P_{NO} is independent of $m_{NO,cham}$, while the NO consumption rate (U_{NO}) is dependent on $m_{NO,cham}$ and can be described by a first order decay process, characterized by the consumption rate coefficient k_{NO}. The compensation point mixing ratio, defined by $J_{NO}(m_{NO,cham}) = 0$, is just

BGD
11, 1187–1275, 2014

$m_{NO,comp} = -P_{NO}/(k_{NO} f_{C,NO})$. Considering Eqs. (1) and (3), the determination (and further characterization) of P_{NO} and U_{NO} (k_{NO}) can be basically achieved by measurements of only two related NO mixing ratio sets, namely (m_{NO,in_1}; $m_{NO,cham\_1}$) and (m_{NO,in_2}; $m_{NO,cham\_2}$), where $m_{NO,cham\_2} > m_{NO,cham\_1}$ (and $m_{NO,in\_2} > m_{NO,in\_1}$).

However, the NO net release rate has been observed to be also strongly dependent on the temperature of the soil (T_{soil}), as well as the moisture content θ_g (i.e., dimensionless gravimetric soil moisture, see Sect. S.1) of the soil sample (e.g. Ludwig et al., 2001). Therefore, J_{NO} is defined to be dependent on a total of three variables, namely θ_g, T_{soil}, and $m_{NO,cham}$

$$J_{NO}(\theta_g, T_{soil}, m_{NO,cham}) = P_{NO}(\theta_g, T_{soil}) - U_{NO}(\theta_g, T_{soil}, m_{NO,cham}) \quad (2a)$$

considering Eq. (3), this is equivalent to

$$J_{NO}(\theta_g, T_{soil}, m_{NO,cham}) = P_{NO}(\theta_g, T_{soil}) + k_{NO}(\theta_g, T_{soil})\, m_{NO,cham}\, f_{C,NO} \quad (3a)$$

Since NO production and NO consumption in the soil are enzymatic processes (e.g., Schuster and Conrad; 1992), an exponential dependence on soil temperature can generally be assumed (s. Fig. 2). Hence, for a constant (fixed) gravimetric soil moisture ($\theta_g = \theta_0$), P_{NO} and U_{NO} are described by

$$P_{NO}(\theta_0, T_{soil}) = P_{NO}(\theta_0, T_0) \exp\left(\frac{\ln Q_{10\_P,NO}}{10}(T_{soil} - T_0)\right) = P_{NO}(\theta_0, T_0)\, Q_{10\_P,NO}^{(T_{soil}-T_0)/10} \quad (4)$$

$$U_{NO}(\theta_0, T_{soil}) = U_{NO}(\theta_0, T_0) \exp\left(\frac{\ln Q_{10\_U,NO}}{10}(T_{soil} - T_0)\right) = U_{NO}(\theta_0, T_0)\, Q_{10\_U,NO}^{(T_{soil}-T_0)/10} \quad (5)$$

where T_0 is a certain reference soil temperature (i.e., where $P_{NO}(\theta_0, T_{soil}) = P_{NO}(\theta_0, T_0)$ and $U_{NO}(\theta_0, T_{soil}) = U_{NO}(\theta_0, T_0)$). $Q_{10\_P,NO}$ and $Q_{10\_U,NO}$ are defined by individual ratios of P_{NO} and U_{NO} at two different temperatures which differ by ten degrees (i.e., without

BGD
11, 1187–1275, 2014

loss of generality, T_0 and $T_1 = T_0 + 10$):

$$Q_{10\_P,NO} = \frac{P_{NO}(\theta_0, T_1)}{P_{NO}(\theta_0, T_0)} = \frac{P_{NO}(\theta_0, T_0 + 10)}{P_{NO}(\theta_0, T_0)} \quad (6)$$

$$Q_{10\_U,NO} = \frac{U_{NO}(\theta_0, T_1)}{U_{NO}(\theta_0, T_0)} = \frac{U_{NO}(\theta_0, T_0 + 10)}{U_{NO}(\theta_0, T_0)} \quad (7)$$

From Eqs. (7), (2a) and (3a) it is evident, that $Q_{10\_U,NO} = Q_{10\_k,NO}$. Combining Eqs. (2a), (4) and (5) leads to

$$J_{NO}(\theta_0, T_0, m_{NO,cham}) = P(\theta_0, T_0) Q_{10\_P,NO}^{(T_{soil}-T_0)/10} + k(\theta_0, T_0) Q_{10\_k,NO}^{(T_{soil}-T_0)/10} m_{NO,cham} f_{C,NO} \quad (3b)$$

The relationships between P_{NO} as well as U_{NO} and the soil temperature are log-linear. Consequently, measurements at least at two different soil temperatures are necessary to characterize their temperature dependency. Since the determination of P_{NO} and k_{NO} for any soil temperature needs already at least two measurements at two different NO mixing ratio levels, the determination of $Q_{10\_P,NO}$ and $Q_{10\_k,NO}$ needs finally at least four measurements of related NO mixing ratio data sets, namely (m_{NO,in_1}; $m_{NO,cham\_1}$) and (m_{NO,in_2}; $m_{NO,cham\_2}$) at $T = T_0$ and (m_{NO,in_3}; $m_{NO,cham\_3}$) and (m_{NO,in_4}; $m_{NO,cham\_4}$) at $T_1 = T_0 + 10$.

During the last two decades, it has repeatedly been shown that J_{NO} follows the soil moisture θ_g in form of an optimum curve (Yang and Meixner, 1997; Otter et al., 1999; Kirkman et al., 2001; van Djik and Meixner, 2001; van Dijk et al., 2002; Garrido et al., 2002; Meixner and Yang, 2006; Yu et al., 2008, 2010; Feig et al., 2008a, b; Ashuri, 2009; Feig, 2009; Laville et al., 2009; Gelfand et al., 2009; Bargsten et al., 2010). This is schematically shown in Fig. 3.

As mentioned above, the optimum curve relationship between J_{NO} and θ_g is in accordance with the general behavior of soil microbial activity in aerobic soils (Skopp et al., 1990). Hence, it is supposed, that both processes, NO production as well as NO consumption follow jointly the optimum curve with θ_g. Consequently, their optimum

BGD
11, 1187–1275, 2014

(maximum) values, namely $P_{NO,opt}$ and $U_{NO,opt}$ (consequently also $k_{NO,opt}$), occur at the same optimum gravimetric soil moisture $\theta_{g,\,opt}$, which henceforth is denoted as θ_0. The form of the optimum curve can be generally described by the product of a (increasing) power function and a (decreasing) exponential function (e.g. Bronstein and Semendajew, 1972). For $T_{soil} = T_0$ and $m_{in\_1} = 0$, the corresponding NO net release' optimum curve $J_{NO}(\theta_g, T_0)$ can be described as follows (c.f., Meixner and Yang, 2008):

$$J_{NO}(\theta_g, T_0) = J(\theta_0, T_0) \left(\frac{\theta_g}{\theta_0}\right)^a \exp\left[-a\left(\frac{\theta_g}{\theta_0} - 1\right)\right] \tag{8}$$

where $J_{NO}(\theta_g, T_0)$ is determined via Eq. (1) from a preset m_{in_1} (preferably $m_{in\_1} = 0$; without loss of generality) and the chamber's NO mixing ratio measured at $\theta_g = \theta_0$ (henceforth denoted as $m_{NO,cham\_1,0}$). The optimum curve's shape-coefficient a is then given by

$$a = \ln\frac{J_{NO}(\theta_0, T_0)}{J_{NO}(\theta_{g,1}, T_0)} \left[\ln\frac{\theta_0}{\theta_{g,1}} + \frac{\theta_{g,1}}{\theta_0} - 1\right]^{-1} \tag{8a}$$

The value of $\theta_{g,1}$ can be arbitrarily be chosen, e.g. such that

$$\frac{J_{NO}(\theta_0, T_0)}{J_{NO}(\theta_{g,1}, T_0)} = R_J \tag{8b}$$

hence, Eq. (8a) will read as

$$a = \frac{\ln R_J}{\ln\frac{\theta_0}{\theta_{g,1}} + \frac{\theta_{g,1}}{\theta_0} - 1} \tag{8c}$$

It is compulsory from Eq. (8)–(8c), that only two data pairs are necessary to define the shape of the optimum curve, namely (i) the optimum (maximum) value of the NO

BGD
11, 1187–1275, 2014

net release rate and the related (optimum) gravimetric soil moisture (i.e. $J_{NO}(\theta_0, T_0)$ and θ_0), and (ii) the value of that gravimetric soil moisture where the NO net release is $1/R_J$ of the maximum value of the NO net release rate (i.e. $\theta_{g,1}$ at $J_{NO}(\theta_{g,1}, T_0) = J_{NO}(\theta_0, T_0)/R_J$). For practical reasons $\theta_{g,1}$ should be selected such, that $\theta_{g,1} > \theta_0$.

Fortunately, $T_{soil} = T_0$ and $m_{in\_1} = 0$ can easily be obtained: (i) the soil temperature can be kept constant by enclosing the dynamic chamber in a thermostat, and (ii) $m_{in\_1} = 0$ is achieved by purging the dynamic chamber with NO-free, so-called "zero" air (see Sect. 3.2.1). The necessary variation of the gravimetric soil moisture over its full range is realized by (i) wetting the soil sample (e.g. to its field capacity, see Sect. 3.1) at the start of the experiment, and (ii) purging the dynamic chamber continuously by air (of any NO mixing ratio) with a dew point (much) less than T_{soil}. The enforced evaporation of water vapor from the soil sample results in a continuous drying out of the soil sample and consequently provides the desired variation of the gravimetric soil moisture over its full range.

This drying out experiment delivers the necessary data to calculate the optimum curve's shape coefficient a (i.e. θ_0 and $\theta_{g,1}$; c.f. Eq. 8c). Then the gravimetric soil moisture's shape-function $g(\theta_g)$ is defined as

$$g(\theta_g) = \left(\frac{\theta_g}{\theta_0}\right)^a \exp\left[-a\left(\frac{\theta_g}{\theta_0} - 1\right)\right] \tag{9}$$

Note, that $g(\theta_g) = 1$ for $\theta_g = \theta_0$. Considering Eq. (8), the dependency of $J_{NO}(\theta_g, T_{soil}, m_{NO,cham})$, $P_{NO}(\theta_g, T_{soil})$, and $U_{NO}(\theta_g, T_{soil}, m_{NO,cham})$ from gravimetric soil moisture becomes,

$$J_{NO}(\theta_g, T_{soil}, m_{NO,cham}) = J_{NO}(\theta_0, T_{soil}, m_{NO,cham})\, g(\theta_g) \tag{10a}$$

$$P_{NO}(\theta_g, T_{soil}) = P_{NO}(\theta_0, T_{soil})\, g(\theta_g) \tag{10b}$$

$$\begin{aligned} U_{NO}(\theta_g, T_{soil}, m_{NO,cham}) &= U_{NO}(\theta_0, T_{soil}, m_{NO,cham})\, g(\theta_g) \\ &= k_{NO}(\theta_0, T_{soil})\, m_{NO,cham}\, f_{C,NO}\, g(\theta_g) \end{aligned} \tag{10c}$$

BGD
11, 1187–1275, 2014

because NO production and NO consumption (consequently also the NO net release) share the same shape of the soil moisture's optimum curve. Combining Eqs. (3a), (3b), and (10a–c) leads to the desired general formulation of the NO net release rate (Eq. 2a) as function of θ_g, T_{soil}, and $m_{NO,cham}$

$$J_{NO}(\theta_g, T_{soil}, c_{NO,cham}) = \left[P(\theta_0, T_0) Q_{10\_P,NO}^{(T_{soil}-T_0)/10} + k(\theta_0, T_0) Q_{10\_k,NO}^{(T_{soil}-T_0)/10} m_{NO,cham} f_{C,NO}\right] g(\theta_g) \quad (11)$$

There are six parameters in Eq. (11) which have to be determined by suitable experiments: θ_0 and a (defining $g(\theta_g)$), as well as $P_{NO}(\theta_0, T_0)$, $k_{NO}(\theta_0, T_0)$, $Q_{10\_P,NO}$ and $Q_{10\_k,NO}$. Given, that T_{soil} and θ_g are known (by direct or indirect measurements, see Sect. 3.4), the quantities which have to be measured during a dynamic chamber experiment are only the NO mixing ratios at the inlet and within the chamber. As already mentioned above, at least four different experiments are necessary over the full range of gravimetric soil moisture θ_g:

exp. 1 : at $T_{soil} = T_0$ and $m_{NO,in} = m_{NO,in\_1}$
exp. 2 : at $T_{soil} = T_0$ and $m_{NO,in} = m_{NO,in\_2}$
exp. 3 : at $T_{soil} = T_1$ and $m_{NO,in} = m_{NO,in\_3}$
exp. 4 : at $T_{soil} = T_1$ and $m_{NO,in} = m_{NO,in\_4}$

At first, experiment (1) delivers the necessary data (θ_0, $\theta_{g,1}$) for the determination of the optimum curve's shape function $g(\theta_g)$. Assuming, that the respective optimum (maximal/minimal) values of J_{NO} in all four experiments will be observed at the same optimum gravimetric soil moisture θ_0 (which could be proofed for each drying-out experiment), the four experiments will provide four data pairs at optimum gravimetric soil moisture, the respective NO mixing ratio within the chamber and the corresponding NO release rate (which is determined by the respective difference of NO mixing ratio within

BGD
11, 1187–1275, 2014

and at the inlet of the chamber; c.f. Eq. 1):

$$\begin{aligned}
&\text{exp. 1}: m_{\mathrm{NO,cham_1,0}} \text{ and } J_{\mathrm{NO}}(\theta_0, T_0, m_{\mathrm{NO,cham_1,0}}) \\
&\quad = Q/m_{\mathrm{soil}}(m_{\mathrm{NO,cham_1,0}} - m_{\mathrm{NO,in_1}})f_{\mathrm{C,NO}} \\
&\text{exp. 2}: m_{\mathrm{NO,cham_2,0}} \text{ and } J_{\mathrm{NO}}(\theta_0, T_0, m_{\mathrm{NO,cham_2,0}}) \\
&\quad = Q/m_{\mathrm{soil}}(m_{\mathrm{NO,cham_2,0}} - m_{\mathrm{NO,in_2}})f_{\mathrm{C,NO}} \\
&\text{exp. 3}: m_{\mathrm{NO,cham_3,0}} \text{ and } J_{\mathrm{NO}}(\theta_0, T_1, m_{\mathrm{NO,cham_3,0}}) \\
&\quad = Q/m_{\mathrm{soil}}(m_{\mathrm{NO,cham_3,0}} - m_{\mathrm{NO,in_3}})f_{\mathrm{C,NO}} \\
&\text{exp. 4}: m_{\mathrm{NO,cham_4,0}} \text{ and } J_{\mathrm{NO}}(\theta_0, T_1, m_{\mathrm{NO,cham_4,0}}) \\
&\quad = Q/m_{\mathrm{soil}}(m_{\mathrm{NO,cham_4,0}} - m_{\mathrm{NO,in_4}})f_{\mathrm{C,NO}}
\end{aligned}$$

For experiments (1) and (2), T_{soil} equals T_0, consequently the exponents of $Q_{10\_\mathrm{P,NO}}$ and $Q_{10\_\mathrm{k,NO}}$ in Eq. (3b) become zero. Then, the reference NO consumption coefficient $k_{\mathrm{NO}}(\theta_0, T_0)$, the slope of the linear relation between J_{NO} and $m_{\mathrm{NO,cham}}$, is determined by

$$k_{\mathrm{NO}}(\theta_0, T_0) = \frac{J_{\mathrm{NO}}\left(\theta_0, T_0, m_{\mathrm{NO,cham\_2,0}}\right) - J_{\mathrm{NO}}\left(\theta_0, T_0, m_{\mathrm{NO,cham\_1,0}}\right)}{\left(m_{\mathrm{NO,cham\_2,0}} - m_{\mathrm{NO,cham\_1,0}}\right) f_{\mathrm{C,NO}}} \tag{12a}$$

which is equivalent to

$$k_{\mathrm{NO}}(\theta_0, T_0) = \frac{Q}{m_{\mathrm{soil}}} \frac{(m_{\mathrm{NO,cham\_2,0}} - m_{\mathrm{NO,in\_2}}) - (m_{\mathrm{NO,cham\_1,0}} - m_{\mathrm{NO,in\_1}})}{m_{\mathrm{NO,cham\_2,0}} - m_{\mathrm{NO,cham\_1,0}}} \tag{12b}$$

Hence, it follows for $P_{\mathrm{NO}}(\theta_0, T_0)$,

$$P_{\mathrm{NO}}(\theta_0, T_0) = J_{\mathrm{NO}}(\theta_0, T_0, m_{\mathrm{NO,cham\_1,0}}) - k_{\mathrm{NO}}(\theta_0, T_0)\, m_{\mathrm{NO,cham\_1,0}}\, f_{\mathrm{C,NO}} \tag{13a}$$

which is equivalent to

$$P_{\mathrm{NO}}(\theta_0, T_0) = \frac{Q f_{\mathrm{C,NO}}}{m_{\mathrm{soil}}} (m_{\mathrm{NO,cham\_1,0}} - m_{\mathrm{NO,in\_1}}) - k_{\mathrm{NO}}(\theta_0, T_0)\, m_{\mathrm{NO,cham\_1,0}}\, f_{\mathrm{C,NO}} \tag{13b}$$

BGD
11, 1187–1275, 2014

Analogously from experiments (3) and (4):

$$k_{NO}(\theta_0,T_1) = \frac{Q}{m_{soil}} \frac{\left(m_{NO,cham\_4,0} - m_{NO,in\_4}\right) - \left(m_{NO,cham\_3,0} - m_{NO,in\_3}\right)}{m_{NO,cham\_4,0} - m_{NO,cham\_3,0}} \quad (14b)$$

$$P_{NO}(\theta_0,T_1) = \frac{Q f_{C,NO}}{m_{soil}} \left(m_{NO,cham\_3,0} - m_{NO,in\_3}\right) - k_{NO}(\theta_0,T_0)\, m_{NO,cham\_3,0}\, f_{C,NO} \quad (15b)$$

The remaining parameters in Eq. (11) are $Q_{10\_P,NO}$ and $Q_{10\_k,NO}$, which are defined by the ratio of $P_{NO}(\theta_0,T_1)/P_{NO}(\theta_0,T_0)$ and $k_{NO}(\theta_0,T_1)/k_{NO}(\theta_0,T_1)$, respectively (note: $T_1 = T_0 + 10$). Combining Eqs. (12b) and (14b), as well as Eqs. (13b) and (15b), after some mathematical re-arrangements, it follows:

$$Q_{10\_k,NO} = \frac{m_{NO,cham\_4,0} - m_{NO,in\_4} - m_{NO,cham\_3,0} + m_{NO,in\_3}}{m_{NO,cham\_2,0} - m_{NO,in\_2} - m_{NO,cham\_1,0} + m_{NO,in\_1}} \cdot \frac{m_{NO,cham\_2,0} - m_{NO,cham\_1,0}}{m_{NO,cham\_4,0} - m_{NO,cham\_3,0}} \quad (16)$$

$$Q_{10\_P,NO} = \frac{m_{NO,cham\_3,0}\left(1 - \frac{m_{soil}}{Q} k(\theta_0,T_1)\right) - m_{NO,in\_3}}{m_{NO,cham\_1,0}\left(1 - \frac{m_{soil}}{Q} k(\theta_0,T_0)\right) - m_{NO,in\_1}} \quad (17)$$

Using Eqs. (12b), (13b), (16) and (17), the six unknown parameters (θ_0, a, $P_{NO}(\theta_0,T_0)$, $k_{NO}(\theta_0,T_0)$, $Q_{10\_P,NO}$, $Q_{10\_k,NO}$) of the general formulation of the NO net release rate (Eq. 11) can be determined from direct and immediate measurements of NO mixing ratios only.

The expected variations of the NO net release rate which should be observed under different conditions of gravimetric soil moisture, soil temperature, and the chamber's headspace NO mixing ratio, are schematically shown in Fig. 4. Moreover, this figure summarizes the methodical concept of the applied dynamic chamber approach.

BGD
11, 1187–1275, 2014

It is worthwhile to note, that the compensation point mixing ratio, defined by $m_{NO,comp} = -P_{NO}/(k_{NO} f_{C,NO})$, is not a function of θ_g, as long as NO production and NO consumption respond identically to variations of gravimetric soil moisture. Furthermore, if $Q_{10\_P,NO} = Q_{10\_k,NO}$ $(:= Q_{10\_NO})$, the temperature dependence of both processes as well as of J_{NO} can be described by

$$h(T_{soil}) = J(\theta_0, T_0)\, Q_{10\_NO}^{(T_{soil}-T_0)/10} \tag{18}$$

Consequently, the general formulation of NO net release, NO production and NO consumption rates as function of θ_g, T_{soil}, and $m_{NO,cham}$ would be reduced to

$$P_{NO}(\theta_g, T_{soil}) = P_{NO}(\theta_0, T_0)\, g(\theta_g)\, h(T_{soil}) \tag{19a}$$

$$\begin{aligned} U_{NO}(\theta_g, T_{soil}, m_{NO,cham}) &= U_{NO}(\theta_0, T_0, m_{NO,cham})\, g(\theta_g)\, h(T_{soil}) \\ &= k_{NO}(\theta_0, T_0)\, m_{NO,cham}\, f_{C,NO}\, g(\theta_g)\, h(T_{soil}) \end{aligned} \tag{19b}$$

$$J_{NO}(\theta_g, T_{soil}, m_{NO,cham}) = [P(\theta_0, T_0) + k(\theta_0, T_0)\, m_{NO,cham} f_{C,NO}]\, g(\theta_g)\, h(T_{soil}) \tag{19c}$$

Consequently, the compensation point mixing ratio $m_{NO,comp}$ would then be neither a function of gravimetric soil moisture, nor of soil temperature: $m_{NO,comp}$ would get the significance of a "fixed" microbiological soil parameter.

2.2 Experimental reality – need and challenges of an improved laboratory method

Since more than two decades (from Remde et al., 1989 until Bargsten et al., 2010), all kind of experiments to determine the net NO release rate from soils have been performed on individual sub-samples out of the respective bulk soil sample from a given ecosystem. Generally, the bulk soil samples have been (i) passed through a screen (usually 2 mm; 16 mm for forest soils of high organic content, c.f. Bargsten et al., 2010) to remove large pieces of rock, roots, and litter, (ii) mechanically homogenized, and (iii) pre-incubated at pre-scribed soil moisture contents before the

BGD
11, 1187–1275, 2014

actual (drying out) experiment started. However, these pre-scribed soil moisture contents, soil temperatures, and the duration of the pre-incubation period varied significantly. In any case, the above mentioned requisite four experiments (exp. 1 to exp. 4) have been performed on four individual sub-samples of the original bulk soil sample. While van Dijk and Meixner (2001) observed good agreement between the measured net NO release rates of soil sub-samples, Gelfand et al. (2009), and Bargsten et al. (2010) found under certain circumstances great differences between θ_0 and $\theta_{g,1}$, as well as between $J_{NO}(\theta_0,T_0)$ and $J_{NO}(\theta_0,T_1)$ of individual sub-samples. These differences became substantial as (i) the organic content of the soil increased (e.g. forest soils), or (ii) the NO consumption rate decreased (particularly in arid and hyper-arid soils). Corresponding examples are presented in Figs. 5 and 6. Replicate measurements of $J_{NO}(\theta_g, T_0 = 25\,^{\circ}C)$ at $m_{NO,in\_1} \approx 0$ ppb of two mechanically homogenized rain forest soil sub-samples from Suriname show substantial difference of θ_0 (0.56 vs. 0.69) and $\theta_{g,1}$ (0.83 vs. 1.21; $R_J = 10$), while the difference of $J_{NO}(\theta_0,T_0)$ from the two experiments is small. For the results shown in Fig. 6, twelve individual experiments have been performed for a desert soil from Mongolia, three replicates each for the four conditions of "exp. 1"–"exp. 4". The differences with respect to θ_0 and $\theta_{g,1}$ might be acceptable; however, differences between net NO release rates measured under conditions of "exp. 1"–"exp. 4" contradict the methodical concept described above. Exponential increase of enzymatic activity with soil temperature necessitates, that $J_{NO}(\theta_g,T_1,m_{NO,in\_2}) > J_{NO}(\theta_g,T_0,m_{NO,in\_1})$ and $J_{NO}(\theta_g,T_1,m_{NO,in\_4}) > J_{NO}(\theta_g,T_0,m_{NO,in\_3})$; linear increase of soil consumption with head space NO mixing ratio requires, that $J_{NO}(\theta_g,T_0,m_{NO,cham\_1}) > J_{NO}(\theta_g,T_0,m_{NO,cham\_2})$ and $J_{NO}(\theta_g,T_1,m_{NO,cham\_3}) > J_{NO}(\theta_g,T_1,m_{NO,cham\_4})$ (c.f. Fig. 4). In Fig. 6, there are a dozen data points which contradict the first paradigm; however, particularly for $\theta_g < 0.03$, fumigation with high NO mixing ratios (144 and 134 ppb) result in considerably higher net NO release rates than for those obtained under "zero"-air fumigation: an obvious contradiction to the second paradigm.

BGD
11, 1187–1275, 2014

It has been suspected, that (i) non-standardized pre-incubation procedures (s. Gödde and Conrad, 1999), and (ii) variability of nutrients and microbial composition in the soil sub-samples (still existing even after mechanical homogenization) might be the most important reasons for contradicting results as shown in Figs. 5 and 6. To tackle these hypotheses, two decisions have been made for this study: (i) to omit any pre-incubation of soil samples (but applying a simple standardized procedure for initial wetting of the soil samples), and (ii) to re-design and improve the existing laboratory dynamic chamber system in that way, that "exp. 1"–"exp. 4" could be performed during one individual drying-out experiment on one soil sample only. Particularly the latter posed two major technical challenges, namely (i) the control of the soil temperature (via the temperature controlled cabinet) must allow the frequent (and fast) change at least between two temperatures differing by 10 K (T_0 and T_1) during an individual drying-out experiment, and (ii) the repeated and fast change of the incoming NO mixing ratio between "zero"-air (m_{NO,in_1}, m_{NO,in_3}) and a pre-scribed high level (m_{NO,in_2}, m_{NO,in_4}) also during the individual drying-out experiment. Temporal changes and equilibration of both, T_{soil} and $m_{NO,in}$ must be so fast, that during one drying-out experiment for each of the conditions of "exp. 1"–"exp. 4" (formerly individually applied to four individual soil sub-samples) a sufficient number of data points would be available to establish experimentally reliable relations between the corresponding net NO release rate and the three variables θ_g, T_{soil} and $m_{NO,cham}$. Besides these technical aspects it had to be tested, whether these repeated changes of environmental conditions would stress the microbial community.

Two additional technical facilities were implemented during the re-design of the laboratory dynamic chamber system, (i) humidification of the incoming air, and (ii) the temporal "switch" of the laboratory chamber system from the state of a dynamic chamber into a static chamber. The first facility accounts for the need to slow down the drying-out of the enclosed soil sample in order to get a temporally higher resolution of data points under "quasi-constant" θ_g-conditions, particularly for arid and hyper-arid soils where θ_0 usually occurs below 0.1. The second facility allows quantification of the

BGD
11, 1187–1275, 2014

emission of carbon dioxide (CO_2) which is usually used as proxy for microbial activity in the soil. There is wide evidence, that the release of gaseous N is strongly coupled to the release of gaseous C (Stark et al., 2002; Dunfield and Knowles, 1998; Gödde and Conrad, 2000). However, small amounts of CO_2 release from less than 0.1 kg soil sample and the limited precision of CO_2 analyzers do not allow application of the dynamic chamber technique.

3 Material and methods

3.1 Soil sampling and preparation of soil samples

The soil samples analysed in this study cover a large range of soil properties to demonstrate the improvement of the analysis of NO production, NO consumption, the NO compensation mixing ratio, and the release rate of CO_2 by the new laboratory system. The capability of the system to study release rates of other trace gases (volatile organic compounds, VOC) in parallel is also demonstrated as this provides a valuable new tool for understanding the processes underlying NO emission. Consequently, the selection of soil samples to be used for this study was guided by most contrasting soil properties (s. Table 1). For instance, soil pH of the samples ranges from 3.2 (mid-latitude spruce forest soil, "EGER blueberry") to 8.3 (arid oasis cornfield soil, "KUCHE corn"), ammonium and nitrate contents of the hyper-arid ("MONGOLIA desert"), arid cornfield and arid wheatfield soils are characterized by very low soil NH_4^+ concentrations (0.64, 2.16, and 2.27 $mg\,kg^{-1}$ (in terms of N) and high soil NO_3^- concentrations (68.80, 105.62, and 54.32 $mg\,kg^{-1}$ (in terms of N)), respectively.

Mechanical homogenisation by sieving was only applied to field-fresh soil samples, since drying inevitably alters the microbial community significantly (Thomson et al., 2010). To minimize these effects on the net NO release rate, fresh soil was passed through 2 mm and 16 mm mesh sieves for mineral (Feig et al., 2008a) and organic soils (Bargsten et al., 2010), respectively. In the field, soil was sampled from

BGD
11, 1187–1275, 2014

0–0.05 m and mid latitude samples were measured immediately, while dryland soils were stored in the dark at 4 °C at very low field moisture content ($< 0.02\theta_g$) until analysis. Storage for up to 3 months at 4 °C is not supposed to lead to microbial alterations (Stotzky et al., 1962).

Mechanically homogenized soil samples of 0.06 kg each were placed into six plexiglas chambers (inner diameter: 0.092 m; height: 0.136 m) and wetted up to field water holding capacity (1.8 pF). This procedure has been chosen, since the gravitational water in the wide macropores will drain a short time after rainfall (up to 2–3 days) and only the water in the smaller macropores, medium pores, and micropores will be available. Therefore, water holding capacity is used within this study as a maximum wetting value. Furthermore, water holding capacity can easily be measured by the so-called filter method (Whatman-filter paper No. 42). As performed in earlier studies (Remde et al., 1989, 1993), we preferred to omit any pre-incubation of the soil samples to come as close as possible to natural field conditions. Therefore, net NO release rates in the dynamic chamber system were always measured immediately after the adjustment to field capacity until the soil was completely dried out. Nevertheless, since six chambers are prepared for one experiment, 30 min were necessary for equilibration of soil temperature, headspace humidity and NO mixing ratio.

3.2 Laboratory chamber system: set-up

The new laboratory chamber system is shown in Fig. 7. The system consists of four units: “gas dilution”, “thermostat valve”, “thermostat cabinet”, and “analyzers”, which are briefly described below (for detailed description, see Supplement Sect. S.1). For clarity only two soil chambers are shown in Fig. 7, one reference cell and one soil sample, although there are six chambers in all.

BGD
11, 1187–1275, 2014

3.2.1 The "gas dilution" unit

Pressurized air is passed through a so-called "Purified Air Generator" (PAG 003, Ecophysics, Switzerland) to filter out particles (< 7µm), water vapour (−30 °C dew point), NO_x, SO_2, ozone (< 10 ppt), as well as hydrocarbons and CO (< 3 ppb). Different (pre-set) NO mixing ratios for flushing the soil chambers are generated by diluting known amounts of NO from a standard gas cylinder (200 ppm, Air Liquide, Germany) through the mass flow controller ("NO MFC", 0–10 $cm^3 min^{-1}$; Bronckhorst, Germany) into the "zero"-air stream. During the entire drying-out experiment, the dilution of NO must be continuously maintained to guarantee stable NO mixing ratios of the flushing air-stream. For that a valve is placed after "NO MFC", to waste the continuous flow of NO to the exhaust in the "analyzer unit", in case "zero"-air flushing of the chambers is applied. There are approx. 3 m of PTFE-tubing (6.35 mm o.d.) between the NO valve and the downstream MFCs to allow for complete mixing of "zero"-air and NO from the standard cylinder. At this point, the flushing air-stream is divided into 4 sub-streams: two "dry" gas streams controlled by "MFC Meas Dry" and by "MFC Flush Dry", as well as two "wet" gas streams controlled by "MFC Meas Wet" and "MFC Flush Wet" (all 4 MFCs: 0–2.5 $L min^{-1}$ or 4.16667×10^{-5} $m^3 s^{-1}$; Bronckhorst, Germany).

3.2.2 "Thermostat valve" unit

Within the "Thermostat valve unit", the air downstream of "MFC Meas Wet" and "MFC Flush Wet" are directed into two humidifiers. Downstream of these devices, "dry" and "wet" streams are mixed together to the "Meas gas" stream and the "Flush gas" stream, respectively. By proper pre-set of "MFC Meas Wet" and "MFC Flush Wet", the water vapour content of both, the "Meas gas" and the "Flush gas" stream can be controlled from 0 to 95 % relative humidity (see appendix I). The "Meas flow" of 2.5 $L min^{-1}$ is led through that soil chamber (via the "Pre valve"), whose headspace mixing ratio is actually measured. The "Flush flow" of 2.5 $L min^{-1}$ is again split up by flow controllers (Omega®, USA) to flush the remaining five chambers (with 0.5 $L min^{-1}$; the reference

BGD
11, 1187–1275, 2014

chamber, containing soil sample was not flushed). To avoid condensation effects, the temperature of the "Thermostat valve unit" is continuously maintained at 40 °C.

3.2.3 The "thermostat cabinet" unit

The pre- and past-valve are switched in such a way that the "Meas flow" is passing through the different chambers and subsequently detected by the NO, PTR-TOF-MS, and H_2O/CO_2 analyzer. In the dynamic chamber mode, which is used for the measurement of net release rates, the chosen combination of chamber volume (9.1405×10^{-4} m^3) and flushing rate (4.16667×10^{-5} m^3 s^{-1}) leads to a very short residence time of the air within the chamber (22 s). Given an incoming CO_2 mixing ratio of $m_{CO_2,in\_1} \approx 350$ ppm, this residence time has been repeatedly observed to be not long enough that the CO_2 respiration (from 0.06 kg of soil) may cause a headspace CO_2 mixing ratio ($m_{CO_2,cham\_1}$) which can be measured as significantly different from the incoming CO_2 mixing ratio (on the basis of common CO_2 analyzers' precision, approx. 0.5 ppm). Consequently, the "static mode" facility has been implemented in the new design of our laboratory chamber system in order to measure the release rate of CO_2 (and potential other trace gases of low soil emission and/or insufficient analyzer's precision). In this mode, that chamber, which is actually being probed, is "closed", i.e. the headspace air is cycled (and analyzed for its increasing CO_2 mixing ratio) for 3.5 min from the chamber's headspace, via corresponding tubing into the measurement cell of the CO_2 analyzer (s. below) and back. In order to change the system from the dynamic into static mode, first the "NO" and "NOtoTherm" valves are switched to allow the "Meas flow" to pass the NO-analyzer and change the incoming mixing ratio of NO. After the incoming mixing ratio of NO is stable (usually 3.5 min), the "LIC_out", "NOCO$_2$", and "overflow" valves for the corresponding box (1–6), are switched to allow the "Flush flow" to pass the CO_2 analyzer. The chamber system stays only in the static mode, after the incoming NO mixing ratio has just been switched from "zero"-air (m_{NO,in_1} or m_{NO,in_3}) to the high mixing ratio level (m_{NO,in_2} or m_{NO,in_4}) and vice versa: after the stabilization time, the mixing ratio of CO_2 of the six soil chambers is measured for 4 min in the static

BGD
11, 1187–1275, 2014

mode, while the NO mixing ratio of the reference chamber is monitored (for details, see Sect. S.1). When the NO mixing ratio of the "Meas flow" is stabilized, the measurement of the temporal increase of CO_2 mixing ratio in the soil chambers is completed; the "$NOCO_2$" and "NOtoTherm" valves are switched again to operate the system back to the dynamic mode.

3.2.4 The "analyzer" unit

The analyzers for the measurement of NO, CO_2, H_2O, and VOC mixing ratios in the incoming and chamber headspace air are as follows: (i) chemiluminescence (gas-phase) NO_x analyzer (Model 42i-TL, Thermo Fisher Scientific Inc., USA), (ii) CO_2/H_2O non dispersive infrared (NDIR) analyzer (Model LI-COR 840A, LI-COR Biosciences Inc., USA), and (iii) Proton Transfer Time of Flight Mass Spectrometer (PTR-TOF-MS 8000, IONICON, Austria).

For the NO_x-analyser, dry oxygen (99.999 %) is used to photolytically generate ozone that reacts in the instrument's reaction cell (at approx. 30 hPa) with the NO of the sample air to form electronically excited NO_2 molecules. The decay to the ground state is accompanied by photon emission (chemiluminescence proportional to NO mixing ratio) which is subsequently detected by a photomultiplier. The NO_x analyzer is regularly calibrated using a commercial gas-dilution device (146C Dynamic Gas Calibrator, Thermo Fisher Scientific Inc., USA) where known amounts of NO from a pressurized standard cylinder (5 ppm; Air Liquide, Germany) are diluted into NO free "zero"-air. From these calibrations the limit of detection (LOD) and the precision (from LOD to 500 ppb) of the analyzer have been determined (s. Sect. 4).

In the dual channel NDIR-CO_2/H_2O analyser sample air flows through a measurement cell consisting of an optical bench with an infrared source, CO_2 filters (3.95×10^{-6} m reference and 4.26×10^{-6} m sample), H_2O filters (2.35×10^{-6} m reference and 2.59×10^{-6} m sample), and detector. The mixing ratios of CO_2 and H_2O are inferred from the difference in infrared absorption between the sample gas and the

BGD
11, 1187–1275, 2014

reference measurement (free of CO_2 and H_2O). For the calibration of the CO_2/H_2O analyzer three gaseous CO_2 standards were used (356.9, 457.3, and 551 ppm; Air Liquide, Germany). For these calibration mixing ratios, corresponding relative precision ($\sigma_{m,CO_2}/m_{CO_2}$) of the analyzer has been determined to 3.15, 1.68, and 1.54×10^{-3}, respectively.

Measurements of volatile organic compounds (VOC) were performed using a commercial PTR-TOF-MS instrument (Ionicon Analytik GmbH, Innsbruck, Austria, s. Grauss et al., 2010). The detection principle relies on the protonation of ambient VOCs by H_3O^+-ions (which are generated in a hollow cathode discharge) that are subsequently detected by mass spectrometry. Such systems can typically measure protonated VOCs with at a detection limit of about 10–100 ppt (Lindinger et al., 1998). The PTR-TOF-MS offers a mass resolution of approx. 3700 m/Δm. Mass spectra were collected ranging from m/z = 10 to 500. The instrument was operated with a drift voltage of 600 V and a drift pressure of 2.20 mbar (E/N 140 Td). Internal mass calibration of the PTR-TOF-MS was performed by permeating 1,3,5- trichlorobenzene into a 1 mm section of 1.58 mm o.d. Teflon tubing used in the inlet flow system controlled to 60 °C. Post-acquisition data analysis was performed according to procedures described elsewhere (Mueller et al., 2013, 2011, 2010; Titzmann et al., 2010). Standards for acetone and acetaldehyde were available from commercial pressurized standard gas cylinders (Apel–Riemer Environmental). The dynamic chamber system provides a "Meas flow" of 2.5 L min^{-1}, where the NOx analyzer receives about 1.3 L min^{-1}, the CO_2/H_2O analyser about 0.5 L min^{-1}, and the PTR-TOF-MS about 0.1 L min^{-1}; the rest is wasted to the exhaust. The limit of detection (LOD) for the PTR-TOF-MS for C_2H_4O and C_3H_6O was determined as 1σ noise (during calibration by standard gas) as 0.081 ppb and 0.024 ppb, respectively.

Since the signal of the NO_x analyzer (s. below) is somewhat sensitive to changing water vapour concentrations (originating from evaporation of the enclosed soil sample), a certain amount of the purified and dry air stream (see "gas dilution unit") was used to continuously flush the outer tube of the 3.6 m Nafion® inverted gas dryer (Model Perma

BGD
11, 1187–1275, 2014

Pure MD™-110, Perma Pure LLC, USA). To avoid gas diffusion from the NO standard gas cylinder (200 ppm, Air Liquide, Germany) into the dryer, approximately 3 m of PTF tubing (6.35 mm o.d.) separates the T-connector and the NO mass flow controller "NO MFC". In order to avoid pressure pulses within the complex valve switching framework of the our laboratory chamber system, the "Depress" valve has been integrated, which is opened before and closed after each operation of any switching valves.

3.3 Determination of the gravimetric soil moisture

Suitable sensors for direct measurement of the gravimetric soil moisture content of the small (0.06 kg) enclosed soil sample are currently not available. Therefore, high precision determination of the actual gravimetric soil moisture content is indirectly achieved by considering the mass balance of H_2O vapor of the dynamic chamber. A detailed description is given in Sect. S.2. During the entire drying-out experiment, H_2O vapor in the incoming flushing air-stream, $s_{H_2O,in}(t)$, and in the well mixed headspace of the laboratory dynamic chamber, $s_{H_2O,cham}(t)$, is measured by the CO_2/H_2O NDIR analyzer. In case of flushing the chambers with dry air, the presence of H_2O vapor in the chamber's headspace is exclusively due to evaporation from the (initially wetted) soil sample, which in turn diminishes the (gravimetric) soil moisture content of the soil sample (in case of flushing the chambers with humidified air, the decrease of H_2O vapor is exclusively due to absorption in the (initially dry) soil sample). For the sake of convenience, data of H_2O vapor are considered only in terms of the measured signal $s_{H_2O,cham}$ (in arbitrary units), where the relation between $s_{H_2O,cham}$ and the H_2O vapor concentration is given by $c_{H_2O,cham}(t) = g\, s_{H_2O,cham}(t)$. The proportionality constant g is "calibrated" by the temporally integrated H_2O vapor signal which is directly related to the amount of evaporated soil water; the latter is simply determined by weighing the soil sample

BGD
11, 1187–1275, 2014

before and after the experiment. Hence, the proportionality constant g is given by:

$$g = \frac{m_{\mathrm{soil}}(t_S) - m_{\mathrm{soil}}(t_0)}{V\left[s_{\mathrm{H_2O,cham}}(t_S) - s_{\mathrm{H_2O,cham}}(t_0)\right] + S_0} \tag{S6}$$

where V is the volume of the chamber (m^3), $m_{\mathrm{soil}}(t_0)$ and $m_{\mathrm{soil}}(t_S)$, given in kg, is the total mass of the soil sample at the begin ($t = t_0$) and the end ($t = t_S$) of the drying-out experiment, $s_{\mathrm{H_2O,cham}}(t_0)$, and $s_{\mathrm{H_2O,cham}}(t_S)$ are the corresponding H_2O signals (arbitrary units), and S_0 is an integration constant (Eq. (S3.4), see Sect. S.1). At any time t_i during the drying-out experiment the total mass of the enclosed soil sample $m_{\mathrm{soil}}(t_i)$ is then given by

$$m_{\mathrm{soil}}(t_i) = m_{\mathrm{soil}}(t_{i-1}) + Vg\left[s_{\mathrm{H_2O,cham}}(t_i) - s_{\mathrm{H_2O,cham}}(t_{i-1})\right] + S_i \tag{S7.2}$$

where

$$S_i = (T_i + T_{i-1})\left[s_{\mathrm{H_2O,cham}}(t_{i-1}) - s_{\mathrm{H_2O,in}}(t_{i-1})\right]; \quad T_i = \frac{t_i - t_{i-1}}{2}; T_0 = T_{S+1} = 0 \tag{S7.3}$$

the dimensionless gravimetric soil moisture is defined by $\theta_g = (m_{\mathrm{soil,\,wet}} - m_{\mathrm{soil,\,dry}})/m_{\mathrm{soil,\,dry}}$. Hence, during the entire period of drying-out a soil sample in the laboratory dynamic chamber, the actual gravimetric soil moisture $\theta_g(t_i)$ is then given by

$$\theta_g(t_i) = \frac{m_{\mathrm{soil}}(t_i) - m_{\mathrm{soil}}(t_S)}{m_{\mathrm{soil}}(t_S)} \tag{S11}$$

3.4 Calculation of release rates of NO, CO_2, C_2H_4O and C_3H_6O

Most analyzers provide measurement data in units of the dimensionless volume mixing ratio of the corresponding trace gas i (m_i in 10^{-9} = ppb), while for the calculation of

BGD
11, 1187–1275, 2014

release rates (J_i in ng kg$^{-1}_{\text{dry soil}}$ s^{-1}) concentration units (c_i in ng m^{-3}) have to be used. Therefore, appropriate conversion factors $f_{C,i}$ are necessary:

$$c_i = f_{C,i} m_i = 10^3 \frac{\rho_{\text{air}} M_i}{M_{\text{air, dry}}} m_i \tag{20}$$

where ρ_{air} is the mean dry air density (kg m^{-3}), M_i is the atomic/molecular weight of the considered trace gas i (kg kmol^{-1}), and $M_{\text{air, dry}}$ is the molecular weight of dry air ($M_{\text{air, dry}} = 28.9644$ kg kmol^{-1}). Release rates and fluxes of NO are often expressed in terms of mass of atomic nitrogen $M_N = 14.0067$ kg kmol^{-1}), because this enables easy comparison with corresponding soil related fluxes and release rates of nitrous oxide (N_2O), nitrogen dioxide (NO_2), nitrous and nitric acid (HONO and HNO_3), as well as ammonia (NH_3). Analogously, the corresponding quantities for CO_2, C_2H_4O and C_3H_6O are expressed in terms of the atomic weight of carbon ($M_C = 12.0107$ kg kmol^{-1}). Here, the mean air density ρ_{air} [kg m^{-3}] is dependent on air temperature of the chamber's headspace (the temperature controlled cabinet) according to:

$$\rho_{\text{air}} = \frac{100\, p_{\text{air}}\, M_{\text{air, dry}}}{R\,(273.15 + T_{\text{headspace}})} \tag{21}$$

where p_{air} is the barometric pressure (hPa), R the universal gas constant (8314.41 J kmol^{-1} K^{-1} (N m kmol^{-1} K^{-1}; kg m^2 kmol^{-1}K^{-1} s^{-2}), and $T_{\text{headspace}}$ the actual air temperature (°C) of the chamber's headspace.

Considering the mass balance of the dynamic chamber (e.g. Meixner and Yang, 2006), the net release rate (J_i) can be calculated from the chamber's purging rate (Q in m^3 s^{-1}), the mass of the enclosed soil (m_{soil} in kg), and the mixing ratio difference between the chamber's out- and inlet ($m_{i,\text{out}} - m_{i,\text{in}}$ in ppb). For the above described set-up of our laboratory dynamic chamber system, $m_{i,\text{in}}$ is replaced by the mixing ratio measured in the reference chamber ($m_{i,\text{ ref}}$), and $m_{i,\text{out}}$ by the mixing ratio the chamber's

BGD
11, 1187–1275, 2014

headspace ($m_{i,\mathrm{cham}}$). The latter is justified by the effective mixing of the headspace's air by the fan and the high purging rate Q, i.e., short exchange time τ of the chamber's headspace volume). Then, J_i is formulated as

$$J_i = \frac{Q}{m_{\mathrm{soil}}} \left(m_{i,cham} - m_{i,in}\right) f_{\mathrm{C},i} \tag{22}$$

where $Q = 4.16667 \times 10^{-5}\,\mathrm{m^3\,s^{-1}}$ ($= 2.5\,\mathrm{L\,min^{-1}}$) for each experiment of this study.

Formulas for the calculation of the net NO release rate J_{NO}, the NO production rate P_{NO}, the NO consumption rate U_{NO}, the NO consumption coefficient k_{NO}, and the Q_{10} values for NO production and consumption are already given in Sect. 2 of this paper. Numeric expressions of optimum curve relationships between J_{NO}, k_{NO}, P_{NO}, U_{NO} and gravimetric soil moisture content θ_{g} have been obtained by fitting Eq. (9) to corresponding data points using the solver-option of Microsoft® Office Excel.

Acetone (C_2H_4O) and acetaldehyde (C_3H_6O) are two of the VOC-species which have been measured by PTR-TOF-MS, which was calibrated by a commercially available, calibrated gas standard (see above). The PTR-TOF-MS signals are converted to corresponding mixing ratios by

$$m_{\mathrm{VOC}} = \left(\frac{\mathrm{ncps}_{\mathrm{VOC,cham}} - \mathrm{ncps}_{\mathrm{VOC,in}}}{C_{\mathrm{f,VOC}}}\right) \tag{23}$$

where $C_{\mathrm{f,VOC}}$ is the VOC specific calibration factor, and $\mathrm{ncps}_{\mathrm{VOC,in}}$ and $\mathrm{ncps}_{\mathrm{VOC,cham}}$ are the normalized PTR-TOF-MS signals (counts per second) at the inlet (measured from the reference chamber box0) and within the chamber's headspace, respectively. Analogously to the calculation of the net NO release rate, the release rate for VOCs (here: C_2H_4O and C_3H_6O) is calculated as:

$$J_{\mathrm{VOC}} = \frac{Q\left(m_{\mathrm{VOC,cham}} - m_{\mathrm{VOC,in}}\right) f_{\mathrm{C,VOC}}}{m_{\mathrm{soil}}} \tag{24}$$

BGD
11, 1187–1275, 2014

where Q is the flushing flow rate (2.5 L min^{-1} or 4.16667 × 10^{-5} m^3 s^{-1}), m_{soil} the dry mass of soil (kg), and $f_{C,VOC}$ is either f_{C,C_2H_4O} or f_{C,C_3H_6O} for conversion of C_2H_4O (C_3H_6O) mixing ratios (ppb) into C_2H_4O (C_3H_6O) concentrations (ng m^{-3}).

To determine the CO_2 release rate J_{CO_2}, the chamber system is operated in the static mode. Consequently, for calculation of J_{CO_2}, the mass balance equation of the closed chamber has to be considered, i.e. the release rate is derived from the temporal change of the CO_2 concentration in the total volume V^* over the soil sample (V^* = 1.273 × 10^{-3} m^3; i.e. chambers' volume + volume of tubing + volume of the CO_2/H_2O analyzer's absorption cell),

$$J_{CO_2} = \frac{[m_{CO_2,cham}(t_1) - m_{CO_2,cham}(t_0)]f_{C,CO_2}}{m_{soil}} \frac{V^*}{t_1 - t_0} \quad (25)$$

where $m_{CO_2,cham}(t_1)$ and $m_{CO_2,cham}(t_0)$ are the CO_2 mixing ratios (ppm) at t_1 and t_0, and f_{C,CO_2} is the factor to convert the CO_2 mixing ratio (ppm) into CO_2 concentration (µg m^{-3}). Note, that $t_1 - t_0$ (= 3.5 min) is the duration of closing the respective soil chamber, s. above).

3.5 Error analysis

The directly measured quantities in this study were the mixing ratios of NO, CO_2, H_2O, and VOCs in the flushing (incoming) air-stream and within the chamber's headspace. Each chamber was measured for 4 min with temporally high resolution of 30 s for NO, VOCs, CO_2, and H_2O. Corresponding averages and standard deviations have been calculated of the last 90 s (3 data points) for each measurement. Therefore, general Gaussian error propagation was applied to calculate the errors of all those quantities, which are derived from measured mixing ratios, i.e. net NO release rate J_{NO}, NO consumption coefficient k_{NO}, NO production rate P_{NO}, NO consumption rate U_{NO}, NO compensation point mixing ratio $m_{NO,comp}$, Q_{10} values of NO production and NO con-

BGD
11, 1187–1275, 2014

sumption, the proportionality factor g, actual mass of enclosed soil sample $m_{soil}(t_i)$, actual gravimetric soil moisture θ_g, (t_i), and the release rates of VOCs and CO_2.

3.5.1 Standard deviations of J_{NO}, k_{NO}, P_{NO}, U_{NO}, $m_{NO,comp}$, $Q_{10\_k,NO}$, and $Q_{10\_P,NO}$

To calculate $\sigma_{J,NO}$, Eq. (1) is recalled (s. Sect. 2):

$$J_{NO} = \frac{Q}{m_{soil}} \left(m_{NO,cham1,0} - m_{NO,in}\right) f_{C,NO} \quad (1)$$

For application of the general Gaussian error propagation, the derivatives of J_{NO} with respect to m_{soil}, Q, $m_{NO,cham}$, $m_{NO,in}$, $f_{C,NO}$ as well as their standard deviations (σ_{msoil}, σ_Q, $\sigma_{mNOcham}$, σ_{mNOin}, and $\sigma_{f,C\ NO}$) have to be considered. However, it can be assumed that $\sigma_{f,C\ NO} \approx 0$, and experimental evidence has shown that both, σ_{msoil} and σ_Q are negilible (less than 1 % of m_{soil}, Q, respectively). Hence, the standard deviation of J_{NO} is given by:

$$\sigma_{J,NO} = \pm J_{NO} \sqrt{\left(\frac{\sigma_{mNOcham}}{m_{NO,cham}}\right)^2 + \left(\frac{\sigma_{mNOin}}{m_{MO,in}}\right)^2} \quad (26)$$

Analogously, according to Eqs. (12a), (14b), (13b), and (15b) only the derivatives of $m_{NO,cham}$ and $m_{NO,in}$, as well as their standard deviations $\sigma_{mNOcham}$ and σ_{mNOin} have to be considered for the calculation of the standard deviations of k_{NO} (U_{NO}), P_{NO}, and

BGD
11, 1187–1275, 2014

$m_{NO,comp}$ (= $-P_{NO}/(k_{NO}f_{C,NO})$), which are given by:

$$\sigma_{k,NO\_T0} = \pm \frac{Q}{m_{soil}(m_{NO,cham2,0} - m_{NO,cham1,0})} \left[\sigma^2_{mNOin2} + \sigma^2_{mNOin1} + \left(\frac{m_{NO,cham1,0}}{m_{NO,cham2,0} - m_{NO,cham1,0}}\right)^2 \left(\sigma^2_{mNOcham2,0} + \sigma^2_{mNOcham1,0}\right)\right]^{\frac{1}{2}} \quad (27)$$

$$\sigma_{U,NO\_T0} = \pm U_{NO\_T0} \left[\left(\frac{\sigma_{k,NO\_T0}}{k_{NO\_T0}}\right)^2 + \left(\frac{\sigma_{mNOcham1,0}}{m_{NO,cham1,0}}\right)^2\right]^{\frac{1}{2}} \quad (28)$$

$$\sigma_{P,NO\_T0} = \pm P_{NO\_T0} \left[\left(\frac{\sigma_{J,NO\_T0}}{J_{NO\_T0}}\right)^2 + \left(\frac{\sigma_{k,NO\_T0}}{k_{NO\_T0}}\right)^2 + \left(\frac{\sigma_{mNOcham1,0}}{m_{NO,cham1,0}}\right)^2\right]^{\frac{1}{2}} \quad (29)$$

$$\sigma_{mNOcomp\_T0} = \pm m_{NO,comp\_T0} \left[\left(\frac{\sigma_{k,NO\_T0}}{k_{NO\_T0}}\right)^2 + \left(\frac{\sigma_{P,NO\_T0}}{P_{NO\_T0}}\right)^2\right]^{\frac{1}{2}} \quad (30)$$

For the standard deviations of k_{NO}, U_{NO}, P_{NO}, and $m_{NO,comp}$ at $T_{soil} = T_1$ (σ_{k,NO_T1}, σ_{U,NO_T1}, σ_{P,NO_T1}, and $\sigma_{m,NOcomp\_T1}$) the indices "1", "2", and "T_0" in Eqs. (27)–(30) have to be replaced by "3", "4", and "T_1", respectively.

The Q_{10} values of NO production and NO consumption are defined by

$$Q_{10\_P,NO} = \frac{P_{NO}(\theta_0, T_1)}{P_{NO}(\theta_0, T_0)} \text{ and} \quad (6)$$

$$Q_{10\_U,NO} = \frac{U_{NO}(\theta_0, T_1)}{U_{NO}(\theta_0, T_0)} = \frac{k_{NO}(\theta_0, T_1)}{k_{NO}(\theta_0, T_0)} \quad (7)$$

BGD
11, 1187–1275, 2014

where $T_1 = T_0 + 10$. Consequently, the standard deviations of $Q_{10\_P,NO}$ and $Q_{10\_U,NO}$ are given by

$$\sigma_{Q10\_PNO} = \pm Q_{10\_P,NO} \left[\left(\frac{\sigma_{P,NO\_T1}}{P_{NO\_T1}} \right)^2 + \left(\frac{\sigma_{P,NO\_T0}}{P_{NO\_T0}} \right)^2 \right]^{\frac{1}{2}} \quad (31)$$

$$\sigma_{Q10\_UNO} = \pm Q_{10\_k,NO} \left[\left(\frac{\sigma_{k,NO\_T1}}{k_{NO\_T1}} \right)^2 + \left(\frac{\sigma_{k,NO\_T0}}{k_{NO\_T0}} \right)^2 \right]^{\frac{1}{2}} \quad (32)$$

3.5.2 Standard deviations of the proportionality factor g, $m_{soil}(t_i)$, and $\theta_g,(t_i)$

According to the definition of the proportionality factor g (see Eq. (S6) and Eq. (S3.4), Sect. S.1), the calculation of σ_g requires the derivatives of g with respect to $m_{soil}(t_0)$, $m_{soil}(t_S)$, V, $s_{H_2O,cham}(t_0)$, $s_{H_2O,cham}(t_S)$, Q, and S_0, as well as their standard deviations ($\sigma_{msoil}(t_0)$, $\sigma_{msoil}(t_S)$, σ_V, $\sigma_{scham}(t_0)$, $\sigma_{scham}(t_S)$, σ_Q, and σ_{S_0}). Application of general Gaussian error propagation leads to:

$$\sigma_g = \pm \left(\frac{\Delta m}{D^2} \right) \left[\left(\frac{D}{\Delta m} \right)^2 \left(\sigma^2_{msoil(t_S)} + \sigma^2_{msoil(t_0)} \right) + V^2 \left(\sigma^2_{scham(t_S)} + \sigma^2_{scham(t_0)} \right) + \sigma^2_{S_0} \right]^{\frac{1}{2}} \quad (33)$$

where $D = V\Delta s + S_0$, $\Delta m = m_{soil}(t_S) - m_{soil}(t_0)$, $\Delta s = s_{H_2O,cham}(t_S) - s_{H_2O,cham}(t_0)$, and σ_{S_0} the standard deviation of the integration constant S_0 (for details, see Sect. S.1).

Typical values for $\sigma_{msoil(t0)}$, $\sigma_{msoil(tS)}$, $\sigma_{scham(t0)}$, and $\sigma_{scham(tS)}$ are within 0.5 % of $m_{soil}(t_0)$, $m_{soil}(t_S)$, $s_{cham}(t_0)$, and $s_{cham}(t_S)$. Consequently, the standard deviation σ_g of the proportionality factor g is as small as 1 % of g.

BGD
11, 1187–1275, 2014

The standard deviation $\sigma_{\theta g(ti)}$ of the actual gravimetric soil water content $\theta_g(t_i)$, defined by Eq. (S11) is given by

$$\sigma_{\theta\,\mathrm{g(ti)}} = \pm \left[\left(\frac{\sigma_{\mathrm{msoil}(t_i)}}{m_{\mathrm{soil}}(t_S)} \right)^2 + \left(- \frac{m_{\mathrm{soil}}(t_i)}{m^2_{\mathrm{soil}}(t_S)} \sigma_{\mathrm{m\,soil\,(tS)}} \right)^2 \right]^{\frac{1}{2}} \tag{34}$$

where $\sigma_{\mathrm{msoil}(t_i)}$ is the standard deviation derived for the actual total soil mass $m_{\mathrm{soil}}(t_i)$ as shown in Sect. S.1.

3.5.3 Standard deviations of the VOC and CO_2 release rates

The error for C_2H_4O and C_3H_6O was calculated as:

$$\sigma_{\mathrm{m,VOC}} = \sqrt{ \left(\frac{\left(\sigma_{\mathrm{m,VOCcham}} + \sigma_{\mathrm{m,VOCin}} \right)}{\mathrm{cnt}_{\mathrm{cham,\,corr}}} \right)^2 + \left(\frac{\sigma_{\mathrm{fcal}}}{f_{\mathrm{cal}}} \right)^2 } \tag{35}$$

where $\sigma_{\mathrm{m,VOC,in}}$ and $\sigma_{\mathrm{m,VOC,cham}}$ are the standard deviations (in counts) for the incoming and chamber's headspace measurements, respectively; $\mathrm{cnt}_{\mathrm{cham,\,cor}}$ are the corrected counts and σ_{fcal} is the standard deviation of the calibration factor f_{cal}.

The release rate of CO_2, measured under static mode conditions of the laboratory chamber system, is defined via Eq. (25). The errors of m_{soil}, $f_{\mathrm{C,CO_2}}$, t_0, and t_1 are considered to be negligible. The relative error of the total volume V^*, determined by the standard gas addition technique, was calculated to 1.5 %. Consequently, the standard deviation $\sigma_{\mathrm{J,CO_2}}$ of the CO_2 release rate is formulated as:

$$\sigma_{\mathrm{J,CO_2}} = \pm \frac{f_{\mathrm{C,CO_2}}\, V^*}{m_{\mathrm{soil}}\,(t_1 - t_0)} \left[\left(\left(m_{\mathrm{CO_2,cham}}(t_1) - m_{\mathrm{CO_2,cham}}(t_0) \right) \sigma_{V^*}/V^* \right)^2 + \sigma^2_{\mathrm{mCO_2cham},t_1} + \sigma^2_{\mathrm{mCO_2cham},t_0} \right]^{\frac{1}{2}} \tag{36}$$

BGD
11, 1187–1275, 2014

3.5.4 Detection limit, precision, and data rejection criteria

The limit of detection (LOD) of the NO mixing ratio could be evaluated during each drying-out experiment where the soil chambers have been flushed by "zero"-air. The LOD is usually defined as the lowest mixing ratio level that can be determined to be statistically different from a measurement of "zero"-air (e.g., MacDougall and Crummett, 1980). In this study, we define the LOD for NO measurements as three times that standard deviation which has been obtained through a statistically significant number (> 100) of "zero"-air measurements. Depending of the actual conditions of the dilution unit and/or the NO_x-analyzer, LOD_{NO} usually varies between 0.07 and 0.130 ppb. Since the errors of the measurement of NO mixing ratio propagate through all quantities which are characterizing net NO release from soil samples, we have chosen for this study LOD_{NO} = 0.15 ppb for further conservative estimates of errors and (minimum) detectability.

For this study, release rates, consumption and production rates, as well as the determination of characteristic Q_{10} values are exclusively derived from differences of mixing ratios (often (very) small, particularly between those measured in the incoming (the chamber's headspace). Hence, the quantification of the analyzers' reproducibility (precision) is as important as that of LOD. In case of NO mixing ratio measurements, we define precision as the dimensionless ratio of the standard deviation (σ_{mNO}) and the corresponding mixing ratio (m_{NO}). Corresponding data have been obtained during (i) routine multipoint calibration exercises and (ii) every drying-out experiment where different NO mixing ratios have been used for flushing the soil chambers. For m_{NO} > 50 ppb, the precision of the used NO_x-analyzer is rather low (< 0.01); however, it is sharply increasing for m_{NO} < 10 ppb (s. Fig. 8).

As mentioned above, mean NO mixing ratios of the incoming air as well as of each chamber's headspace have recorded every 30 s for a total of 240 s, and only data of the last 90 s have been used for further evaluation. Only those NO mixing ratios measured in each chamber's headspace have been considered for further evaluation which

BGD
11, 1187–1275, 2014

have been found to exceed the detection limit of the NO-analyzer (0.15 ppb; s. above). Remaining NO mixing ratios had to pass a simple statistical test to ensure consistency of the data. Instead of applying an outlier test, the combinations of corresponding differences have been calculated. Those data which exceeded 95 % of the corresponding cumulative frequency distribution have been rejected. Then, the difference between NO mixing ratios of the incoming and each chamber's headspace air has been calculated for use in Eq. (1). Since these differences can be very small (particularly for high and very small θ_g values, c.f. Fig. 4), they had to pass a statistical standard test to ensure their significance (F test for standard deviations, and a subsequent T test for averages). Only those data pairs whose difference was significant (p value 0.05) have been included in subsequent calculations. Consistency and significance of measured H_2O-signals (and respective differences) have been treated analogously.

4 Results

4.1 Response of microbial activity to changing experimental conditions

Knowledge of the microbial activity's response to temporal changes of soil moisture content, soil temperature, and incoming mixing ratios is important for any kind of incubation experiments. Wetted to the level of water-holding capacity and flushed with dry air, highly organic soils need between 48–96 h for dry-out. For most dryland soils, only about 24 h are necessary to completely dry-out the enclosed soil sample. However, with the new humidification facility (s. Sect. 3), the drying-out period for these soils can easily be extended to 48–96 h. Such periods are well comparable with those drying periods, which occur naturally after rainfalls. With respect to changes of soil temperature, microbial activity's response is assumed to be quick. Using the NO compensation point mixing ratio (as an integral quantity for the combined action of production and consumption), Gödde and Conrad (1999) have already demonstrated, that during a step-wise increase of soil temperature (4 to 45 °C; 5–10 K per 1–3 h) the response of microbial

BGD
11, 1187–1275, 2014

activity is much less than 1 h. This has guided the design of the heating/cooling facility of our improved laboratory dynamic chamber system. As described in the supplement, this facility needs about 30 min for the pre-scribed 10 K-increase or -decrease of soil temperature; another 10–15 min are allowed for final equilibration of the chamber system. Gödde and Conrad (1999) give no information concerning the microbial activity's response to changes of incoming NO mixing ratio. To examine that, firstly the response time of the laboratory dynamic chamber system was determined. For repeated step-wise changes of incoming NO mixing ratios between 10 and approx. 30 ppb, $m_{NO,in}$ data (30 s means) were plotted vs. the time elapsed after switching. From that, the 98 % response time of the system (τ_{98}) has been determined to 113 s. Since mean analyzer signals were logged every 30 s, it was decided for the measurement of NO (H_2O, VOC) mixing ratio of incoming as well of every chamber's headspace air to discard the first 150 s and to keep the remaining 90 s (3 data points) for further evaluation (s. Sect. 3). Consequently, each of the seven soil chambers of the laboratory system was probed for 4 min; in any case, no significant temporal trends of $m_{NO,cham}$ have been observed after 150 s of probing each chamber. One entire cycle (i.e., probing all seven chambers at constant soil temperature, constant incoming NO mixing ratio, and "quasi-constant" gravimetric soil moisture content) lasted for 28 min. Twenty different soil samples (including those studied in this work) were tested for potential trend of J_{NO}; for that the cycle for all seven chambers was just repeated after switching $m_{NO,in}$ from "zero"-air to 130 ppb. In any case, there was no significant difference between $m_{NO,cham}$ data of the respective chamber measured in the first and in second cycle. From that it is concluded that microbial activity's response to step-changes of incoming NO mixing ratio might be as fast as for step-wise changes of soil temperature.

4.2 Minimum detectable level of the net release rate J_{NO}

For a given ratio of flushing rate (Q) and dry mass of the enclosed soil sample ($m_{soil,dry}$), the minimum detectable level of J_{NO} is dependent on the precision and the LOD of NO mixing ratio (s. Eq. 1), because J_{NO} is defined as the difference of two

BGD
11, 1187–1275, 2014

measured, error prone NO mixing ratios. Minimum detectable levels have been estimated for the condition, that $m_{NO,cham}$ and $m_{NO,in}$ in Eq. (1) must differ at least by the square root of the sum of their variances (squared standard deviations).

In Fig. 9 the minimum detectable net NO release rate is shown as function of the NO mixing ratio in the soil chamber's headspace ($m_{NO,cham}$). At the LOD_{NO}-level of this study (= 0.15 ppb), the minimum detection level of J_{NO} is 0.34 and 0.08 ng kg^{-1} s^{-1} for $m_{soil,\,dry}$ = 0.015 kg ("EGER blueberry and spruce") and 0.06 kg (for the remainder of the soil samples), respectively. In earlier studies (e.g. Feig et al., 2008a; Gelfand et al., 2009; Bargsten et al., 2010), where 0.1 kg of dry soil mass has been used, the minimum detection level of J_{NO} (at LOD_{NO}) has been experimentally determined to 0.08 and 0.11 ng kg^{-1} s^{-1}. For $m_{soil,\,dry}$ = 0.1 kg, our calculations would result in 0.08 ng kg^{-1} s^{-1}.

4.3 Five contrasting soils – results of net NO release rates

To demonstrate the wide capability of the improved laboratory dynamic chamber system, we present results of net NO release rates from soil samples which have been taken from five different and highly contrasting soils (s. Sect. 3, Table 1). It should be emphasized, that -in contrast to earlier studies- only one soil sample has been exposed to conditions "exp. 1"–"exp. 4" (s. Sect. 2) during one drying-out experiment. Individual data of $m_{NO,in}$, $m_{NO,cham}$, $J_{NO}(\theta_0, T_0, m_{NO,cham})$, and $J_{NO}(\theta_0, T_1, m_{NO,cham})$ for "exp. 1"–"exp. 4" are listed in Table 2.

Results of net NO release rates from an arid, but agriculturally managed soil are shown in Fig. 10. The soil has been taken from the top soil layer (5 cm) of a fertilized and irrigated wheatfield of Kaga (Kuche) oasis, northern Taklimakan desert (Uighur Autonomous Region Xinjiang, China). Comparing Fig. 10 with Fig. 4 of Sect. 2, the results from this arid soil provide a textbook-style illustration of the methodical concept described in Sect. 2. Net NO release rates observed for conditions "exp. 1"–"exp. 4" reveal a mean optimum value at $\theta_0 = 0.063 \pm 0.0026$; agreement of individual θ_0 values is statistically highly significant. The same is valid for $\theta_{g,1}$, the second value to deter-

BGD
11, 1187–1275, 2014

mine the gravimetric soil moisture's shape coefficient ($\theta_{g,1} = 0.19 \pm 0.008$ for $R_J = 2$, s. Eq. 8c). For this soil sample, it was not necessary to slow down the drying-out process by humidification of the incoming air. Hence the error of the incoming water-vapor signal s_{in} was negligible. Only the error of the water-vapor signal s_{cham} (measured in the chamber's headspace; s. Sect. 3.5.2) contributed to the θ_g-error of all data points, which are very small (error bars of θ_g in Fig. 10 are smaller than the size of symbols). Analogously, the same is valid for the J_{NO}-error bars in Fig. 10 for conditions of "exp. 1" and "exp. 3" (i.e. m_{NO,in_1}, $m_{NO,in\_1} \approx 0$ ppb). Only when m_{NO,in_3} and m_{NO,in_4} were around 137 ppb ("exp. 2" and "exp. 4"), the error of both mixing ratios ($m_{NO,in}$ and $m_{NO,cham}$; s. Eq. 1) contribute to a larger error of J_{NO}. All NO net release rates for the arid soil sample are positive. As described in Sect. 2 (c.f. Fig. 4), this is equivalent to the fact, that the corresponding NO compensation point mixing ratio $m_{NO,comp}$ must be higher then $m_{NO,cham\_3}$ and $m_{NO,cham\_4}$, respectively; indeed, $m_{NO,comp}$ of this soil sample has been determined to > 500 ppb.

Net NO release rates from a soil sample which has been taken from the "O" horizon of an 80 yr old spruce forest soil ("Fichtelgebirge", SE Germany) are shown in Fig. 11. The understory of the sampling patch consisted in young spruce (0.3–0.8 m). A mean optimum value of $\theta_0 = 2.12$ (±0.148) has been identified for all net NO release rates observed for conditions "exp. 1"–"exp. 4" (highly significant agreement between individual θ_0 values). The observed optimum gravimetric soil moistures, which exceed unity, are due to the high content of soil organic matter (indicated by total C-content of 44 %, s. Table 1) which has a strong capability to absorb water. The mean of individual $\theta_{g,1}$ value is 4.71 ± 0.447 (for $R_J = 2$); agreement between them is highly significant. For this forest soil sample, it was necessary to slow down the drying-out process by humidification of the incoming air (in order to yield enough data points for quasi-constant θ_g-conditions during each switching-cycle between different temperatures and incoming mixing ratios, s. Sect. 3). Hence both, the errors of s_{in} and s_{cham} contributed to the θ_g-error of all data points, which are considerably larger than those for the arid soil sample (s. Fig. 10). This spruce covered forest soil revealed highest net NO release

BGD
11, 1187–1275, 2014

rates of all soils investigated in this study (21 and 35 ng kg^{-1} s^{-1} for T_{soil} = 20 °C and 30 °C, respectively). As already mentioned for the arid soil sample, considerable J_{NO}-errors in Fig. 11 are due to larger errors of (non-zero) NO mixing ratios measured in both, the incoming and the chamber's headspace air (s. Sect. 3.5.4). As for the arid soil sample, all NO net release rates are positive. This means, that $m_{NO,cham\_3}$ as well as $m_{NO,cham\_4}$ are lower than the corresponding NO compensation point mixing ratio $m_{NO,comp}$. The latter have been determined to be 928 ppb (T_{soil} = 20 °C) and 1187 ppb (T_{soil} = 20 °C), respectively.

Net NO release rates from a mid-latitude natural grassland, shown in Fig. 12, are in considerable contrast to those from the arid, but agriculturally managed soil from NW-China. Though the grassland at Finthen (W-Germany) is classified as natural steppe-like ecosystem, it was not cultivated (fertilized) for the last 30 yr. Net NO release rates from this grassland are the lowest observed for all five soils investigated in this study. This is certainly due to the low nutrient status of this soil (s. Table 1). For conditions "exp. 1"–"exp. 4", individual values of optimum value of θ_0 are statistically not different from each other, their mean is θ_0 = 0.20 (±0.025). The mean of $\theta_{g,1}$, however, reveals higher scatter (0.40 ± 0.118 for R_J = 2, s. Eq. 8c). Like for the spruce covered forest soil, it was necessary to slow down the drying-out process by humidification of the incoming air. Consequently, the θ_g-error of all data points is correspondingly larger. Net NO release rates observed for m_{NO,in_2} = 131 ppb (T_{soil} = 20 °C) are negative and very small (less than −0.6 ng kg^{-1} s^{-1}), but still exceeding the minimum detectable net NO release rate. Since they are negative, the corresponding NO compensation point mixing ratio $m_{NO,comp}$ (90 ± 23.0 ppb) is smaller than $m_{NO,cham\_2}$ (129 ± 0.6 ppb). For m_{NO,in_4} = 125 ppb (T_{soil} = 30 °C), however, all data points are lower than the corresponding minimum detectable net NO release rate and they scatter around J_{NO} = 0. This is a logical consequence that $m_{NO,cham\_4}$ (125 ± 0.6 ppb) was close to the corresponding NO compensation point mixing ratio $m_{NO,comp}$ which has been determined to 150 ± 43.3 ppb.

BGD
11, 1187–1275, 2014

The soil sample from the blueberry covered forest soil has been taken close to that from the young spruce covered soil. Therefore, indicated by its high total C-content (41 %, s. Table 1), its soil organic matter content is also high and optimum gravimetric soil moisture content of this soil also exceed unity (s. Figure 13). The mean optimum gravimetric soil moisture content for conditions "exp. 1"–"exp. 4" is $\theta_0 = 1.16$ (±0.102), individual values are indistinguishable from each other on a highly significant level, which is also valid for corresponding $\theta_{g,1}$ values (mean $\theta_{g,1} = 2.80 \pm 0.211$ for $R_J = 2$). Whereas the net NO release rates of this sample are positive for m_{NO,in_1} = 0.17 ppb (T_{soil}=20 °C) and m_{NO,in_3} = 0.18 ppb (T_{soil} = 30 °C), they are negative for m_{NO,in_2} = 470 ppb (T_{soil}=20 °C) and m_{NO,in_4} = 472 ppb (T_{soil} = 30 °C). Compared with the remainder of the soils in this study, the positive values are rather low (2.01 and 3.66 ng kg^{-1} s^{-1}). Negative net NO release rates (obtained at approx. 470 ppb of the incoming air), are as low as −17.5 and −18.0 ng kg^{-1} s^{-1}, respectively. Moreover, these net NO release rates are hardly distinguishable, despite the fact that they have been obtained at different soil temperatures.

Out of the five investigated soil samples, that from the Gobi desert (Mongolia) is the most exotic one. The mean optimum gravimetric soil moisture content, θ_0, for conditions "exp. 1"–"exp. 4" is as low as 0.02 (±0.002), the mean $\theta_{g,1}$ value is 0.04. Even at these very low θ_g-levels, individual θ_0- and $\theta_{g,1}$ values are indistinguishable from each other on a highly significant level. Surprisingly, all net NO release rates from this hyper-arid soil (s. Figure 14) are higher than the values observed for the mid-latitude (nutrient poor) grassland soil (s. Figure 12). The most striking result, however, is that there is no significant difference between net NO release rates obtained for T_{soil} = 20 °C and T_{soil} = 20 °C, neither for low (0.27 and 0.64 ppb) nor for high (133 and 134 ppb) NO mixing ratios of the incoming air. This will be discussed in detail in Sect. 5.

4.4 Net release rates of acetone (C_2H_4O), acetaldehyde (C_3H_6O), and CO_2

The improved laboratory dynamic chamber system was also used to measure net release rates of volatile organic compounds (VOC). Here, release rates of only two VOC-

BGD
11, 1187–1275, 2014

compounds are shown, namely acetone (C_2H_4O) and acetaldehyde (C_3H_6O), because soil net release rates of VOCs (detectable by PTR-TOF-MS) are dominated by C_2H_4O and C_3H_6O. Results of net C_2H_4O and C_3H_6O release rates from an arid, but agriculturally managed soil are shown in Figs. 15 and 16, respectively. Soil samples have been taken from the first 5 cm of a fertilized and irrigated cornfield of Kaga (Kuche) oasis, northern Taklimakan desert (Uighur Autonomous Region Xinjiang, China). Net C_2H_4O release rates fumigated with "zero"-air exhibit identical values of θ_0 (0.027) and $\theta_{g,1}$ (0.10) at T_{soil} = 20 °C as well as at T_{soil} = 30 °C (s. Figure 15), while corresponding optimum net C_3H_6O release rates occur for θ_0 = 0.025 and $\theta_{g,1}$ = 0.08 (s. Figure 16). For the entire range of gravimetric soil moisture, net C_2H_4O release rates are approx. double as much than C_3H_6O release rates. In both cases, net release rates are about 20-fold lower than those for nitric oxide. Remarkably, the shape of the θ_g-function of all three release rates is identical. Compared to the J_{NO} data, however, C_2H_4O and C_3H_6O data points own much larger errors. This is due to the fact, that the make-up of corresponding "zero"-air could not provide an incoming air stream which was 100 % free of C_2H_4O and C_3H_6O; corresponding noise (σ_{m,C_2H_4O,in_1} and σ_{m,C_3H_6O,in_1}) contribute most to the observed error of $J_{C_2H_4O}$ and $J_{C_3H_6O}$.

Net release rates for CO_2 were measured in the static mode of the laboratory chamber system (s. Sect. 3). Highest J_{CO_2} values have been observed from the organic rich forest soils (5641 ng kg^{-1} s^{-1} for "EGER spruce"; 2824 ng kg^{-1} s^{-1} for "EGER blueberry"), the lowest J_{CO_2} value, 105.6 ng kg^{-1} s^{-1} (in terms of C), has been calculated for the hyper-arid desert soil (however, statistically not different from zero, s. Table 1). Total organic carbon contents and C/N ratios correlate well with J_{CO_2} (s. Table 1).

BGD
11, 1187–1275, 2014

5 Discussion

5.1 Standardized procedure for initial wetting and sub-sample variability

As described in Sect. 2, only four experiments ("exp. 1"–"exp. 4") are necessary to completely characterize the net NO release from a soil sample in terms of gravimetric soil moisture content, soil temperature, and NO mixing ratio of the incoming air. However, former experiments have been performed on four individual sub-samples of the original soil sample, which led (i) to non-consistent values of θ_0 and $\theta_{g,1}$, and (ii) to non-consistent, even contradicting net NO release rates under varying conditions of (prescribed) soil temperatures and incoming NO mixing ratios. Our decision to omit any pre-incubation of soil samples, but applying a simple standardized procedure for initial wetting of the soil samples (i.e., wetting up to corresponding water-holding capacity) resulted in very uniform θ_0- and $\theta_{g,1}$ values for conditions "exp. 1"–"exp. 4". It has to be emphasized, that this is valid for a very wide range of optimum gravimetric soil moisture contents, namely from 0.02 (desert soil) to 2.12 (spruce covered forest soil). The second decision, namely to perform "exp. 1"–"exp. 4" on only one (sub-)sample, has drastically reduced the effect of sub-sample variability with respect to non-consistent net NO release rates. This is best demonstrated by comparing the results of net NO release rates shown in Fig. 6 and those in Fig. 14. In both cases, sub-samples were from the same original soil sample of a hyper-arid desert soil of Mongolia. While the data in Fig. 6 result from a total of 12 sub-samples (3 replicates using 4 sub-samples each), those in Fig. 14 were obtained for only two sub-samples. The overwhelming scatter of data points in Fig. 6 does not allow any meaningful conclusions about relations between net NO release rates, soil temperature, and incoming NO mixing ratio. In contrast, it is hard to distinguish each pair of data points in Fig. 14 which originate from two replicate studies under identical conditions of "exp. 1"–"exp. 4" (i.e., each pair of circles and diamonds in Fig. 14). Moreover, there is a very clear picture how the net NO release rate for this hyper-arid soil depends on soil temperature. Since the reddish ("exp. 3" and "exp. 4") as well as the blueish ("exp. 1" and "exp. 2") fitted curves are

BGD
11, 1187–1275, 2014

statistically indistinguishable, there is evidence, that in this hyper-arid soil sample NO consumption obviously does not occur. Potential microbial reasoning for this observation is discussed in detail below.

5.2 Minimum detectable levels of k_{NO}, $Q_{10\_U,NO}$, P_{NO}, and $Q_{10\_P,NO}$

Particularly on the minimum detectable level of k_{NO}, and $Q_{10\_k,NO}$, precision and LOD of NO mixing ratio measurements have a decisive impact, because these quantities are defined as difference of differences and as the ratio of differences of differences of NO mixing ratio, respectively. Respective minimum detectable levels have been estimated for the condition that (i) $J_{NO}(\theta_0, T_0, m_{NO,cham\_1,0})$ and $J_{NO}(\theta_0, T_0, m_{NO,cham\_2,0})$ in Eqs. (12a) and (14b), and (ii) $k_{NO}(\theta_0, T_1)$ and $k_{NO}(\theta_0, T_0)$ in Eq.(7), must (significantly) differ at least by the square root of the sum of their variances (squared standard deviations).

In Fig. 17, the minimum detectable level of the NO consumption rate coefficient k_{NO} is shown as function of that NO mixing ratio ($m_{NO,cham\_1,0}$), which will establish in the soil chamber for $m_{NO,in\_1} \approx 0$ ppb, $\theta_g = \theta_0$, and $T_{soil} = T_0$. According to Eq.(12a) and Fig. 1, k_{NO} is the slope of $J_{NO}(\theta_0, T_0, m_{NO,cham})$. Besides on the NO mixing ratio's precision, the minimum detectable level of k_{NO} depends decisively on the magnitude of the NO compensation point mixing ratio $m_{NO,comp}$ (where J_{NO} =0). This is shown by the colored curves (indicating different $m_{NO,comp}$) in Fig. 17. With the present NO_x-analyzer, minimum detectable levels of k_{NO} range between -4×10^{-7} and -4×10^{-6} $m^3\,kg^{-1}\,s^{-1}$. This information is particularly important for arid and hyper-arid soils, where extremely low k_{NO} values have been found (e.g. Gelfand et al., 2009). In our study, values of $k_{NO}(\theta_0, T_0)$ and $k_{NO}(\theta_0, T_1)$ for the hyper-arid desert soil are indeed exceeding respective minimum detectable levels of k_{NO}, but due to their large standard deviations they are statistically not different from zero (s. Table 2). Consequently, for determination of corresponding NO compensation point mixing ratios of this soil,

BGD
11, 1187–1275, 2014

$P_{NO}(\theta_0,T_0)$ and $P_{NO}(\theta_0,T_1)$ have been divided by the minimum detectable k_{NO} value ($= -4 \times 10^{-7}\,m^3\,kg^{-1}\,s^{-1}$).

The minimum detectable level of $Q_{10\_U,NO}$, as function of $m_{NO,cham\_1,0}$ and $m_{NO,comp}$ is shown in Fig. 18. Data have been calculated for $LOD_{NO} = 0.15$ ppb and the precision curve shown in Fig. 8. As an exponential increase of the NO consumption rate U_{NO} ($= k_{NO} \cdot m_{NO,cham} \cdot f_{C,NO}$) is assumed (s. Sect. 2), $Q_{10\_U,NO}$ cannot fall below unity. With respect to the NO_x-analyzer's precision, the $Q_{10\_U,NO}$ value is the most error prone quantity, because six individual differences of NO mixing ratios have to be used for its calculation (s. Eq. 16). Consequently, the minimum detectable level of $Q_{10\_U,NO}$, strongly increases with increasing $m_{NO,comp}$ and decreasing headspace NO mixing ratio (particularly for $m_{NO,cham\_1,0} < 10$ ppb). All calculated $Q_{10\_U,NO}$ values of this study had to pass this minimum detectable $Q_{10\_U,NO}$-test. Data calculated for the "Finthen grassland" and "KUCHE wheat" soil samples do not pass this criterion; in both cases the respective minimum detectable $Q_{10\_U,NO}$ value has been used for further evaluation (1.366 and 1.278, respectively; s. Table 2).

Minimum detectable levels of $P_{NO}(\theta_0,T_0)$ and $Q_{10\_P,NO}$ have also been calculated and have been proven to be only marginally dependent on the NO mixing ratio in the chamber's headspace (corresponding figures not shown). For $m_{NO,cham} < 60$ ppb, $P_{NO}(\theta_0,T_0)$ and $Q_{10\_P,NO}$ are virtually independent of $m_{NO,cham}$. In total, $P_{NO}(\theta_0,T_0)$ and $Q_{10\_P,NO}$ range between 0.4 and 1.6 $ng\,kg^{-1}\,s^{-1}$ and 1.02 and 1.1 for $100 < m_{NO,comp} < 500$ ppb, respecttively.

5.3 P_{NO} and k_{NO} of five contrasting soils

As mentioned already in Sect. 4, five soil samples of very contrasting soil properties have been used to determine that set of quantities which is necessary to completely characterize biogenic NO emission. In Table 2, individual data of NO production rate (P_{NO}) and NO consumption rate coefficients (k_{NO}) are listed for conditions of respective optimum gravimetric soil moisture content (θ_0), $T_{soil} = 20\,^{\circ}C$, and $T_{soil} = 30\,^{\circ}C$. Depen-

BGD
11, 1187–1275, 2014

dencies of P_{NO} and k_{NO} over the entire range of gravimetric soil moisture content are shown in Figs. 19 and 20, respectively. Double logarithmic scaling has to be chosen to illustrate the wide ranges of P_{NO}, k_{NO}, and θ_g, (two orders of magnitude for each quantity), which have been observed in this study. This also demonstrates the obvious large contrast of microbial activities within these five soil samples.

The wide range of observed $g\theta_g$ values is certainly due to the wide range of individual soil textures and soil organic matter, which in turn determine the water-holding capacity (i.e., sandy soils usually exhibit θ_g values $\ll 1$, while organic rich soils easily exceed unity; Bargsten et al., 2010; Wickland and Neff, 2008). However, the fact, that the distribution of optimum gravimetric water contents is quite similar (i.e., $\theta_0 > 1$ for the mid-latitude forest soils, $\theta_0 \ll 1$ for the remainder of soil samples) may point to different microbial communities acting in these contrasting soils; different contribution of these communities to NO production and NO consumption might be due to microbial ecology which results in diverse microbial adaptation to prevailing field conditions, niche differentiation, and habitat preference.

Considering the wide range of observed k_{NO} values for $T_{soil} = 20\,^{\circ}C$ (s. Figure 20), similar ecosystems seem to exhibit similar behaviour, i.e., "KUCHE wheat" and "FINTHEN grassland" vs. "EGER blueberry" and "EGER spruce"; but this is obviously not the case if the maxima of P_{NO} at $T_{soil} = 20\,^{\circ}C$ are considered (s. Figure 19). However, the high maximum P_{NO} value of the arid wheat-field soil is certainly a result of agricultural management, which includes fertilization and irrigation by flooding every 14 days in the growing season. Frequent flooding (i.e., water saturation of the soil), followed by nearly complete dry-out (within a couple of days) should be considered to explain the relative large shape width of the θ_g-curve: soil microbial communities might be adapted to and being active within this wide range of θ_g.

In Figs. 19 and 20, the response of P_{NO} and k_{NO} of all five soils to other soil temperatures (10 °C and 30 °C) is indicated by respective thinner lines. It should be noted, that these curves are calculated according to Eq. (4) using $P_{NO}(\theta_0, T_0)$ and $k_{NO}(\theta_0, T_0)$ and those $Q_{10\_P,NO}$ and $Q_{10\_k,NO}$ values which are listed in Table 2 ($Q_{10\_k,NO} = Q_{10\_U,NO}$;

BGD
11, 1187–1275, 2014

s. Sect. 2). $Q_{10\_U,NO}$ for "FINTHEN grassland" and "KUCHE wheat" represent data of lower detectable limit of $Q_{10\_U,NO}$, rather than data from respective measurements. With increasing soil temperature all soils show corresponding increase in P_{NO} as well as in k_{NO}. The hyper-arid desert soil from Mongolia exhibits the by far the largest temperature response: the relative increase of $P_{NO}(\theta_0, T_{soil} = 20\,^{\circ}C)$ to $P_{NO}(\theta_0, T_{soil} = 30\,^{\circ}C)$ exceeds 200 % (note, there are no corresponding k_{NO}-curves in Fig. 20, since the respective $Q_{10\_U,NO}$ value could not be calculated due to non-significant $k_{NO}(\theta_0, T_0)$- and $k_{NO}(\theta_0, T_1)$-data). There is also a remarkable temperature response of the NO consumption rate coefficient for the "KUCHE wheat" soil.

Observed P_{NO} and k_{NO} values are considered with respect to the soil property data given in Table 1. Both mid-latitude forest soils ("EGER spruce" and "EGER blueberry") are characterized by high CO_2 release rates suggesting the dominance of heterotrophic processes. High ammonium and nitrate contents of "EGER spruce" suggest that heterotrophic nitrification might be the relevant process for the observed higher P_{NO} rates in that soil, while comparatively lower ammonium and nitrate contents (approx. 4 and 2 fold, respectively) point to heterotrophic denitrification in the "EGER blueberry" soil. The remarkably high ammonium and nitrate contents in both mid-latitude soils are due to (i) high ability of organic matter constituents to absorb these nutrients, and (ii) very large NH_4^+ and NO_3^- inputs to this ecosystem by precipitation (Wolff et al., 2010). Due to low nitrate ($2.2\,mg\,kg^{-1}$) content heterotrophic denitrification seems to prevail also in the "FINTHEN grassland" soil. In the arid and hyper-arid soils ("KUCHE wheat" and "MONGOLIA desert") autotrophic nitrification might be the dominating process for NO production, since these soils are obviously ammonium limited, enriched in nitrate, low in total carbon, and both experience most of the time very low soil moistures.

Both mid-latitude forest soils exhibit very low pH (approx. 3). Under these acidic conditions the activity of bacteria is usually limited and the activity of archaea (Gubry-Rangin et al., 2010) and fungi (Pennanen et al., 1998) dominates. Therefore, it might be possible that co-denitrification of fungi, as found in an earlier study (Kumon et al.,

BGD
11, 1187–1275, 2014

2002), might be of relevance for NO emission from these soils. However, whether NO is produced and/or consumed by this process needs still further investigation.

5.4 NO compensation point mixing ratios of five contrasting soils

In this study, NO compensation point mixing ratios were found to be dependent on soil temperature, but not on soil moisture (s. Table 2). Among all quantities characterizing biogenic NO release, $m_{NO,comp}$ values cover the widest range (from 47 ppb to > 6000 ppb). For the mid-latitude forest soils ("EGER blueberry" and "EGER spruce") corresponding $m_{NO,comp}$ values are 47 ± 13.7 and 928 ± 472 ppb (T_{soil}=20 °C), and 82 ± 20 and 1187 ± 466 ppb (T_{soil} = 30 °C), respectively. This is contrasting $m_{NO,comp}$ = 380 ppb (blueberry) and $m_{NO,comp}$ = 510 ppb (spruce) which have been reported by Bargsten et al. (2010) for the same ecosystem (T_{soil} = 10 °C, θ_g = 1). Since Bargsten et al. (2010) observed only very weak relationships to soil properties, the potential of ectomycorhizza as a major contributor to NO production has been suspected. However, since (i) soil samples of this study as well as by Bargsten et al. (2010) have been taken on very small spatial scales (within some tens of meters), and (ii) ectomycorhizza is found in symbiosis with both, the roots of spruce and blueberries, it is unlikely that ectomycorhizza should entirely explain the large differences of $m_{NO,comp}$ found in both studies. However, the data of Bargsten et al. (2010) have been observed by a former version of the laboratory dynamic chamber system, initial non-standardized wetting of soil samples, ≥ 3 h pre-incubation, and performing "exp. 1"–"exp. 4" with four individual sub-samples each.

NO compensation point mixing ratios for "FINTHEN grassland", classified as steppe-like grassland, are 90 ± 23 ppb (T_{soil} = 20 °C) and 150 ± 43 ppb (T_{soil} = 30 °C). This is in agreement with $m_{NO,comp}$ = 157 ± 16 ppb for the savannah grassland ecosystem of Nylsvley (Otter et al., 1990). For T_{soil} = 20 °C, NO compensation point mixing ratio for "KUCHE wheat", an arid agriculturally managed soil, is 506 ± 112 ppb and very close to $m_{NO,comp}$ = 600 ppb (20 °C) which has been reported for a dryland farming soil in Egypt by Saad and Conrad (1993). However, in this study a decrease of the NO com-

BGD
11, 1187–1275, 2014

pensation point mixing ratio from 20 °C to 30 °C has been observed, which could not be confirmed by our study (because corresponding Q_{10}-data fall short of the minimum detectable value for $Q_{10\_U,NO}$; s. Table 2). Since the calculated k_{NO} values of the hyper-arid Mongolian desert soil have been found to be statistically indistinguishable from zero, corresponding $m_{NO,comp}$ (6590 ppb) has been derived using the minimum detectable k_{NO} value instead (s. Table 2). This is in great contrast to $m_{NO,comp} < 100$ ppb for soils from the Namib, Kalahari, and Sahara deserts reported by Feig (2009). However, also these data have been observed by a former version of the laboratory dynamic chamber system, initial non-standardized wetting of soil samples, 48 h pre-incubation, and performing "exp. 1"–"exp. 4" with four individual sub-samples each.

As already mentioned, the NO compensation point mixing ratio is defined by $m_{NO,comp} = f_{C,NO}^{-1} P_{NO}(\theta_g, T_{soil})/k_{NO}(\theta_g, T_{soil})$. Since both, NO production and NO consumption exhibit the same shapes of optimum curves with respect to θ_g (s. Section 2), $m_{NO,comp}$ is a sole function of soil temperature, but only if P_{NO} and k_{NO} will own different dependencies on soil temperature. According to Eqs. (4) and (5) this is equivalent that $Q_{10\_P,NO}$ and $Q_{10\_U,NO}$ ($= Q_{10\_k,NO}$) must be different. For the two mid-latitude forest soils, the dependency of $m_{NO,comp}$ on soil temperature is shown in Fig. 21 for the soil temperature range 10–35 °C. NO compensation point mixing ratios of "EGER spruce" are 10-fold higher than those from "EGER blueberry"; however, the increase of $m_{NO,comp}$ from $T_{soil} = 10$ °C to $T_{soil} = 35$ °C is 4-fold for "EGER blueberry" and only about 2-fold for "EGER spruce". Up to now, increasing NO compensation point mixing ratios with increasing soil temperature has only been reported by Gödde and Conrad (1999). Moreover, for two mid-latitude soil samples (grassland and arable land), they have shown, that with increasing soil temperature the ratio of nitrifiers to denitrifiers (both contributing to the net release of NO) was decreasing. High $m_{NO,comp}$ values of "KUCHE wheat" and "MONGOLIA desert" soils are characterically low in total carbon, high in nitrate, and are fast drying-out under field conditions. Since these factors hinder the development of anaerobic conditions, denitrification might be limited in these soils. That is confirmed by a very recent study of Orlando et al. (2012), who found in dryland

BGD
11, 1187–1275, 2014

soils only a low abundance of denitrifiers. Due to very low ammonium contents, limited NO production within those soils is most likely by autotrophic nitrification. Compared to "EGER spruce", the nitrate content of the "EGER blueberry" sample is lower and its $m_{NO,comp}$ value is comparable with that of the "FINTHEN grassland" soil, which has a low nitrate content, too. Therefore, it is suggested, that even small differences of pH and total carbon of the "EGER blueberry" soil, compared with the "EGER spruce" soil, might promote denitrification by fungi in "EGER blueberry", which results in a considerable low $m_{NO,comp}$ value. The pH value of the "FINTHEN grassland" soil is 6.2; most likely, the activity of denitrifying bacteria might cause its low $m_{NO,comp}$ value. Already Pennanen et al. (1998) have shown, that pH is an important factor that controls the activity of bacteria and fungi.

More than two decades ago, Saad and Conrad (1993) investigated the temperature dependence of both, NO production and NO consumption. However, the results have shown a rather inconsistent pattern, namely either an optimum response (about 25–30 °C) or a continuous increase with soil temperature for P_{NO} and k_{NO}, which led to complex responses of $m_{NO,comp}$ to soil temperature. Gödde and Conrad (1999), however, assumed that nitrifiers and denitrifiers differ in their ability to adapt to different temperatures within different soils and with different incubation conditions. It is well known, that nitrifiers and denitrifiers use different enzymes to produce and consume NO (Braker and Conrad, 2011). Since the enzymes of nitrifiers and denitrifiers differ in their K_m and V_{max} values (Koper et al., 2010; Betlach and Tiedje, 1981) and thereby in their efficiency, it seems reasonable to assume that both processes, NO production and consumption, show different response to changing soil temperatures.

As mentioned at the beginning of this section, the amount of errors of measured NO mixing ratio is entirely due to the precision of our NO_x-analyser. Since six individual differences of NO mixing ratios have to be used for the calculation of $Q_{10\_U,NO}$ (s. Eq. 16), this quantity is the most error prone and propagation of NO mixing ratio errors generates considerably large errors of $Q_{10\_U,NO}$, which in turn determine the minimum

BGD
11, 1187–1275, 2014

detectable value of $Q_{10\_U,NO}$. Only the $Q_{10\_U,NO}$ values of the "EGER blueberry" and "EGER spruce" soil samples passed this criterion.

5.5 Soil temperature parameterization of net potential NO fluxes – a *caveat*

Using the algorithm of Galbally and Johansson (1989), the net potential NO flux from soil to the atmosphere (in units of $ng\,m^2\,s^{-1}$) is derived from observed P_{NO} and k_{NO} values, as well as from data of soil bulk density and effective soil diffusion coefficient of NO. Bargsten et al. (2010), Feig et al. (2008a), van Dijk et al. (2002), Yu et al. (2008, 2010), Kirkman et al. (2001), and Otter et al. (1999) parameterized the net potential NO flux with respect to soil temperature by applying a constant Q_{10} value. This value has been determined as the ratio of optimum net NO release rates obtained under "zero"-air fumigation at T_{soil} = 30 °C and T_{soil} = 20 °C, respectively (i.e., $Q_{10\_J,mNO,in\_1/3} = J_{NO}(\theta_0, T_1, m_{NO,in\_3,0})/J_{NO}(\theta_0, T_0, m_{NO,in\_1,0})$; s. Table 2). The NO mixing ratio in the chamber's headspace, $m_{NO,cham}$, is usually in the range of a few tenths to a few ppb. Hence, the contribution of NO consumption (linearly increasing with $m_{NO,cham}$) to the observed net NO release is rather small, and it is justified to assume $Q_{10\_J,mNO,in\_1/3} = Q_{10\_P,NO}$. However, as (negatively) larger k_{NO} values (lower $m_{NO,comp}$ values) occur, as larger becomes the contribution of NO consumption to J_{NO}, and the temperature dependence of J_{NO} is more and more determined by both, $Q_{10\_P,NO}$ and $Q_{10\_U,NO}$. Whereas the number of samples is limited in our study, the attempt is made to estimate the potential impact of these findings. As shown in Table 2, $Q_{10\_U,NO}$ values are about 1.3, while corresponding $Q_{10\_P,NO}$ values are consistently higher (1.44–2.03). This is equivalent to the fact, that – with increasing soil temperature – NO production will increasingly dominate NO consumption, which in turn will lead to the increase of the net potential NO flux. However, verification of this effect, particularly by field experiments, is missing. A first indication, however, has been provided by the recent and comprehensive study of Laville et al. (2009). Performing both, laboratory and field measurements by chamber techniques on a mid-latitude fertilized agricultural

BGD
11, 1187–1275, 2014

soil, they have identified two different Q_{10} values for the temperature dependence of their NO fluxes, namely Q_{10} = 4.3 (0–20 °C) and Q_{10} = 1.39 (20–45 °C).

It should be stated, that non-consistent temperature response of NO net release rates and/or NO fluxes obviously require individual parameterization of the temperature dependence of both, NO production and NO consumption. Largest impact is expected for fertilized soils and higher soil temperatures.

5.6 NO production rate (P_{NO}) vs. NO consumption rate (U_{NO})

As mentioned in Sect. 2, the net release of NO is the result of simultaneous NO production and NO consumption in the top layers of every soil ($J_{NO} = P_{NO} - U_{NO}$, Eq. 2). All parameters are known to calculate two dimensional distributions of P_{NO} (as function of θ_g and T_{soil}). The NO consumption rate U_{NO}, however, is the product of the NO consumption rate coefficient (k_{NO}) and the chamber's headspace NO concentration (= $m_{NO,cham} f_{C,NO}$). While $m_{NO,cham}$ is an intrinsic quantity of the applied chamber technique, it has a definite relevance for ambient (field) conditions. Generally, the NO flux across the soil–atmosphere interface is proportional to the difference between NO compensation point and atmospheric NO mixing ratios (c.f. Galbally and Johansson, 1989), where the proportionality coefficient is the integral diffusion coefficient of the interface layer (which may be defined as the top soil layer and the so-called quasi-laminar boundary layer (some few millimeters above soil surface). Since the well mixed laboratory dynamic chamber is characterized by very high turbulent diffusion, measured data of $m_{NO,cham}$ are very close to those found at the top of the quasi-laminar boundary layer in the field (c.f. Pape et al., 2009). Using (temperature dependent) values of those $m_{NO,cham}$ which have been observed under "zero"-air fumigation at optimum gravimetric soil moisture content, two dimensional distributions of $U_{NO}(\theta_g, T_{soil})$ have been calculated. In Figs. 22 and 23, two dimensional distributions of both, P_{NO} and U_{NO} are shown for the "EGER blueberry" and the "KUCHE wheat" soil sample, respectively.

Expressed by the (negatively) highest k_{NO} value of all investigated soils, the "EGER blueberry" soil has the highest potential to consume NO. However, P_{NO} values of this

BGD
11, 1187–1275, 2014

soil are comparatively low (2.07 and 3.79 ng kg^{-1} s^{-1} for T_{soil} = 20 °C and 30 °C, respectively), chamber's headspace NO mixing ratios are also low (1.5 and 2.7 ppb for T_{soil} = 20 °C and 30 °C, respectively). Consequently, this results in U_{NO} values which are not exceeding −0.12 ng kg^{-1} s^{-1} for all conditions of θ_g and T_{soil} (s. Figure 22). Obviously, this soil is characterized by well-balanced P_{NO} and U_{NO} resulting in low soil-atmosphere NO fluxes. In contrast, the k_{NO} value of the "KUCHE wheat" soil is only one third of the "EGER blueberry" soil; its potential to consume NO is correspondingly lower. However, maximum U_{NO} (−1.2 ng kg^{-1} s^{-1}) is about ten-fold higher than that of the "EGER blueberry" soil, which is caused by much higher values of P_{NO} and $m_{NO,cham}$ (see Table 2). For the "KUCHE wheat" soil five-fold higher P_{NO} values lead to ten-fold higher U_{NO} values compared with the "EGER blueberry" soil, despite of lower k_{NO} values of for the "KUCHE wheat" soil. In the field, where atmospheric turbulence causes strong vertical mixing within the lower troposphere, near-surface NO mixing ratios are in the order of a few ppb (or even fractions of ppb). Under these conditions, U_{NO} is expected to be quite low, and NO production will dominate the NO flux across the soil–atmosphere interface. Under very stable atmospheric conditions, which preferably occur within deep canopies, atmospheric turbulence might be very low or even be intermitting (e.g. Foken et al., 2012); then quite high NO mixing ratios (> 10 ppb) could be present very close (< 3 mm) to the soil surface facilitating enhanced impact of NO consumption to the NO flux.

5.7 Measurement of net CO_2 release rates – a proxy for heterotrophic activity

The described improved laboratory dynamic chamber system provides the facility to "switch" into the static chamber mode, which permits the measurement of net CO_2 release rates (J_{CO_2}). For the organic rich soils of this study, namely "EGER spruce". "EGER blueberry", and "SURINAME rainforest", J_{CO_2} values are 5641, 2824, and 417 ng kg^{-1} s^{-1} (in terms of C), respectively. These values are in a similar range as those for raw peat soils (Howard and Howard, 1993). According to Stark et al. (2002),

BGD
11, 1187–1275, 2014

soils which are characterized by high organic carbon contents and high C : N ratios exhibit lower NO emissions. Following Dunfield and Knowles (1998), there is evidence that the organic carbon content of soil and the concomitant evolution of CO_2 are good predictors for soil NO consumption. Gödde and Conrad (2000), found significant correlation between the NO consumption rate coefficient (k_{NO}) and the heterotrophic activity in the soil samples. This confirms our finding for the "EGER blueberry" soil, where high heterotrophic activity (indicated by high J_{CO_2} value) is related to high k_{NO}-, but low P_{NO} values. The "EGER spruce" soil sample is contrasting; here its high J_{CO_2} value opposes a very high J_{NO}. Our results indicate, that the composition and degradability of organic matter might be of greater importance in driving both, the net CO_2 release and the NO release, than the total C content alone. Therefore, total C content seems to be a good predictor for J_{CO_2}, but not necessarily for J_{NO}. Furthermore, it is certainly meaningful to assume that limited organic carbon contents of arid and hyper-arid soils result in very low (if any) NO consumption.

5.8 Net release of C_2H_4O and C_3H_6O

To our knowledge, net VOC release rates have been studied with respect to soil temperature (Asensio et al., 2007), but never for the entire range of gravimetric soil moisture content of soil samples. However, experimental proof for a release of VOCs by microbes in soil is very difficult. This is due to the fact that bacteria can lead to the increase of the net release of a certain VOC compound by indirect effects e.g. increase in surface area (Schulz and Dickschat, 2007). Distinguishing between abiotic and biotic controls of net VOC release is surprisingly difficult since current methods for sterilizing the soil can (i) affect the abiotically active moieties, and (ii) kill the organisms present. The analysis of an autoclaved reference sample is not recommended, since the process of autoclaving may cause the release VOCs (Schulz and Dickschat, 2007). Therefore, the possibility of abiotic release of C_2H_4O and C_3H_6O from soil particles – such as soil organic matter – cannot be excluded. However, it has been shown for the first time in this study, that (at least) the net release of C_2H_4O and C_3H_6O fol-

BGD
11, 1187–1275, 2014

lows the gravimetric soil moisture content in the form of an optimum curve, as it is generally observed for NO. This might point to biological processes responsible for the release of C_2H_4O and C_3H_6O. Acetone was identified as an intermediate in aerobic acetylene metabolism (Kanner and Bartha, 1982). C_3H_6O is known as intermediate of fermentation (Jones and Woods, 1986). From the results presented in Figs. 15 and 16, Q_{10} values of 1.830 ± 0.243 for the release of C_2H_4O and 1.562 ± 0.218 for the release of C_3H_6O have been calculated. These values are in considerably good agreement with the Q_{10} values of net NO release rates in this study (data of $Q_{\_J,mNO,in\_1/3}$, s. Table 2). This provides strong indication for microbial release of C_2H_4O and C_3H_6O, because abiotic processes exhibit usually higher Q_{10} values (> 3), as reported for the release of methyl chloride and methyl bromide from different plant materials (Yassaa et al., 2009; Wishkerman et al., 2008).

6 Conclusion

To completely characterize soil NO production and soil NO consumption in terms of the three major influencing factors (soil moisture, soil temperature, and NO mixing ratio) by measurements of the net NO release rate, a comprehensive concept for the laboratory dynamic chamber method has been formulated. However, there were obvious and large discrepancies between the postulated response of net NO release rates to these variables and that observed by earlier versions of the laboratory dynamic chamber system. This made the development of an improved system necessary. The improved system – consisting of six individual soil chambers – is described with respect to design and function, benchmark tests have been performed, and the overall performance of the system has been demonstrated by a series of experiments on five soil samples which are characterized by very contrasting soil properties.

The methodical concept of the improved system is focussed on the precise measurement of NO mixing ratio (a) in the air stream flushing the soil chambers, and (b) in the chambers' headspace. The difference of these NO mixing ratios define the net

BGD
11, 1187–1275, 2014

NO release rate, from which a series of further quantities for the characterization of NO production and consumption are derived (NO production rate, NO consumption rate coefficient, NO compensation point mixing ratio, Q_{10} values of NO production and consumption). Finally, for calculation of all these quantities, a set of only four pairs of precisely measured NO mixing ratios is necessary.

Introducing a standardized method of initial wetting (up to water-holding capacity), the response of net NO release rates to the entire range of gravimetric soil moisture content was invesigated by slow drying-out of the soil samples (by flushing soil chambers with air of low dew point). The actual gravimetric soil moisture content of each soil sample was precisely determined by a mass balance approach of the chamber's headspace water vapor concentration. The response of net NO release rates to soil temperature and NO mixing ratio has been studied by step-wise changing (i) the temperature of the entire chamber system, and (ii) using pre-scribed NO mixing ratios (from a standard gas diluting system). Proper control and automation of the chamber system with respect to these step-wise changes has been designed such, that all experiments for characterization of NO production and consumption could be performed on one soil sample and during one drying-out process only. With former versions of the laboratory dynamic chamber system these experiments have to be performed with four different sub-samples; corresponding sub-sample variability has been identified to lead quite often to non-consistent results, particularly of NO consumption rate coefficients and Q_{10} values. In order to study the impact of heterotrophic microbial activitiy on the net NO release, knowledge of a suitable proxy, the CO_2 release, is important. Therefore, the improved laboratory dynamic chamber system has been extended by a facility which temporarily "switches" the system into the static chamber mode which has shown as necessary to measure net CO_2 release rates.

Successful application of the improved laboratory dynamic chamber system to five very contrasting soils has demonstrated

1. with respect to gravimetric soil moisture, the response of net NO as well as C_2H_4O and C_3H_6O release rates follows a very distinct optimum curve; its shape is inde-

BGD
11, 1187–1275, 2014

pendent of soil temperature and NO mixing ratio. Maximum release rates occur at distinct so-called optimum gravimetric soil moisture contents; two data pairs of net release rate and corresponding gravimetric soil moisture content are sufficient to mathematically describe the corresponding shape function of the optimum curve,

2. with respect to increasing soil temperatures, the response of net NO as well as C_2H_4O and C_3H_6O release rates is exponential; only two experiments (e.g. at 20 °C and 30 °C) are necessary to derive corresponding Q_{10} values which mathematically describe individual temperature response of both, NO production and NO consumption,

3. the choice to omit any pre-incubation and to apply standardized initial wetting of soil samples, as well as the proper control and automation of the improved system allows the complete characterization of NO production rates, NO consumption rate coefficients, and NO compensation point mixing ratio over at least two orders of magnitude for a gravimetric soil moisture contents ranging from 0.02 to 2,

4. thorough quantification of the NO-analyzer's precision over a large range of NO mixing ratios (0.15 to 500 ppb) is substantial (a) to quantify corresponding errors of NO mixing ratio, (b) to enable quantitative error assessment of all derived quantities by consequent error propagation, (c) to establish significant, statistically based criteria, particularly limits of detection for all measured and derived quantities, and (d) to enable rigorous tests for data rejection.

Finally, it has been found, that the NO compensation point mixing ratio of a given soil sample (defined as the quotient of NO production rate and NO consumption rate coefficient) is independent of the gravimetric soil moisture content, but explicitely on soil temperature, because NO production and NO consumption are characterized by different Q_{10} values. As already reported by Gödde and Conrad (1999), there is strong evidence that the temperature dependence of the NO compensation point mixing ratio might be caused by different contribution of different microbial groups to the net release of NO, e.g. denitrifiers/nitrifiers or heterotrophs/autotrophs.

BGD
11, 1187–1275, 2014

Only with the improved laboratory dynamic chamber system, which eliminates any effects of sub-sample variability, it was possible to show, that the NO consumption rate coefficient of arid and hyper-arid soils is statistically indistinguishable from zero, but at least less than $-4 \times 10^{-7}\,m^3\,kg^{-1}\,s^{-1}$ (= minimum detectable limit). Using this minimum detectable limit, the NO compensation point mixing ratio would be 6590 ppb. From these result we hypothezise that (at least) in these hyper-arid soils the abundance of denitrifiers might be (very) low and denitirifiers even might lack the correponding enzyme, NO reductase (NOR), which is used for detoxification of NO, respectively consumption of NO (c.f., Falk et al., 2010). Then, it would be justified to assume, that autotrophic nitrifier activity dominate biogenic NO emissions from drylands.

Designing the improved laboratory dynamic chamber system included the option to apply the system also for soil release studies of other trace gases. Using a PTR-TOF-MS in parallel to the NO_x-, CO_2-, and H_2O-analyzers, a first attempt has been made to determine net release rates of volatile organic compounds (VOCs) from soil samples. Applying "zero"-air for fumigation, corresponding soil net VOC release rates from an agriculturally managed, irrigated and heavily fertilized oasis soil (Xinjiang, China) were dominated by substantial amounts of acetone (C_2H_4O) and acetaldehyde (C_3H_6O) release. Surprisingly, net release rates of C_2H_4O and C_3H_6O share with NO identical shapes of optimum curves (with respect to gravimetric soil moisture), and Q_{10} values of the three compounds are also quite similar. These analogies between NO and C_2H_4O/C_3H_6O strongly support the hypothesis, that biological processes are responsible for the soil release of C_2H_4O and C_3H_6O rather than abiotic processes. Next steps in this research will focus experiments where soil samples will be fumigated with elevated VOC mixing ratios to explore the potential existence of VOC compensation points. Knowledge of soil release rates of VOCs is of high interest for tropospheric chemistry, particularly for remote regions. However, complete characterization of VOC production and VOC consumption with the improved laboratory dynamic chamber system may enable soil specific fingerprinting of corresponding microbial activities is certainly of great importance for the new emerging field of soil volatilomics.

BGD
11, 1187–1275, 2014

Supplementary material related to this article is available online at http://www.biogeosciences-discuss.net/11/1187/2014/bgd-11-1187-2014-supplement.pdf.

Acknowledgements. The authors want to thank the Max Planck Graduate Centre with Johannes Gutenberg-University Mainz (MPGC) and the MPG for their financial support. This work was part of the German Research Foundation (DFG) funded project "DEQNO – Desert Encroachment in Central Asia – Quantification of soil biogenic Nitric Oxide" (DFG-MA 4798/1-1) and has also been supported by the DFG research unit 763 (HALOPROC). Soil sampling has been supported by C. Becker, N. Hempelmann, M. Ermel, and G. Khorsha. We are grateful to Z. Wu, B. Kraft, and S. Thiele for fruitful discussions. Our deep gratitude goes to the "ancestors" of the laboratory dynamic chamber system (former versions): W. X. Yang, L. Otter, S. van Dijk, I. Trebs, M. Kortner, M. Welling, G. Feig, J. Yu, and A. Bargsten.

The service charges for this open access publication have been covered by the Max Planck Society.

References

Asensio, D., Penuelas, I. F., and Llusia, J.: On-line screening of soil VOCs exchange responses to moisture, temperature and root presence, Plant Soil, 291, 249–261, 2007.

Ashuri, F. A.: Der Austausch von Stickstoffmonoxid zwischen Boden und Atmosphäre unter besonderer Berücksichtigung des Bodenwassergehaltes, Einfluss kulturlandschaftlicher Verhältnisse auf den Umsatz eines Spurengases, Ph.D. thesis, Johannes Gutenberg University Mainz, Germany, 1–169, 2009.

Bargsten, A., Falge, E., Pritsch, K., Huwe, B., and Meixner, F. X.: Laboratory measurements of nitric oxide release from forest soil with a thick organic layer under different understory types, Biogeosciences, 7, 1425–1441, doi:10.5194/bg-7-1425-2010, 2010.

Betlach, M. R. and Tiedje, J. M.: Kinetic explanation for accumulation of nitrite, nitric oxide, and nitrous oxide during bacterial denitrification, Appl. Environ. Microb., 42, 1074–1084, 1981.

Braker, G. and Conrad, R.: Diversity, structure, and size of N_2O-producing microbial communities in soils – what matters for their functioning?, Adv. Appl. Microbiol., 75, 33–70, 2011.

BGD
11, 1187–1275, 2014

Bronstein, I. N. and Semendjajew, K. A.: Taschenbuch der Mathematik, Empirische Formeln und Interpolation, BSBBG, Teubner Verlagsgesellschaft Leipzig, 515–527, 1970.
Chameides, W. L., Fehsenfeld, F., Rodgers, M. O., Cardelino, C., Martinez, J., Parrish, D., Lonneman, W., Lawson, R., Rasmussen, R. A., Zimmerman, P., Greenberg, J., Middleton, P., and Wang, T.: Ozone precursor relationships in the ambient atmosphere, J. Geophys. Res., 97, 6037–6055, 1992.
Conrad, R.: Compensation concentration as critical variable for regulating the flux of trace gases between soil and atmosphere, Biogeochemistry, 27, 155–170, 1994.
Conrad, R.: Soil Microorganisms as controllers of atmospheric trace gases (H_2, CO, CH_4, N_2O and NO), Microbiol. Rev., 60, 609–640, 1996.
Crutzen, P. J., Lawrence, M., and Pöschl, U.: On the background photochemistry of tropospheric ozone, Tellus, 51, 123–146, 1999.
Denman, K. L., Brasseur, G., Chidthaisong, A., Ciais, P., Cox, P. M., Dickinson, R. E., Hauglustaine, D. Heinze, C., Holland, E., Jacob, D., Lohmann, U., Ramachandran, S., da Silva Dias, P. L., Wofsy, S. C., and Zhang, X.: Couplings between changes in the climate system and biogeochemistry, in: Climate Change 2007: The Physical Science Basis, Contribution to Working Group I to the Fourth Assessment Report of the Intergovernmental Panel on Climate Change, 499–587, 2007.
Dunfield, P. F. and Knowles, R.: Organic matter, heterotrophic activity, and NO consumption in soils, Glob. Change Biol., 4, 199–207, 1998.
Falk, S., Liu, B., and Braker, G.: Isolation, genetic and functional characterization of novel soil nirK-type denitrifiers, Syst. Appl. Microbiol., 33, 337–347, 2010.
Feig, G. T.: Soil Biogenic Emissions of Nitric Oxide from Arid and Semi-Arid Ecosystems, Ph.D. thesis, Johannes Gutenberg University Mainz, Germany, 1–222, 2009.
Feig, G. T., Mamtimin, B., and Meixner, F. X.: Soil biogenic emissions of nitric oxide from a semi-arid savanna in South Africa, Biogeosciences, 5, 1723–1738, doi:10.5194/bg-5-1723-2008, 2008a.
Feig, G. T., Mamtimin, B., and Meixner, F. X.: Use of laboratory and remote sensing techniques to estimate vegetation patch scale emissions of nitric oxide from an arid Kalahari savanna, Biogeosciences Discuss., 5, 4621–4680, doi:10.5194/bgd-5-4621-2008, 2008b.
Foken, T., Meixner, F. X., Falge, E., Zetzsch, C., Serafimovich, A., Bargsten, A., Behrendt, T., Biermann, T., Breuninger, C., Dix, S., Gerken, T., Hunner, M., Lehmann-Pape, L., Hens, K., Jocher, G., Kesselmeier, J., Lüers, J., Mayer, J.-C., Moravek, A., Plake, D., Riederer, M.,

BGD
11, 1187–1275, 2014

Rütz, F., Scheibe, M., Siebicke, L., Sörgel, M., Staudt, K., Trebs, I., Tsokankunku, A., Welling, M., Wolff, V., and Zhu, Z.: Coupling processes and exchange of energy and reactive and non-reactive trace gases at a forest site – results of the EGER experiment, Atmos. Chem. Phys., 12, 1923–1950, doi:10.5194/acp-12-1923-2012, 2012.

Garrido, F., Henault, C., Gaillard, H., Perez, H., and Germon, J. C.: N_2O and NO emissions by agricultural soils with low hydraulic potentials, Soil Biol. Biochem., 34, 559–575, 2002.

Galbally, I. E. and Johansson, C.: A model relating laboratory measurements of rates of nitric oxide production and field measurements of nitric oxide emission from soils, J. Geophys. Res., 94, 6473–6480, 1989.

Galbally, I. E. and Roy, C. R.: Loss of fixed nitrogen from soil by nitric oxide exhalation, Nature, 275, 734–735, 1978.

Gelfand, I., Feig, G., Meixner, F. X., and Yakir, D.: Afforestation of semi-arid shrubland reduces biogenic NO emission from soil, Soil Biol. Biochem., 41, 1561–1570, 2009.

Gödde, M. and Conrad, R.: Simultaneous measurement of nitric oxide production and consumption in soil using a simple static incubation system, and the effect of soil water content on the contribution of nitrification, Soil Biol. Biochem., 30, 439–442, 1998.

Gödde, M. and Conrad, R.: Immediate and adaptational temperature effects on nitric oxide production and nitrous oxide release from nitrification and denitrification in two soils, Biol. Fert. Soils, 30, 33–40, 1999.

Gödde, M. and Conrad, R.: Influence of soil properties on the turnover of nitric oxide and nitrous oxide by nitrification and denitrification at constant temperature and moisture, Biol. Fert. Soils, 32, 120–128, 2000.

Gubry-Rangin, C., Nicol, G. W., and Prosser, J. I.: Archaea rather than bacteria control nitrification in two agricultural acidic soils, FEMS Microbiol. Ecol., 74, 566–574, 2010.

Gut, A., Blatter, A., Farni, M., Lehmann, B. E., Neftel, A., and Staffelbach, T.: A new membrane tube technique (METT) for continuous gas measurements in soils, Plant Soil, 198, 79–88, 1998.

Howard, D. M. and Howard, P. J. A.: Relationships between CO_2 evolution, moisture content and temperature for a range of soil types, Soil Biol. Biochem., 25, 1537–1546, 1993.

Insam, H. and Seewald, M. S. A.: Volatile organic compounds (VOCs) in soils, Biol. Fert. Soils, 46, 199–213, 2010.

Jones, D. T. and Woods, D. R.: Acetone-butanol fermentation revisited, Microbiol. Rev., 50, 484–524, 1986.

BGD
11, 1187–1275, 2014

Kanner, D. and Bartha, R.: Metabolism of acetylene by Nocardia rhodochros, J. Bacteriol., 150, 989–992, 1982.
Kirkman, G. A., Yang, W. X., and Meixner, F. X.: Biogenic nitric oxide emissions upscaling: An approach for Zimbabwe, Global Biogeochem. Cy., 15, 1005–1020, 2001.
Koper, T. E., Stark, J. M., Habteselassie, M. Y., and Norton, J. M.: Nitrification exhibits Haldane kinetics in an agricultural soil treated with ammonium sulfate or dairy-waste compost, FEMS Microbiol. Ecol., 74, 316–322, 2010.
Kumon, Y., Sasaki, Y., Kato, I., Takaya, N., Shoun, H., and Beppu, T.: Codenitrification and Denitrification are dual metabolic Pathways through which dinitrogen evolves from nitrate in *Streptomyces antibioticus*, J. Bacteriol., 184, 2963–2968, 2002.
Laville, P., Flura, D., Gabrielle, B., Loubet, B., Fanucci, O., Rolland, M.-N., and Cellier, P.: Characterisation of soil emissions of nitric oxide at field and laboratory scale using high resolution method, Atmos. Environ., 43, 2648–2658, 2009.
Lindinger, W., Hansel, A., and Jordan, A.: Proton-transfer-reaction mass spectrometry (PTR–MS): On-line monitoring of volatile organic compounds at pptv levels, Chem. Soc. Rev., 27, 347–354, 1998.
Ludwig, J., Meixner, F. X., Vogel, B., and Forstner, J.: Soil-air exchange of nitric oxide: an overview of processes, environmental factors, and modelling studies, Biogeochemistry, 52, 225–257, 2001.
MacDougall, D. and Crummett, W. B.: Guidelines for data acquisition and data quality evaluation in environmental chemistry, Anal. Chem., 52, 2242–2249, doi:10.1021/ac50064a004, 1980.
Mayer, J. C., Bargsten, A., Rummel, U., Meixner, F. X., and Foken, T.: Distributed modified bowen ratio method for surface layer fluxes of reactive and non-reactive trace gases, Agr. Forest Meteorol., 151, 655–668, 2011.
Meixner, F. X. and Yang, W. X.: Biogenic emissions of nitric oxide and nitrous oxide from arid and semiarid land, in: Dryland Ecohydrology, Springer, Netherlands, 233–255, 2006.
Müller, M., Graus, M., Ruuskanen, T. M., Schnitzhofer, R., Bamberger, I., Kaser, L., Titzmann, T., Hörtnagl, L., Wohlfahrt, G., Karl, T., and Hansel, A.: First eddy covariance flux measurements by PTR-TOF, Atmos. Meas. Tech., 3, 387–395, doi:10.5194/amt-3-387-2010, 2010.
Müller, M., George, C., and D'Anna, B.: Enhanced spectral analysis of C-TOF aerosol mass spectrometer data: iterative residual analysis and cumulative peak fitting, Int. J. Mass Spectrom., 306, 1–8, doi:10.1016/j.ijms.2011.04.007, 2011.

BGD
11, 1187–1275, 2014

Müller, M., Mikoviny, T., Jud, W., D'Anna, B., and Wisthaler, A.: A new software tool for the analysis of high resolution PTR-TOF mass spectra, Chemometr. Intell. Lab., 127, 158–165, 2013.
Orlando, J., Caru, M., Pommerenke, B., and Braker, G.: Diversity and activity of denitrifiers of Chilean arid soil ecosystems, Front. Microbiol., 3, 1–9, 2012.
Oswald, R., Behrendt, T., Ermel, M., Wu, D., Su, H., Cheng, Y., Breuninger, C., Moravek, A., Mougin, E., Delon, C., Loubet, B., Pommerening-Röser, A., Sörgel, M., Püschl, U., Hoffmann, T., and Trebs, I.: HONO Emissions from Soil Bacteria as a Major Source of Atmospheric Reactive Nitrogen, Science, 341, 1233–1235, 2013.
Otter, L. B., Yang, W. X., Scholes, M. C., and Meixner, F. X.: Nitric Oxide emissions from a southern African Savannah, J. Geophys. Res., 104, 18471–18485, 1999.
Pape, L., Ammann, C., Nyfeler-Brunner, A., Spirig, C., Hens, K., and Meixner, F. X.: An automated dynamic chamber system for surface exchange measurement of non-reactive and reactive trace gases of grassland ecosystems, Biogeosciences, 6, 405–429, doi:10.5194/bg-6-405-2009, 2009.
Pennanen, T., Fritze, H., Vanhala, P., Kiikkila, O., Neuvonen, S., and Baath, E.: Structure of a microbial community in soil after prologed addition of low levels of simulated acid rain, Appl. Environ. Microb., 64, 2173–2180, 1998.
Remde, A., Slemr, F., and Conrad, R.: Microbial production and uptake of nitric oxide in soil, FEMS Microbiol. Ecol., 62, 221–230, 1989.
Remde, A., Ludwig, J., Meixner, F. X., and Conrad, R.: A study to explain the emission of nitric oxide from a marsh soil, J. Atmos. Chem., 17, 249–275, 1993.
Rudolph, J. and Conrad, R.: Flux between soil and atmosphere, vertical concentration profiles in soil, and turnover of nitric oxide: 2. Experiments with naturally layered soil cores, J. Atmos. Chem., 23, 275–300, 1996.
Rudolph, J. Rothfuss, F., and Conrad, R.: Flux between soil and atmosphere, vertical concentration profiles in soil, and turnover of nitric oxide: 1. Measurements on a model soil core, J. Atmos. Chem., 23, 253–273, 1996.
Rütting, T., Boeckx, P., Müller, C., and Klemedtsson, L.: Assessment of the importance of dissimilatory nitrate reduction to ammonium for the terrestrial nitrogen cycle, Biogeosciences, 8, 1779–1791, doi:10.5194/bg-8-1779-2011, 2011.
Saad, O. A. L. O. and Conrad, R.: Temperature dependence of nitrification, denitrification and turnover of nitric oxide in different soils, Biol. Fert. Soils, 15, 21–27, 1993.

BGD
11, 1187–1275, 2014

Schulz, S. and Dickschat, J. S.: Bacterial volatiles: the smell of small organisms, Nat. Prod. Rep., 24, 814–842, 2007.
Schuster, M. and Conrad, R.: Metabolism of nitric oxide and nitrous oxide during nitrification and denitrification in soil at different incubation conditions, FEMS Microbiol. Ecol., 101, 133–143, 1992.
Sillman, S.: The relation between ozone, NO_x, and hydrocarbons in urban and polluted rural environments, Atmos. Environ., 33, 1821–1845, 1999.
Skopp, J., Jawson, M. D., and Doran, J. W.: Steady-state aerobic microbial activity as a function of soil water content, Soil Sci. Soc. Am. J., 54, 1619–1625, 1990.
Slemr, F. and Seiler, W.: Field study of environmental variables controlling the NO emission from soil and the NO compensation point, J. Geophys. Res., 96, 13017–13031, 1991.
Stark, J. M., Smart, D. R., Hart, S. C., and Haubensack, K. A.: Regulation of nitric oxide emissions from forest and rangeland soils of Western North America, Ecology, 83, 2278–2292, 2002.
Steinkamp, J. and Lawrence, M. G.: Improvement and evaluation of simulated global biogenic soil NO emissions in an AC-GCM, Atmos. Chem. Phys., 11, 6063–6082, doi:10.5194/acp-11-6063-2011, 2011.
Stotzky, G., Goos, R. D., and Timonin, M. I.: Microbial changes occurring in soil as a result of storage, Plant Soil, 16, 1–18, 1962.
Titzmann, T., Graus, M., Müller, M., Hansel, A., and Ostermann, A.: Improved peak analysis of signals based on counting systems: illustrated for proton-transfer-reaction time-of-flight mass spectrometry, Int. J. Mass Spectrom., 295, 72–77, 2010.
Thomson, B. C., Ostle, N. J., McNamara, N. P., Whiteley, A. S., and Griffiths, R. I.: Effects of sieving, drying and rewetting upon soil bacterial community structure and respiration rates, J. Microbiol. Meth., 83, 69–73, 2010.
UNEP: World Atlas of Desertification, Edward Arnold, Sevenoaks, 1–182, 1997.
Van Cleemput, O. and Samater, A. H.: Nitrite in soils: accumulation and role in the formation of gaseous N compounds, Fert. Res., 45, 81–89, 1996.
Van Dijk, S. and Meixner, F. X.: Production and consumption of NO in forest and pasture soils from the amazon basin, Water Air Pollut.-Focus, 1, 119–130, 2001.
Van Dijk, S. M., Gut, A., Kirkman, G. A., Meixner, F. X., Andreae, M. O., and Gomes, B. M.: Biogenic NO emissions from forest and pasture soils: relating laboratory studies to field measurements, J. Geophys. Res., 107, 8058, doi:10.1029/2001JD000358, 2002.

BGD
11, 1187–1275, 2014

Wang, R., Willibald, G., Feng, Q., Zheng, X., Liao, T. Brüggemann, N., and Butterbach-Bahl, K.: Measurement of N_2, N_2O, NO and CO_2 emissions from soil with the Gas–Flow–Soil–Core Technique, Environ. Sci. Technol., 45, 6066–6072, 2011.
Wickland, K. P. and Neff, J. C.: Decomposition of soil organic matter from boreal black spruce forest: environmental and chemical controls, Biogeochemistry, 87, 29–47, 2008.
Williams, E. J., Hutchinson, G. L., and Fehsenfeld, F. C.: NO_x and N_2O emissions from soil, Global Biogeochem. Cy., 6, 351–388, 1992.
Wishkerman, A., Gebhardt, S., McRoberts, C. W., Hamilton, J. T. G., Williams, J., and Keppler, F.: Abiotic methyl bromide formation from vegetation and its strong dependence on temperature, Environ. Sci. Technol., 42, 6837–6842, 2008.
Wolff, V., Trebs, I., Foken, T., and Meixner, F. X.: Exchange of reactive nitrogen compounds: concentrations and fluxes of total ammonium and total nitrate above a spruce canopy, Biogeosciences, 7, 1729–1744, doi:10.5194/bg-7-1729-2010, 2010.
Yang, W. X. and Meixner, F. X.: Laboratory studies on the release of nitric oxide from subtropical grassland soils: the effect of soil temperature and moisture, in: Gaseous Nitrogen Emissions from Grasslands, Wallingford, England, 67–70, 1997.
Yassaa, N., Wishkerman, A., Keppler, F., and Williams, J.: Fast determination of methyl chloride and methyl bromide emissions from dried plant matter and soil samples using HS-SPME and GC-MS: method and first results, Environ. Chem., 6, 311–318, doi:10.1071/EN09034, 2009.
Yu, J., Meixner, F. X., Sun, W., Liang, Z., Chen, Y., Mamtimin, B., Wang, G., and Z. Sun: Biogenic nitric oxide emission from saline sodic soils in a semiarid region, northeastern China: a laboratory study, J. Geophys. Res., 113, 1–11, 2008.
Yu, J., Meixner, F. X., Sun, W., Mamtimin, B., Wang, G., Qi, X., Xia, C., and Xie, W.: Nitric oxide emissions from black soil, northeastern China: a laboratory study revealing significantly lower rates than hiterto reported, Soil Biol. Biochem., 42, 1784–1792, 2010.

BGD
11, 1187–1275, 2014

Table 1. Compilation of soil properties of all soil samples used in this study. All soil samples have been taken from the top soil of corresponding ecosystems (0–5 cm depth).

sample ID	eco-system	coordinates latitude [° N]	coordinates longitude [° E]	pH [1]	soil type	NH_4^+ [mg kg^{-1}] (N)	NO_3^- [mg kg^{-1}] (N)	total N [%]	total C [%]	$J_{CO_2}(\theta_0, T_0)$ [2] [ng kg^{-1} s^{-1}] (C)
MONGOLIA desert (Mongolia)	hyper-arid desert	44.1367	96.6314	7.9	sandy loam	0.64	68.80	< 0.05	0.96	105.6 [4]
KUCHE corn (Xinjiang, China)	arid oasis agriculture	41.5358	82.855	8.3	silty loam	2.16	105.62	0.11	4.89	n. a.
KUCHE wheat (Xinjiang, China)	arid oasis agriculture	41.5357	82.8541	8.0	silty loam	2.27	54.32	0.09	4.77	n. a.
FINTHEN grassland (Germany)	grass-land steppe	49.9685	8.1479	6.2	loam	7.00	2.20	0.31	4.54	n. a.
SURINAME rainforest (Suriname)	rainforest[1]	05.0763	−55.0029	4.0	–	83.40	4.88	0.59	8.12	416.7
EGER blueberry (Germany)	spruce forest	50.1425	11.8665	3.2	–	239.6	36.9	1.89	41.00	2824
EGER spruce (Germany)	spruce forest	50.1420	11.8673	3.0	–	982.6	90.2	n. d.	43.84[3]	5641

[1] from Oswald et al. (2013).
[2] θ_0: optimum gravimetric soil moisture content of net NO release rate.
[3] data obtained by "loss on ignition" measurements (conversion factor: 2.13).
[4] calculated data statistically not significant ($\Delta m_{CO_2}/\Delta t$ not significantly different from zero (s. Eq. 25).

BGD
11, 1187–1275, 2014

Table 2. Summary of results necessary to characterize NO consumption and NO consumption for the mid-latitude forest soils, mid-latitude grassland soil, and the arid and hyper-arid soils from Xinjiang and Mongolia used in this study. For the four experimental conditions "exp. 1"–"exp. 4" (see Sect. 2), only those NO mixing ratios of the incoming (m_{NO,in_x}) and chamber's headspace air ($m_{NO,cham\_x,0}$) are listed which have been observed at $\theta_g = \theta_0$. J_{NO} data have been calculated with Eq. (1), k_{NO} data with Eqs. (12b) and (14b), P_{NO} data with Eqs. (13b) and (15b), Q_{10_U} (=Q_{10_k}) data with Eq. (16), and Q_{10_P} data with Eq. (17). NO compensation point mixing ratios, $m_{NO,comp}$, are defined by the corresponding ratio of P_{NO} and k_{NO}. The value $Q_{10\_J,mNO,in\_1/3}$ is defined by the ratio $J_{NO}(\theta_0,T_1,m_{NO,cham\_3,0}) : J_{NO}(\theta_0,T_0,m_{NO,cham\_1,0})$.

quantity	EGER blueberry avg	EGER blueberry std dev	EGER spruce avg	EGER spruce std dev	FINTHEN grassland avg	FINTHEN grassland std dev	KUCHE wheat avg	KUCHE wheat std dev	MONGOLIA desert avg	MONGOLIA desert std dev	unit
exp.1: $m_{NO,cham\_1,0}$	1.5	0.15	13.2	0.17	3.0	0.15	17.5	0.18	4.1	0.15	ppb
exp.1: m_{NO,in_1}	0.16	0.150	0.17	0.150	0.30	0.150	0.08	0.150	0.30	0.150	ppb
exp.2: $m_{NO,cham\_2,0}$	459.7	2.30	478.8	2.39	128.9	0.65	148.9	0.75	133.2	0.67	ppb
exp.2: m_{NO,in_2}	471.9	2.36	472.4	2.36	130.1	0.65	136.2	0.68	129.7	0.65	ppb
exp.3: $m_{NO,cham\_3,0}$	2.7	0.15	22.0	0.19	4.2	0.15	26.7	0.20	8.3	0.16	ppb
exp.3: m_{NO,in_3}	0.19	0.150	0.19	0.150	0.36	0.150	0.15	0.150	0.63	0.151	ppb
exp.4: $m_{NO,cham\_4,0}$	457.9	2.29	484.1	2.42	125.2	0.63	162.2	0.81	133.7	0.67	ppb
exp.4: m_{NO,in_4}	469.7	2.35	471.0	2.35	124.5	0.62	137.3	0.69	126.2	0.63	ppb
$J(\theta_0,T_0,m_{NO,cham\_1,0})$	2.01	0.316	21.11	0.367	1.09	0.088	6.99	0.094	1.51	0.086	$ng\,kg^{-1}\,s^{-1}$
$J(\theta_0,T_0,m_{NO,cham\_2,0})$	−18.0	4.88	10.4	5.45	−0.49	0.375	5.11	0.406	1.4	0.37	$ng\,kg^{-1}\,s^{-1}$
$J(\theta_0,T_1,m_{NO,cham\_3,0})$	3.66	0.318	35.28	0.392	1.58	0.088	10.7	0.101	3.07	0.088	$ng\,kg^{-1}\,s^{-1}$
$J(\theta_0,T_1,m_{NO,cham\_4,0})$	−17.5	4.86	21.3	5.47	0.00[a]	0.361	9.99	0.427	3.0	0.37	$ng\,kg^{-1}\,s^{-1}$
$k(\theta_0,T_0)\times10^{-5}$	−7.642	1.865	−4.032	2.049	−2.192	0.5339	−2.502	0.5539	−0.120[b]	0.5188[b]	$m^3\,kg^{-1}\,s^{-1}$
$k(\theta_0,T_1)\times10^{-5}$	−8.110	1.869	−5.288	2.073	−1.895	0.5371	−0.852	0.5662	−0.091[b]	0.5294[b]	$m^3\,kg^{-1}\,s^{-1}$
$P(\theta_0,T_0)$	2.07	0.321	21.41	0.401	1.13	0.089	7.24	0.111	1.51	0.087	$ng\,kg^{-1}\,s^{-1}$
$P(\theta_0,T_1)$	3.79	0.324	35.94	0.475	1.63	0.090	10.78	0.134	3.07	0.092	$ng\,kg^{-1}\,s^{-1}$
$m_{NO,comp}(\theta_0,T_0)$	47	13.7	928	471.6	90	23.0	506	112	6590[c]	–	ppb
$m_{NO,comp}(\theta_0,T_1)$	82	20.0	1187	465.8	150	43.3	2211	1471	6590[c]	–	ppb
Q_{10_U}	1.061[d]	0.3562	1.311	0.8416	1.366[e]	–	1.278[e]	–	n.d.	–	[1]
Q_{10_P}	1.826	0.3234	1.679	0.0385	1.443	0.1395	1.488	0.0293	2.034	0.1327	[1]
$Q_{10\_J,mNO,in\_1/3}$	1.825	0.3284	1.671	0.0345	1.450	0.1416	1.523	0.0250	2.035	0.1308	[1]
θ_0	1.16	0.102	2.12	0.148	0.20	0.025	0.06	0.003	0.023	0.002	[1]
$\theta_{g,1}$	2.80	0.211	4.71	0.447	0.40	0.118	0.19	0.008	0.040	0.000	[1]
R_J	2.0	–	2.0	–	2.0	–	2.0	–	2.0	–	[1]
a	1.2907	–	1.6377	–	2.5339	–	0.7721	–	3.5559	–	[1]

[a] calculated value is lower than the corresponding minimum detectable.
J_{NO} value (see Fig. 9) and significantly not different from zero (s. Fig. 12); consequently J_{NO} = 0 is being assumed here.
[b] calculated data are statistically not significantly different from zero.
[c] data have been calculated using the respective P_{NO} value and the respective minimum detectable k_{NO} value (= $-4 \times 10^{-7}\,m^3\,kg^{-1}\,s^{-1}$, s. Fig. 17).
[d] data is just at the corresponding minimum detectable Q_{10_U} level (s. Fig. 18.).
[e] data falls short of minimum detectable values and has been replaced by minimum detectable Q_{10_U} value.

BGD
11, 1187–1275, 2014

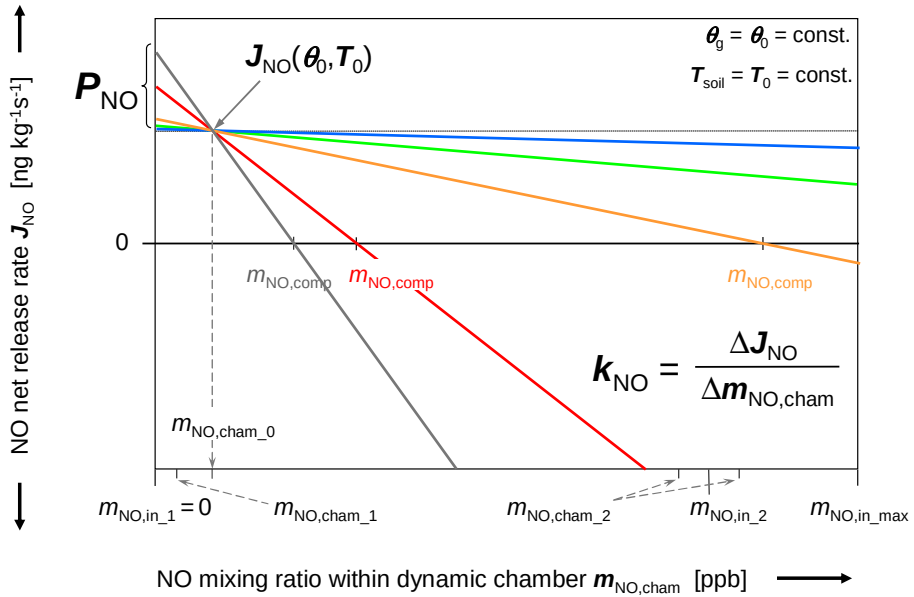

Fig. 1. Schematic of NO net release rate J_{NO} *vs.* NO mixing ratio $m_{NO,cham}$ in the headspace of the dynamic chamber at constant soil temperature and soil moisture; different indices on NO mixing ratios at the inlet ($m_{NO,in}$) or within the dynamic chamber ($m_{NO,cham}$) are explained in the text (note: $m_{NO,cham\_2} < m_{NO,in\_2}$, if $m_{NO,cham\_2} > m_{NO,comp}$, and $m_{NO,cham\_2} > m_{NO,in\_2}$, if $m_{NO,cham\_2} < m_{NO,comp}$).

BGD
11, 1187–1275, 2014

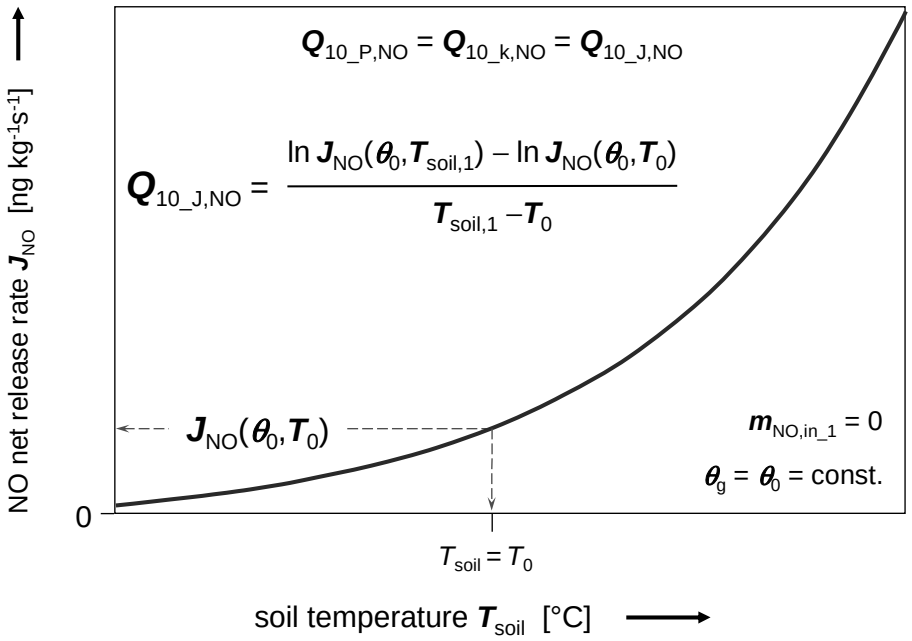

Fig. 2. Schematic of NO net release rate J_{NO} vs. temperature T_{soil} of the enclosed soil sample at constant gravimetric soil moisture and "zero"-air at the dynamic chamber's inlet (note: the shown exponential dependence for $J_{NO}(T_{soil})$ is only valid, if Q_{10} values of both, NO production ($Q_{10\_P,NO}$) and NO consumption ($Q_{10\_k,NO}$) are identical; in this case $Q_{10\_J,NO}$ equals $Q_{10\_P,NO}$ = $Q_{10\_k,NO}$, see Eq. 3b).

BGD
11, 1187–1275, 2014

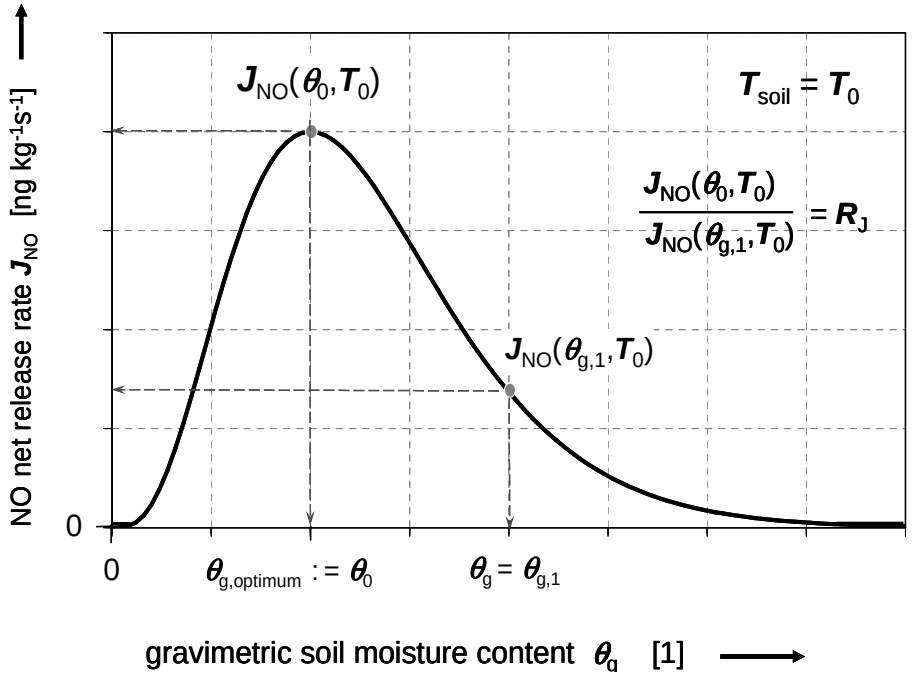

Fig. 3. Schematic of NO net release rate J_{NO} vs. gravimetric soil moisture θ_g at constant soil temperature. The ratio $J_{NO}(\theta_0)/J_{NO}(\theta_{g,1}) = R_J$ is chosen arbitrarily (without loss of generality).

BGD
11, 1187–1275, 2014

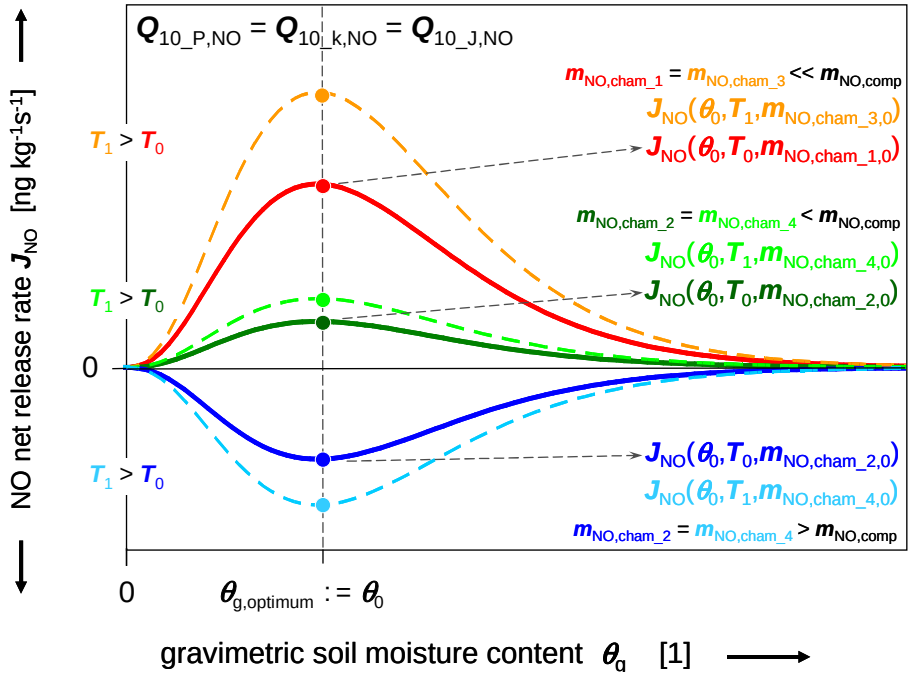

Fig. 4. Schematic of NO net release rate (J_{NO}) variations, which should be observed under different conditions of gravimetric soil moisture (θ_g), soil temperature (T_{soil}), and the dynamic chamber's headspace NO mixing ratio ($m_{NO,cham}$). Note, that the shown variations of J_{NO} with T_{soil} are only valid, if $Q_{10\_P,NO} = Q_{10\_k,NO}$; then, also $Q_{10\_J,NO} = Q_{10\_P,NO} = Q_{10\_k,NO}$, see Eq. 3b).

BGD
11, 1187–1275, 2014

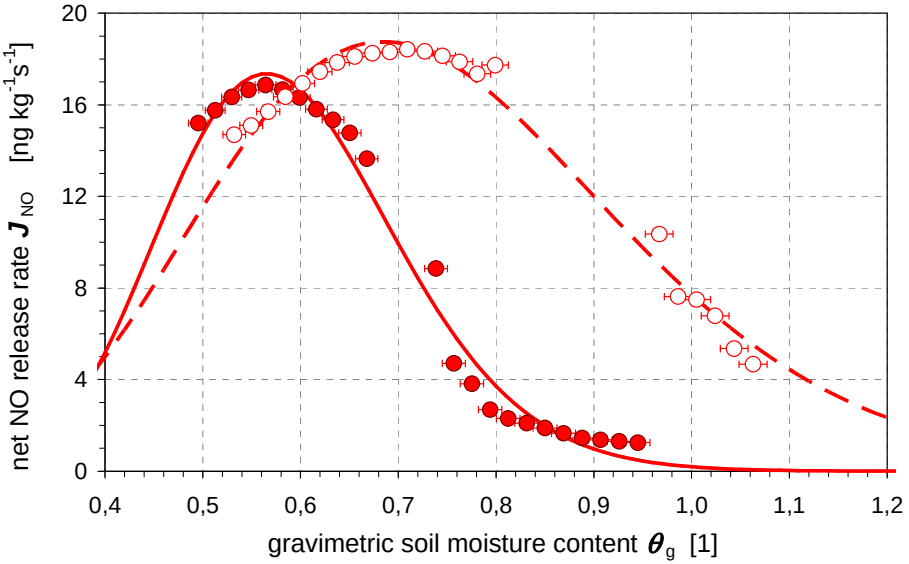

Fig. 5. Results of two replicate NO net release rate (JNO) measurements performed on two individual sub-samples of a organic rainforest soil from Suriname; both experiments have been performed at T_{soil} = 25 °C and m_{NO,in_1} < 0.15 ppb.

BGD
11, 1187–1275, 2014

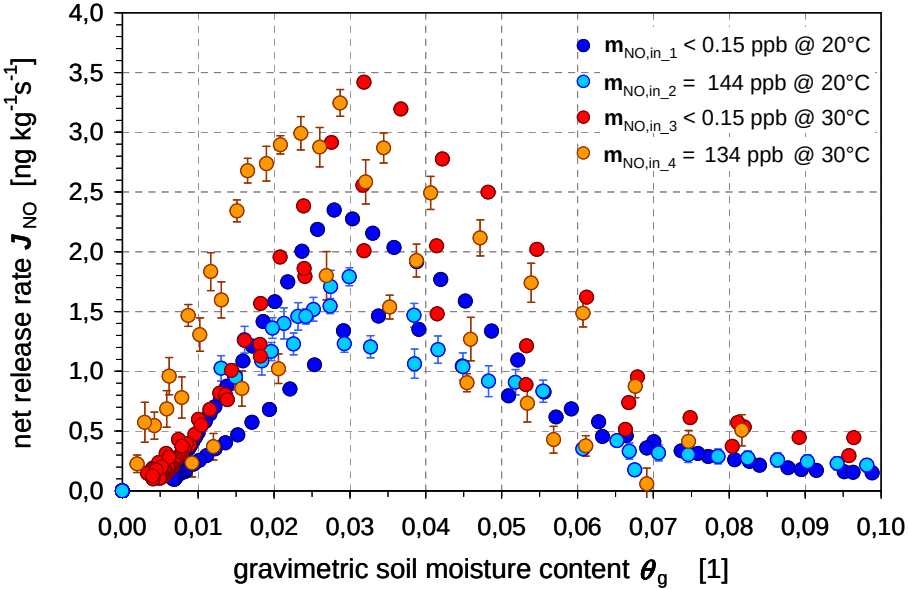

Fig. 6. Results of individual NO net release rate (J_{NO}) measurements performed on 12 sub-samples of a desert soil from Mongolia; three replicates have been measured for each of the four measurement conditions indicated by the four different colors of shown data points.

BGD
11, 1187–1275, 2014

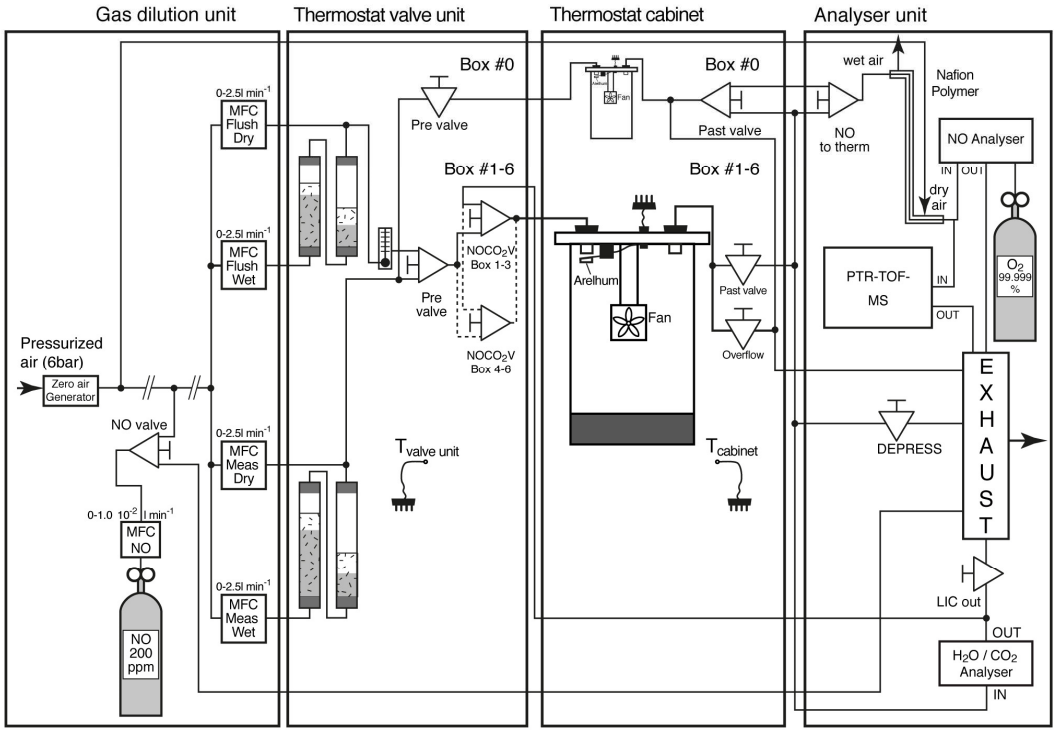

Fig. 7. Schematic of the improved laboratory dynamic chamber system, consisting of four units: "gas dilution", "thermostat valve", "thermostat cabinet", and "analyzers". For simplification only two soil chambers are shown in the figure: one reference cell and one soil sample, although there are six soil chambers in all.

BGD
11, 1187–1275, 2014

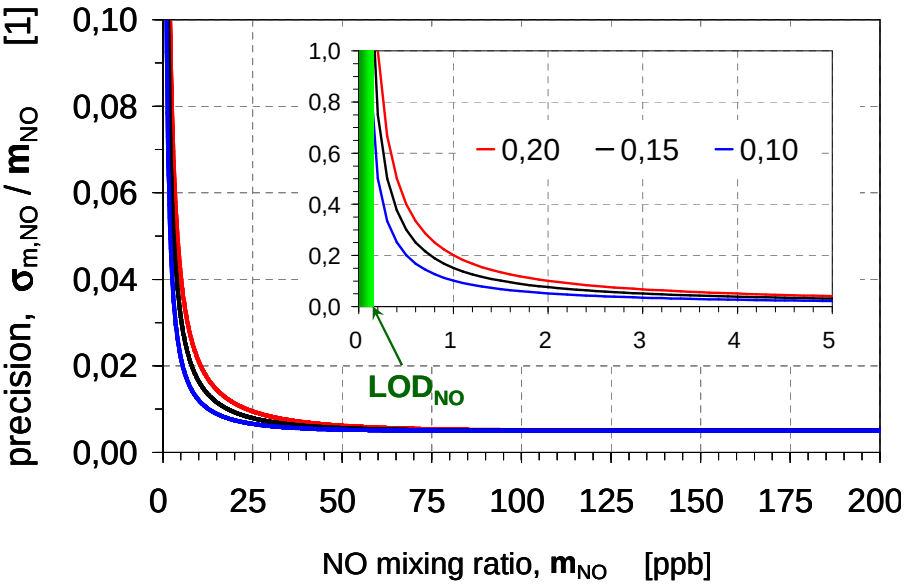

Fig. 8. Precision of NO mixing ratios measured by the used NO_x-analyzer. Data have been obtained **(a)** during routine multipoint calibration exercises, and **(b)** during each drying-out experiment using different $m_{NO,in}$. Note LOD_{NO} and the sharp of precision for $m_{NO} < 10$ ppb as shown in the insert of Fig. 8.

BGD
11, 1187–1275, 2014

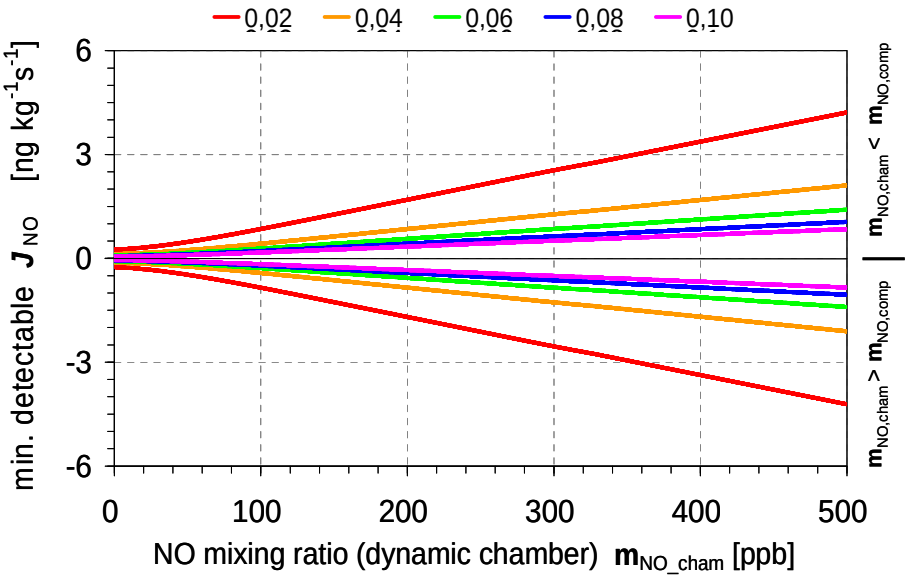

Fig. 9. Minimum detectable net NO release rate as function of the NO mixing ratio in the soil chamber's headspace. Data have been calculated for LOD_{NO} = 0.15 ppb on the basis of the NOx-analyzer's precision (s. Fig. 8). Color code indicates different values of dry mass of the enclosed soil ($m_{soil,\ dry}$ in kg).

BGD
11, 1187–1275, 2014

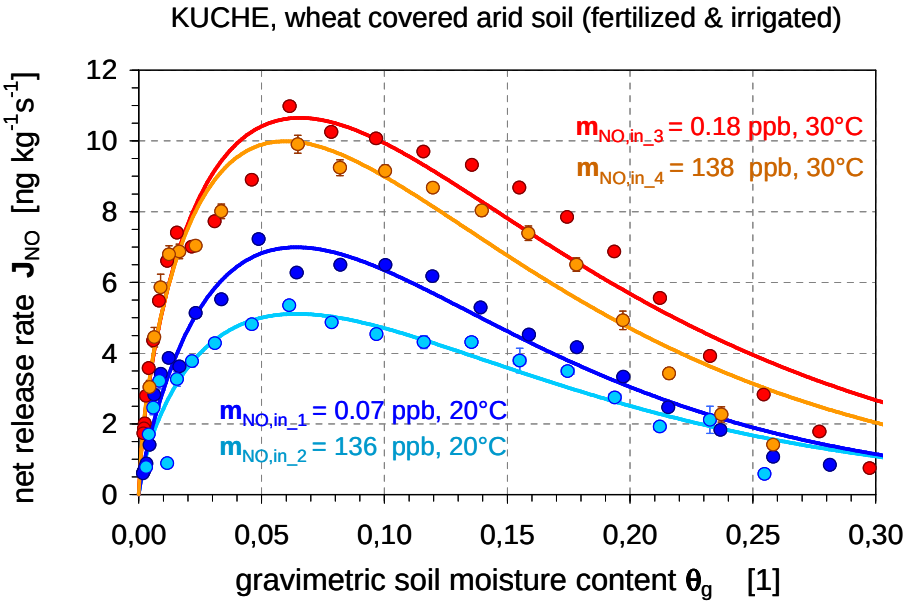

Fig. 10. Net NO release rates of a sample taken from an arid, but agriculturally managed (fertilized & irrigated) wheat covered soil in southern Xinjiang, China. Measurements under the four conditions of exp. 1–exp. 4 (s. Sect. 2) have been performed on one single soil sample; the color code represents these four conditions.

BGD
11, 1187–1275, 2014

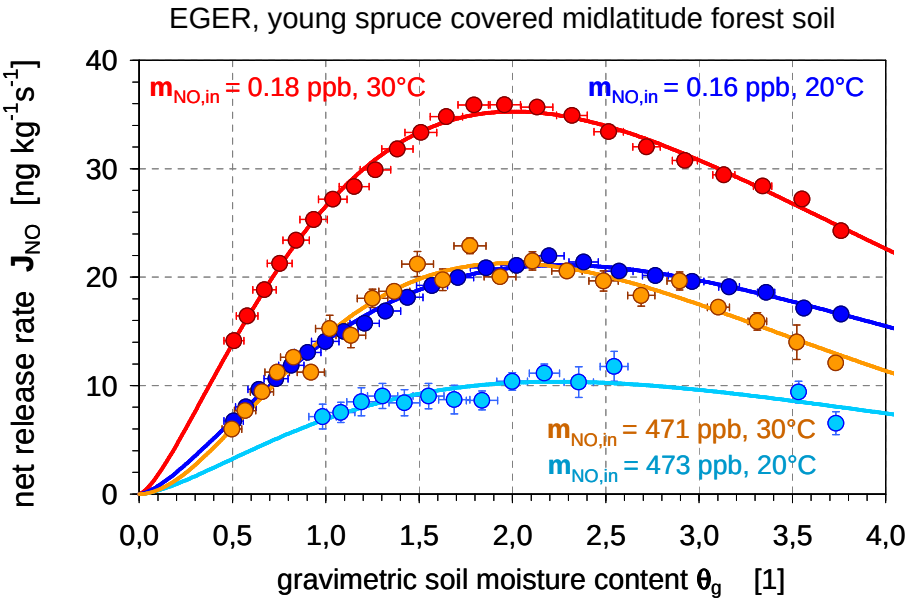

Fig. 11. As Fig. 10, but for a sample taken from an organic rich forest soil covered with young spruce ("Fichtelgebirge", SE Germany).

BGD
11, 1187–1275, 2014

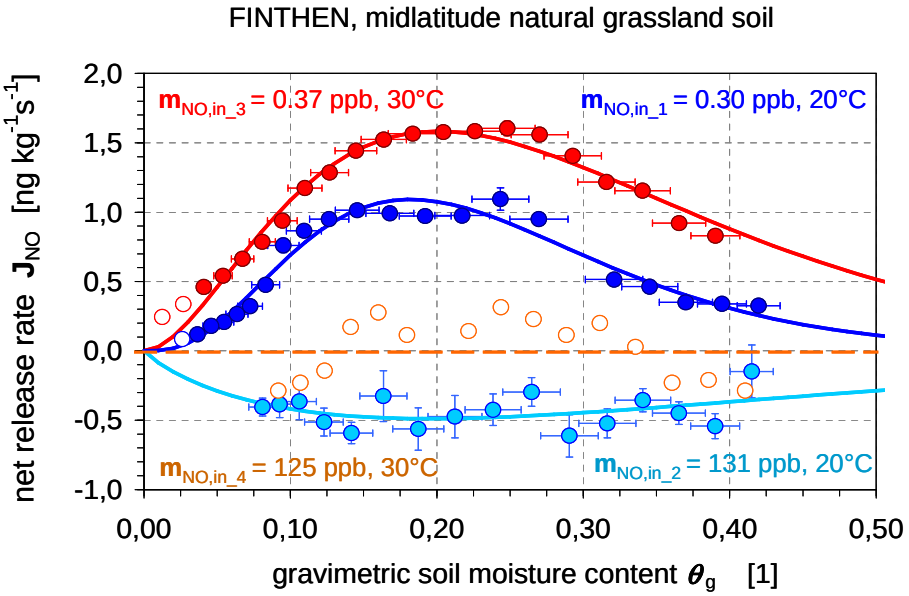

Fig. 12. As Fig. 10, but for a sample taken from a grassland soil (Finthen, W-Germany). Data points marked by empty circles fall within the "deadband" of non-detectable J_{NO} values (defined by ± minimum detectable net NO release rate; s. Sect. 4.2).

BGD
11, 1187–1275, 2014

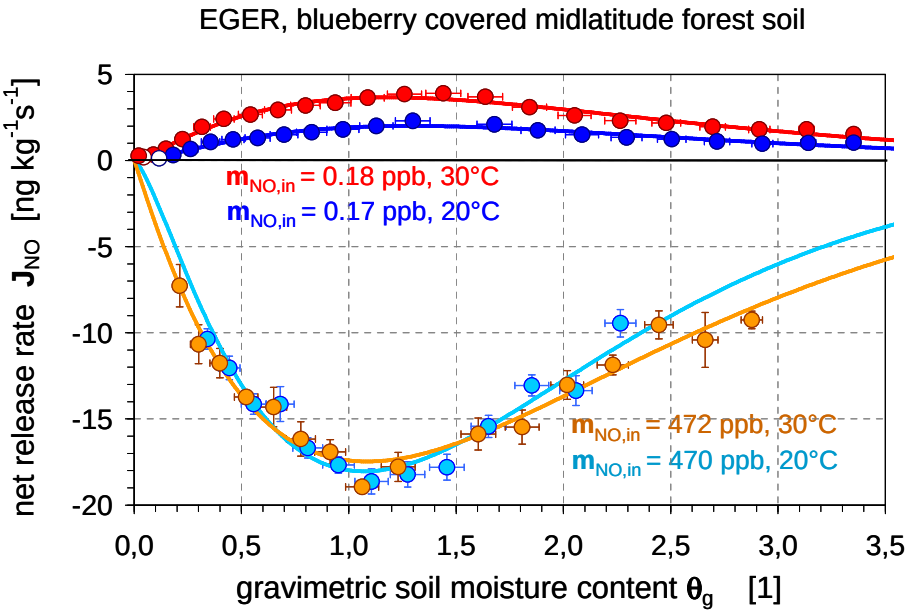

Fig. 13. As Fig. 10, but for a sample taken from an organic rich forest soil covered with blueberries ("Fichtelgebirge", SE Germany). Data points marked by empty circles fall within the "deadband" of non-detectable J_{NO} values (defined by ± minimum detectable net NO release rate; s. Sect. 4.2).

BGD
11, 1187–1275, 2014

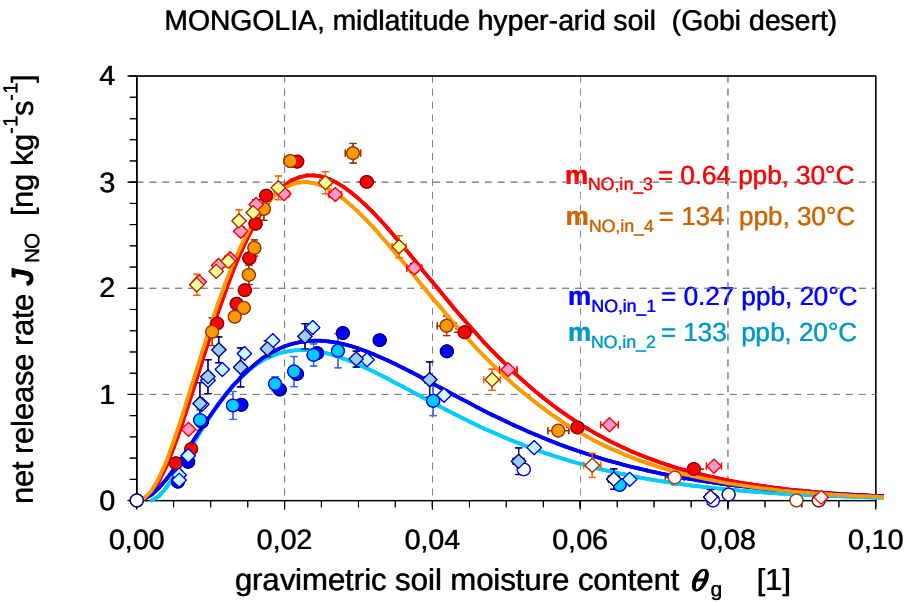

Fig. 14. As Fig. 10, but for a sample taken from a hyper-arid soil in the Gobi desert, Mongolia. Data points originated from two replicate measurements (two different sub-samples) which are identified by corresponding circles and diamonds. Data points marked by empty circles and diamonds fall within the "deadband" of non-detectable values (defined by ± minimum detectable net NO release rate).

BGD
11, 1187–1275, 2014

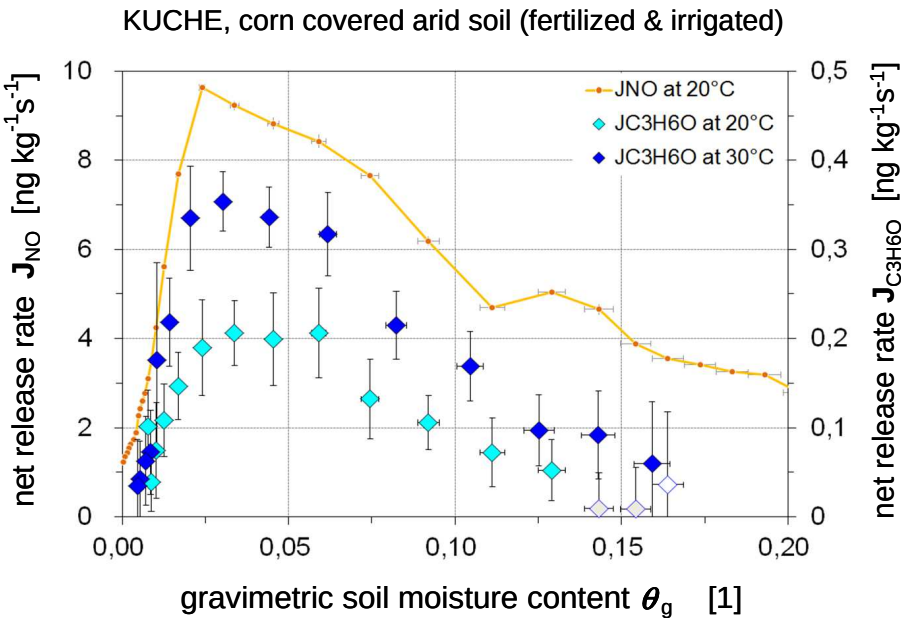

Fig. 15. Net NO release rate (T_{soil} = 20 °C) and net acetaldehyde (C_3H_6O) release rates (T_{soil} = 20 and 30 °C) at fumigation with "zero"-air of a sample taken from an arid, but agriculturally managed (fertilized & irrigated) corn covered soil in southern Xinjiang, China. Data points marked by empty diamonds fall within the "deadband" of non-detectable values. Note, that net NO release rates are expressed in terms of mass of nitrogen (N), while those of C_3H_6O in terms of mass of carbon (C).

BGD
11, 1187–1275, 2014

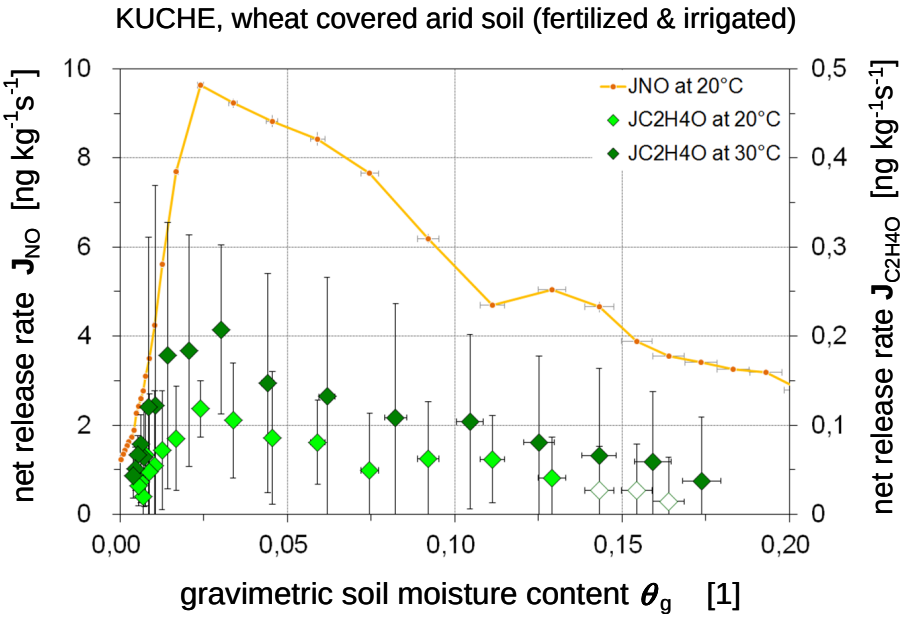

Fig. 16. Net NO release rate (T_{soil} = 20 °C) and net acetone (C_2H_4O) release rates (T_{soil} = 20 °C and 30 °C) at fumigation with "zero"-air of a sample taken from an arid, but agriculturally managed (fertilized & irrigated) corn covered soil in southern Xinjiang, China. Data points marked by empty diamonds fall within the "deadband" of non-detectable values. Note, that net NO release rates are expressed in terms of mass of nitrogen (N), while those of C_3H_6O in terms of mass of carbon (C).

BGD
11, 1187–1275, 2014

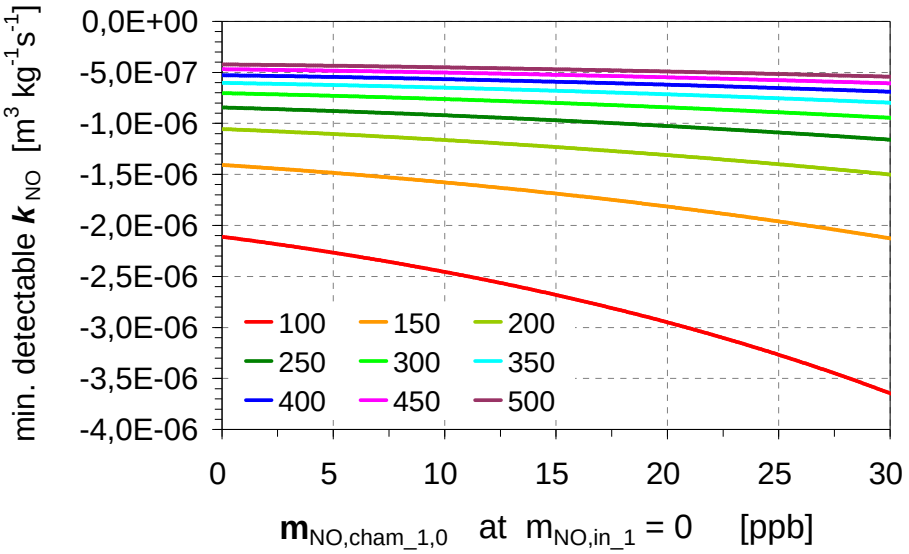

Fig. 17. Minimum detectable NO consumption coefficient (at θ_0 and T_0) as function of the NO mixing ratio in the soil chamber's headspace ($\theta_g = \theta_0$; $m_{NO,in\_1/3} = 0$). Data have been calculated for $m_{soil,\,dry}$ = 0.06 kg and LOD_{NO} = 0.15 ppb on the basis of the NO_x-analyzer's precision. Color code indicates different NO compensation point mixing ratios, $m_{NO,comp}$.

BGD
11, 1187–1275, 2014

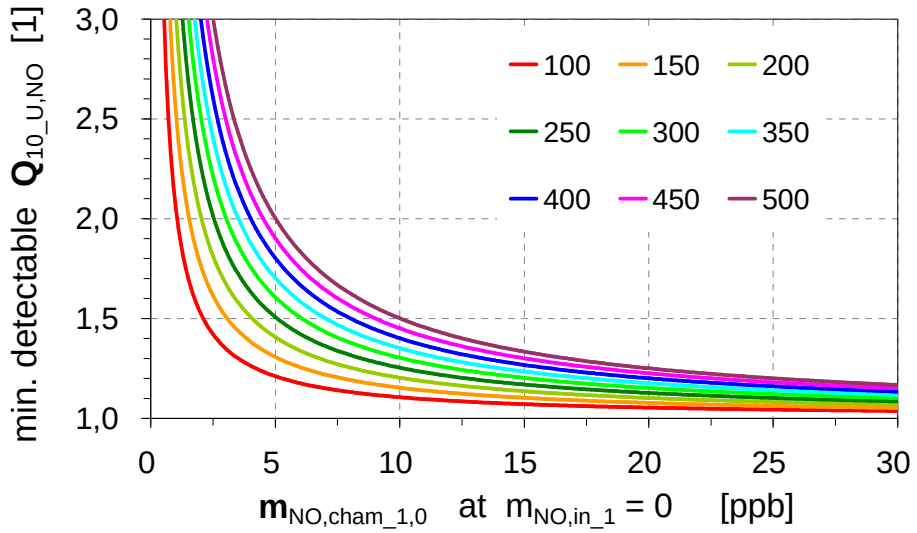

Fig. 18. Minimum detectable Q_{10} value of NO consumption rate U_{NO} as function of the NO mixing ratio in the soil chamber's headspace ($\theta_g = \theta_0$; $m_{NO,in\_1/3} = 0$). Data have been calculated for $m_{soil,\,dry} = 0.06$ kg and $LOD_{NO} = 0.15$ ppb, $T_0 = 20\,^{\circ}C$, and $T_1 = 30\,^{\circ}C$ on the basis of the NO_x-analyzer's precision (s. Fig. 8). Color code indicates different NO compensation point mixing ratios, $m_{NO,comp}$.

BGD
11, 1187–1275, 2014

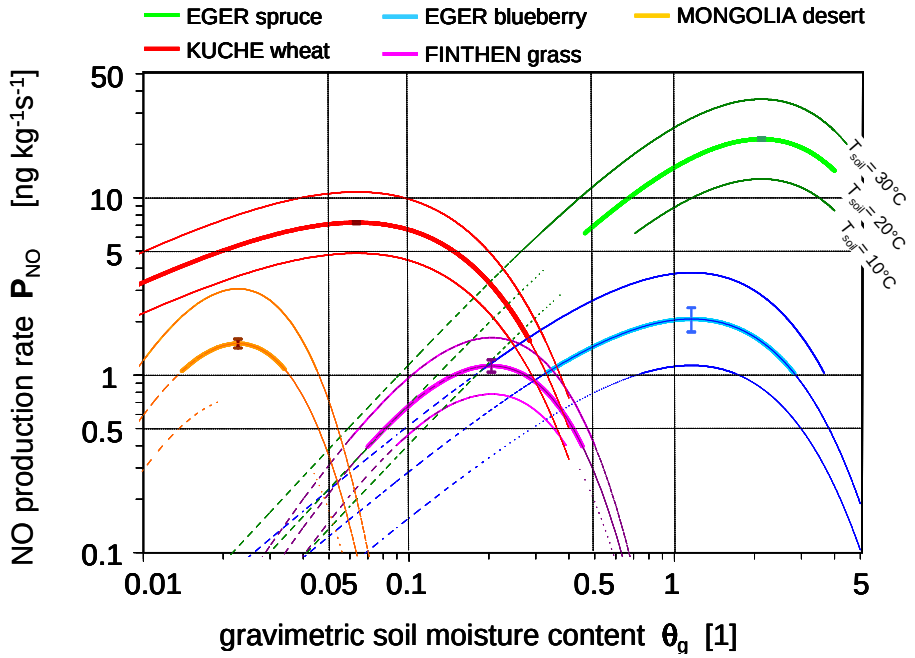

Fig. 19. Summary of NO production rate (P_{NO}) results of the five soil samples in this study. The curves have been calculated using the $P_{NO}(\theta_0, T_0)$, θ_0, $\theta_{g,1}$, and $Q_{10\_P,NO}$-data listed in Table 2. Thick solid lines represent conditions at T_{soil} = 20 °C, thinner solid lines above and below conditions of T_{soil} = 10 °C and T_{soil} = 30 °C, respectively. Solid lines cover the range of those values which have passed corresponding rejection criterion (= minimum detectable P_{NO}, s. Sect. 5.2). Error bars of $P_{NO}(\theta_0, T_0)$ are from Table 2 and indicate respective optimum gravimetric soil moisture contents (θ_0).

BGD
11, 1187–1275, 2014

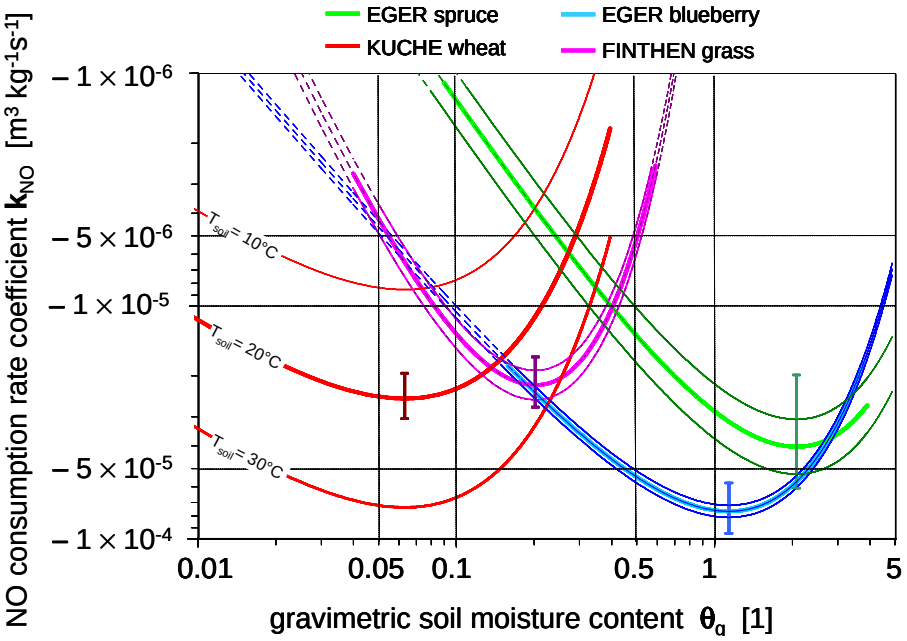

Fig. 20. Summary of NO consumption rate coefficient (k_{NO}) results of the five soil samples in this study. The curves have been calculated using the $k_{NO}(\theta_0,T_0)$, θ_0, $\theta_{g,1}$, and $Q_{10\_U,NO}$-data listed in Table 2. Thick solid lines represent conditions at T_{soil} = 20 °C, thinner solid lines above and below conditions of T_{soil} = 10 °C and T_{soil} = 30 °C, respectively. Solid lines cover the range of those values which have passed corresponding rejection criterion (= minimum detectable k_{NO}, s. Sect. 5.2). Error bars of $k_{NO}(\theta_0,T_0)$ are from Table 2 and indicate respective optimum gravimetric soil moisture contents (θ_0). Note, that there is no k_{NO}-curve for "MONGOLIA desert" soil, since the respective $Q_{10\_U,NO}$ value could not be calculated due to non significant $k_{NO}(\theta_0,T_0)$- and $k_{NO}(\theta_0,T_1)$-data, s. Table 2)

BGD
11, 1187–1275, 2014

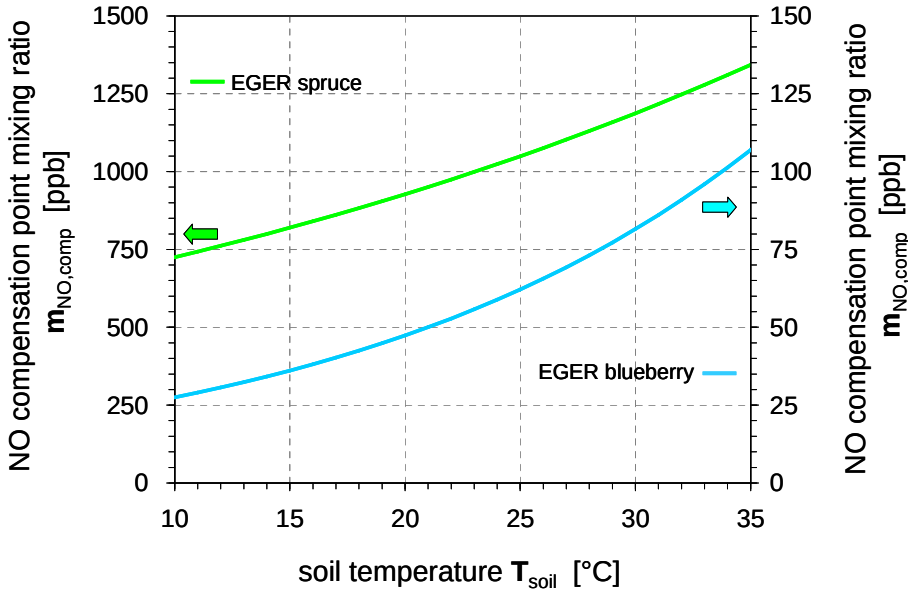

Fig. 21. Soil temperature dependence of NO compensation point mixing ratio ($m_{NO,comp}$) for "EGER blueberry" and "EGER spruce" samples. The curves have been calculated using the $P_{NO}(\theta_0,T_0)$, $k_{NO}(\theta_0,T_0)$, $Q_{10\_P,NO}$, and $Q_{10\_U,NO}$-data listed in Table 2.

BGD
11, 1187–1275, 2014

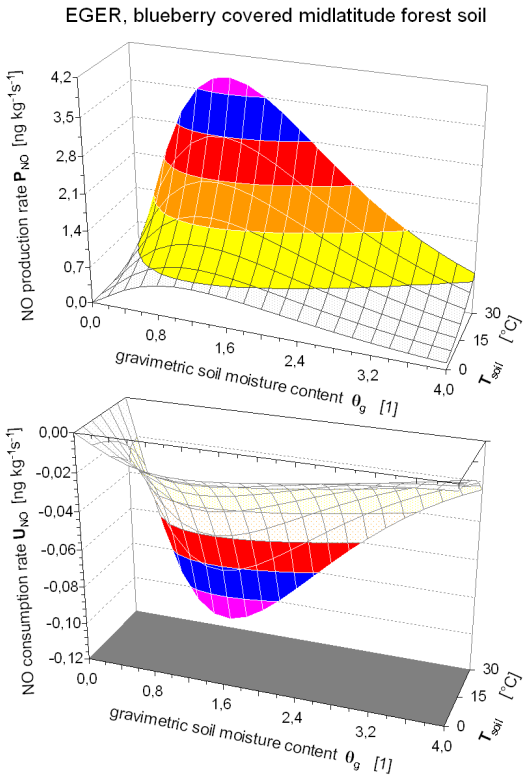

Fig. 22. Two dimensional illustration of NO production rate $P_{NO}(\theta_g,T_{soil})$ and NO consumption rate $U_{NO}(\theta_g,T_{soil})$ for the "EGER blueberry" soil. Light shaded areas represent P_{NO}- and U_{NO} values which fall short of corresponding data rejection criteria (i.e. minimum detectable levels of P_{NO} and U_{NO}; s. Sect. 5.2). $P_{NO}(\theta_0,T_0)$, $k_{NO}(\theta_0,T_0)$, $Q_{10\_P,NO}$, and $Q_{10\_U,NO}$-data listed in Table 2.

BGD
11, 1187–1275, 2014

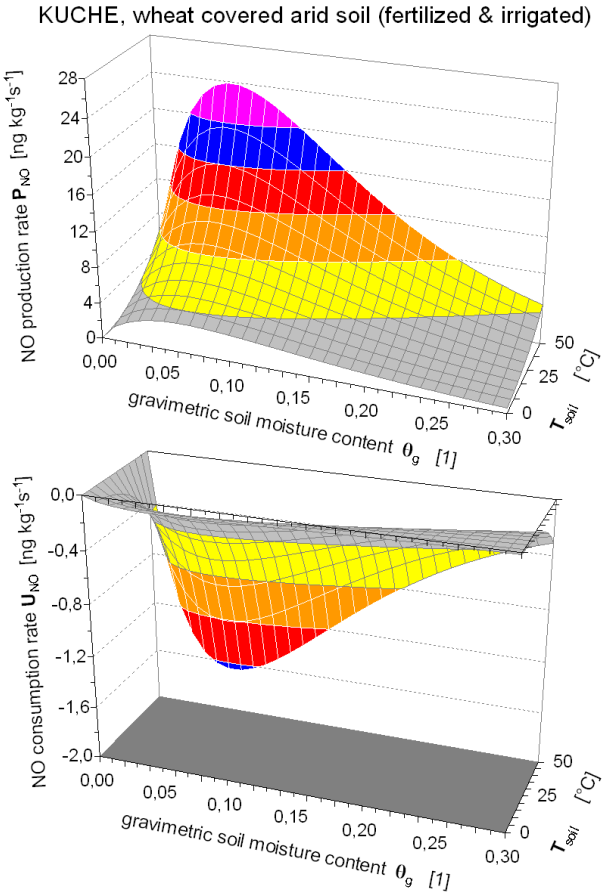

Fig. 23. Two dimensional illustration of NO production rate $P_{NO}(\theta_g,T_{soil})$ and NO consumption rate $U_{NO}(\theta_g,T_{soil})$ for the "KUCHE wheat" soil. Data have been calculated using $P_{NO}(\theta_0,T_0)$, $k_{NO}(\theta_0,T_0)$, $Q_{10\_P,NO}$, and $Q_{10\_U,NO}$-data listed in Table 2.

BGD
11, 1187–1275, 2014